



# VYSOKÉ UČENÍ TECHNICKÉ V BRNĚ

BRNO UNIVERSITY OF TECHNOLOGY

## FAKULTA STROJNÍHO INŽENÝRSTVÍ

FACULTY OF MECHANICAL ENGINEERING

## ÚSTAV FYZIKÁLNÍHO INŽENÝRSTVÍ

INSTITUTE OF PHYSICAL ENGINEERING

## KOREKTOR ABERACÍ PRO NÍZKONAPĚŤOVOU ELEKTRONOVOU MIKROSKOPII

ABERRATION CORRECTOR FOR AN EXCLUSIVELY LOW-VOLTAGE ELECTRON MICROSCOPY

### DIZERTAČNÍ PRÁCE

DOCTORAL THESIS

### AUTOR PRÁCE

AUTHOR

Ing. JAROMÍR BAČOVSKÝ

### VEDOUCÍ PRÁCE

SUPERVISOR

RNDr. VLADIMÍR KOLAŘÍK, CSc.

BRNO 2020

## Abstrakt

Současný vývoj v oblasti nízkovoltové elektronové mikroskopie vede ke zlepšování prostorového rozlišení cestou korekce elektronově-optických vad. V posledních letech se implementace korektorů u konvenčních elektronových mikroskopů (50-200 kV) stává standardem. Nicméně zabudování korektoru do malého stolního prozařovacího mikroskopu pracujícího s nízkým urychlovacím napětím je stále výzva.

Velmi vhodným řešením korekce otvorové vady u takovýchto přístrojů se zdá být koncept hexapólového korektoru založeného na bázi permantních magnetů umožňující zachovat minimální rozměry stolního transmisního mikroskopu.

Přednosti a potenciál Roseho hexapólového korektoru vzhledem k použití v nízkovoltových systémech jsou předmětem kritické analýzy obsažené v této práci, včetně zásadního příspěvku tohoto korektoru k celkové chromatické vadě přístroje.

Chromatická vada zůstává, navzdory veškeré snaze o její minimalizaci, zcela zásadním aspektem při návrhu korektoru.

Koncept představený v rámci této dizertační práce je určen především pro skenovací prozařovací transmisní mód z důvodu omezení nárůstu chromatické vady způsobeného průchodem elektronového svazku preparátem. V práci lze také nalézt podrobný popis navržených kompenzačních systémů korektoru určených k precíznímu seřízení optické soustavy.

## Summary

Current development of low voltage electron microscopy has led to an aberration correction of the instrument in order to improve its spatial resolution. In recent years, aberration correction has slowly become standard in high-end conventional transmission electron microscopy (50-200kV). However, the integration of a corrector to a desktop transmission electron microscope with exclusively low-voltage design seems to be a challenging task.

The hexapole corrector based on permanent magnet technology seems to be a promising solution for the correction of the primary spherical aberration, especially if the compact dimensions and low complexity are to be preserved.

The benefits and potential of the Rose hexapole corrector implemented to such low-voltage systems are critically considered in this thesis. The feasibility of a miniaturized corrector suitable for desktop LVEM is thoroughly discussed, including the aspect of corrector contribution to chromatic aberration that appears to be crucial.

However, despite the effort to minimize the effect of chromatic aberration, its high importance with respect to the microscope resolution still remains a serious obstacle. It must be taken into account when the design is made.

The presented concept is intended exclusively for STEM mode to avoid additional chromatic deterioration caused by electron passage through the specimen. The design of the key segment (transfer lens doublet) is discussed in detail, including its compensation system, which guarantees proper alignment.

Optimal corrector parameters and theoretical resolution limits of such a system are proposed.

**Klíčová slova**

Hexapólový korektor, nízkovoltová prozařovací elektronová mikroskopie, dublet přenosových čoček na bázi permanentních magnetů, otvorová vada, chromatická vada

**Keywords**

Hexapole corrector, low-voltage scanning transmission electron microscopy, permanent magnet transfer lens doublet, spherical aberration, chromatic aberration

BAČOVSKÝ, J. *Korektor aberací pro nízkonapětovou elektronovou mikroskopii*. Brno: Vysoké učení technické v Brně, Fakulta strojního inženýrství, 2020. 91 s. Vedoucí RNDr. Vladimír Kolařík, CSc.

# Contents

Acknowledgements . . . . .	i
Preface . . . . .	iii
Introduction . . . . .	1
<b>1 HISTORICAL BACKGROUND</b>	<b>4</b>
1.1 Precorrected ages . . . . .	5
1.2 Czech contribution to the development of electron optics . . . . .	5
1.3 Beginnings of scanning modes of electron microscopy . . . . .	6
1.4 Development of aberration correctors . . . . .	7
1.5 Aberration-corrected era . . . . .	9
1.5.1 CEOS . . . . .	10
1.5.2 Hitachi . . . . .	10
1.5.3 NION . . . . .	11
1.5.4 JEOL . . . . .	11
1.5.5 FEI . . . . .	11
1.5.6 Sub-Angstrom Low-Voltage Electron Microscope . . . . .	12
<b>2 LOW-VOLTAGE ELECTRON MICROSCOPY</b>	<b>14</b>
2.1 Parameters of current LVEM5 & LVEM25 . . . . .	17
<b>3 METHODS OF ABERRATION CORRECTION</b>	<b>20</b>
3.1 Multipole correctors . . . . .	20
3.1.1 Hexapole corrector . . . . .	21
3.1.2 Quadrupole-octupole corrector . . . . .	25
3.2 Electron mirror . . . . .	26
3.3 Potential on the axis . . . . .	29
3.3.1 Aberration correction by space charge cloud . . . . .	30
3.3.2 Foil lenses . . . . .	30
3.3.3 Axial Conductors . . . . .	31
3.4 High-Frequency Lenses . . . . .	32
<b>4 ABERRATIONS</b>	<b>33</b>
4.1 Spherical aberration . . . . .	35
4.1.1 Plane with minimal spherical aberration disc . . . . .	37
4.1.2 Dependence of the spherical aberration on aperture . . . . .	39
4.2 Chromatic aberration . . . . .	40
<b>5 BENEFIT ANALYSIS OF THE ABERRATION CORRECTION</b>	<b>42</b>
5.1 Estimated resolution of corrected LVEM . . . . .	42
5.2 Wave aberration theory . . . . .	46
<b>6 ENHANCEMENT OF CHROMATIC ABERRATION BY A HEXAPOLE CORRECTOR</b>	<b>53</b>
<b>7 OUTLINE OF THE CORRECTOR</b>	<b>58</b>

*CONTENTS*

<b>8</b>	<b>ADJUSTMENT OF THE CORRECTOR</b>	<b>62</b>
8.1	Compensation coils . . . . .	62
8.2	Required manufacturing accuracy . . . . .	63
8.2.1	Correction for the amount of magnetic charge . . . . .	64
8.2.2	Balancing of doublet asymmetry . . . . .	66
8.3	Residual beam rotation caused by compensation and asymmetry elimination coils . . . . .	66
8.4	Parameters of Extended Hexapoles . . . . .	67
<b>9</b>	<b>CORRECTION POWER OF THE HEXAPOLE CORRECTOR</b>	<b>70</b>
<b>10</b>	<b>MANUFACTURING NOTES</b>	<b>76</b>
<b>11</b>	<b>CONCLUSIONS AND FUTURE DIRECTIONS</b>	<b>78</b>
<b>12</b>	<b>List of abbreviations</b>	<b>91</b>

# ACKNOWLEDGEMENTS

During the first year of my doctoral study, I made a very fundamental but also tricky decision to move my research activities to the private sector and thus, this thesis has become a reality with the kind support of Delong Instruments. The company provided me with a working environment, where I could count on not only a friendly atmosphere but also all possible support.

My gratitude goes firstly to my supervisor RNDr. Vladimír Kolařík, CSc., who guided me through the entire graduate education. His mentoring and deep insight into physics granted me valuable knowledge and encouragement during hard research periods. His unwavering enthusiasm for electron optics kept me constantly engaged with my research goals and his unprecedented overview, as well as intuition gathered over the years of practice, has provided me with reassurance whenever needed. He has taught me from the beginning of the project when I was getting acquainted with the new scientific field, that it was necessary to deal not only with the theory but also with the practical aspects of the future technical solution. He always led me to present the conclusions of our research as clearly as possible.

I would also like to express my sincere gratitude to other colleagues. Namely to Mgr. Petr Štěpán, who introduced me to the practical electron microscopy operation and creative troubleshooting. I would also like to thank him for his friendship, empathy and a great sense of humour during the hours we spent together in our laboratory.

Special thanks also go to Ing. Pavel Jánský Ph.D. for many critical comments and stimulating discussions and also to Ian Tailor for linguistic and stylistic proofreading.

It has been a great privilege and honor to work under your guidance and learn from your experiences.

Besides my advisors in the field of physics, I am also extremely grateful to my parents and all family members for their unconditional love, caring and sacrifices for my future education. Of course, I cannot forget to the circle of closest friends, who enrich my life and remind me that real life and joy is above all outside the science and work.

I would like to extend my sincere thanks to all who participated. This work would never have existed without your support.



# PREFACE

The following dissertation was prepared with the kind support of Delong Instruments. When I finished a master's degree, I was searching for a new research challenges and motivations. I was approached by my future supervisor RNDr. Vladimír Kolařík, CSc very early. Electron microscopy, as a scientific discipline, was completely new to me. At first, I was skeptical because this field has a reputation that almost every student of physics in Brno will work in this scientific field anyway and I wanted to do something unique. However, I was convinced of the beauties of this field very soon and I realized that there is a very exceptional background for this work in Brno.

The research goals have slightly changed and developed over the years of my doctoral study. The original intention, defined together with my supervisor during the initial period of my study, was to analyse the significance of each individual aberration affecting low-voltage transmission electron microscopes. We tried to find a way in confusing chaos of aberration coefficients, half-truths, and even blunders, traditionally transcribed from one book to another, apparently without a proper understanding of the problem.

With a deeper insight into the problem, we set the goal of preparing a corrector design intended exclusively for low-voltage transmission electron microscopes. This ambitious project led to the proposal of the aberration corrector tailored to the specific needs of benchtop transmission electron microscopes produced by Delong Instruments.

The majority of the presented research has been already published and these articles are indexed in the references together with other relevant sources referring to the discussed issues. I tried to support all mentioned statements by a carefully selected set of references providing an understandable explanation even to an inexperienced reader.

My supervisor also often encouraged me to pursue my goal and present my results clearly in such a way that all potential questions arising from the text were fully answered immediately. I did my best to provide comprehensive text containing all the necessary information so that the reader does not need to search in the original publication.



# INTRODUCTION

*Elektronový mikroskop, přestože se zdá mít nejlepší léta za sebou, je přístrojem, jehož vývoj nekončí. Bilance jeho uplatnění je pozoruhodná. Tisíce, ne-li desetitisíce publikací jeho přičiněním dosažených nemají konkurenci. V současné době neexistuje přístroj, který by měl takové rezervy. Elektronový mikroskop stojí před novou vývojovou etapou. Zdá se, že se našly technické prostředky, jak posunout jeho parametry, zejména rozlišovací schopnost, výrazně kupředu. Nejnovější technologie na nanometrové úrovni slibují materiály, které nemají v současné době obdobu, studium biologických objektů na submolekulární úrovni přinese poznatky o jejich funkci. Elektronové mikroskopy nové generace budou moci významně k dosažení uvedených cílů přispět.*

— prof. Ing. Armin Delong [1]

The human desire to explore nature in all possible scales undoubtedly lags behind the technological progress of scientific instrumentation. From its origin, mankind has been attracted to the investigation of the universe from the biggest structures to the tiniest known objects.

Scientific and technological evolution driven by the ambition to see more, further and deeper has already allowed us to observe incredible things, proving the astonishing diversity of nature. Although it might seem that smaller and smaller objects can be examined with better and better microscopes, nature provides only a limited set of objects or, said differently, natural samples. The current microscopes, in fact, have revealed specimen details of all scales all the way down to the atomic structure. However, the difficulties to reach such a high resolution are currently enormous and the most advanced and expensive high-voltage electron-optical devices are required. Moreover, technology has to be supported by immense effort, perfect sample preparation and an experienced operator.

It should also be emphasized that extreme atomic resolution is practically in vain or even redundant for most of the applications. Thus, the effort for further magnifying beyond such dimensions seems to be a marginal issue, due to the fact that there are no other natural structures accessible by electrons.

On the other hand, there is still plenty of room for improvement. In contrast to advanced light-optical microscopy techniques capable of resolution beyond the diffraction limit, which is considered the physical limit for classical microscopy, electron microscopy has not yet approached this physical limitation. Uncorrected conventional electron microscopy limited mainly by chromatic and spherical aberration is not able to achieve spatial resolution better than  $50\lambda$  [2].

There are two approaches to resolve smaller objects with the help of electrons: reduction of the De Broglie wavelength and correction of aberrations. The most effective, or even inevitable, way is to combine both approaches.

Although  $\lambda$  itself is small enough even for low accelerating voltage, its reduction has a significant influence on system aberrations. On the contrary, increasing accelerating voltage, as well as the dimensions of the main microscope column and sample stability against radiation damage have high requirements for technical parameters of electronics. The appropriate way to exploit the physical potential of the instruments is to correct the most serious aberrations.

Basic principles of aberration correction have been known for 70 years [3], but practical implementation has been complicated by technological limitations for a very long time. The first generation of correctors called "proof of principle" confirmed the possibility to use rotationally asymmetric multipole electron-optical components for aberration correction. However, their own imperfections severely deteriorated image resolution.

The rapid development of accuracy of mechanical manufacturing and stability of electronics over the past decades has enabled the practical use of correctors in the most advanced electron microscopes [4].

The current commercially available corrected transmission electron microscopes work with an accelerating voltage in the range of 100–200kV, but corrected systems with lower energy are still under development.

Low-voltage transmission electron microscopy (LVEM) uses an electron beam with an energy of 5 – 30 kV, corresponding to the wavelength interval of 17.3 – 7.1 pm. The reduction of radiation damage of the sample and contrast enhancement necessary for investigation of sensitive samples containing light atoms and weak bonds can be considered as the main advantage of such systems. Certain technical aspects, discussed later, also allow the LVEMs to be constructed in desktop design, in contrast to the bigger common dimensions of conventional TEM/STEM devices.

The main goal of this thesis is to propose a technical solution of a corrector exclusively tailored to the needs of low-voltage electron microscopes.

The first section is devoted to the introduction of the historical context. The evolution of correctors is briefly summarized from the first corrector generation (with "proof-of-principle" ambitions) to the novel generation of SALVE III project.

The unique properties of low-voltage transmission electron microscopes emerge in section 2, which thoroughly describes these unconventional scientific instruments. This is further elaborated and substantiated by precise numbers in section 3 for a particular case of LVEM5 and LVEM25, produced by DeLong Instruments.

Section 4 is dedicated to the aberrations themselves with special attention to the most essential ones, spherical and chromatic aberrations.

The gradually build-up of knowledge necessary for understanding the following chapters leads the reader to sections 5 and 6, presenting a feasibility study of the idea of a low-voltage corrected transmission electron microscope. Special attention is paid to the increase of chromatic aberration, which is not corrected. However, the corrector itself introduces an additional contribution to the global chromatic aberration of the system.

The next three key sections are centred around the outline of the designed corrector concept, its properties and correction abilities. It is shown that the hexapole corrector based on permanent magnet technology seems to be a promising solution for the correction of primary spherical aberration, especially if the compact dimensions and low complexity are to be preserved. However, the high importance of chromatic aberration with respect to the microscope resolution still remains a serious obstacle and must be taken into account when the design is made.

Hence, the concept presented in this thesis is intended exclusively for scanning transmission (STEM) mode to avoid additional chromatic deterioration caused by electron passage through the sample. The design of the key segment (transfer lens doublet) is discussed in detail, including its adjusting systems, which guarantees proper alignment.

The following thesis is closed with a concluding section filled with a summary of the most important aspects of the presented corrector concept. Remarks, which naturally

emerged during the development, and prospects for future work are also included in this final section.

# 1. HISTORICAL BACKGROUND

*Bref, j'ai développé des idées nouvelles pouvant peut-être contribuer à hâter la synthèse nécessaire qui, de nouveau, unifiera la physique des radiations aujourd'hui si étrangement scindées en deux domaines où règnent respectivement deux conceptions opposées : la conception corpusculaire et celle des ondes. J'ai pressenti que les principes de la Dynamique du point matériel, si on savait les analyser correctement, se présenteraient sans doute comme exprimant des propagations et des concordances de phases et j'ai cherché, de mon mieux, à tirer de la, l'explication d'un certain nombre d'énigmes posées par la théorie des Quanta.*

— Louis De Broglie [5]

The following chapter briefly summarizes the most important milestones in the development of electron optics and its endeavor to correct crucial electron-optical aberrations. The beginning of this section will cover the historical aspects that led to the uprising of the scientific field of electron microscopy. The first attempts to design transmission electron microscopes will then be presented herewithin, with special attention to the work of professor Armin Delong's research group in Brno.

According to the diffraction limit statement published by German physicist Ernst Abbe in 1873, the resolution of all optical instruments is commonly limited by the wavelength of investigating particles used as a probe. Any further magnification beyond the above-mentioned restriction does not lead to obtaining new information about the investigated sample. Structures appear to be larger; however, no more details are resolved. A practically achievable resolution when standard aperture angles are used can reach 200 nm for the best light optical microscopes. It corresponds to the maximal magnification of about 1000x-1400x [6]. Everything beyond this limit is called empty magnification.

A very special light optical technique capable of resolution beyond the diffraction limit was presented in 2008 [7]. The more logical way how to reach a higher resolution is to find a more suitable probe with a shorter wavelength than light. It has, however, appeared to be a relevant problem for electromagnetic waves due to the fact that such high-quality optical materials for an electromagnetic radiation with a short wavelength do not exist. The most promising alternative seemed to be electron optics.

Common light optical elements, such as lenses and mirrors, have their counterparts in electron optics. Although the mathematical description of geometrical optics is the same for electrons as well as for photons, aberration correction must be performed by specific methods in the case of electron optics, because boundaries of electron-optic elements cannot be shaped arbitrarily according to the strict needs of aberration correction, as they are shaped in light optics.

From an historical point of view, the discovery of an electron particle by British experimental physicist, Sir Joseph John Thomson working for Cavendish laboratory in University of Cambridge, can be considered the beginning of the scientific field of electron microscopy.

The historical context of the aberration correction technique has been presented in numerous articles. The basic overview of electron optics development can be obtained from a short article Electron Optics and Electron Microscopy: A Personal Retrospective

written by Peter Hawkes [8]. The history of corrector development has been recently summarised by Hawkes in detail [9].

## 1.1. Precorrected ages

Electron optics was born during the second decade of the 20th century. It emerged during a period of revolutionary breakthroughs in the field of theoretical physics. The foundation stone was laid by French physicist Louis de Broglie, who claimed that a wavelength should be associated also with all moving particles, as is the case with light. This calling for natural corpuscular-wave symmetry was summarized in his thesis "RECHERCHES SUR LA THEORIE DES QUANTA" published in 1924 [5].

This breakthrough discovery of particle-wave dualism was independently confirmed by Davisson with Germer and, at nearly the same time, by Thomson with Reider using electron diffraction. As a result of their experiments, which convincingly demonstrated dualism of electrons, the exclusively corpuscular concept was definitively abandoned. The wavelength  $\lambda$  was accordingly assigned to electrons considering their energy  $E$ .

Another pioneer of electron optics was Hans Busch from Germany, who published a paper wherein he proved that the action of an axially symmetric coil on electrons is comparable with light optical converging lenses [10].

In the early 1930s, Max Knoll and his young student Ernst Ruska, working at the Technical University of Berlin, used Busch's ideas of the analogy between the classical light optics glass lens and electron optics to construct the first prototype of an electron microscope. Their endeavour leading to the first transmission electron microscope was published in 1932, together with a description of the electromagnetic lens design. After graduation, Ernst Ruska worked for Fernseh Ltd. He later, in 1937, began his future career at Siemens-Reiniger-Werke AG company in Siemens & Halské laboratories, where he participated in the development of the first commercially produced transmission electron microscope launched in 1939. He was awarded the Nobel Prize in Physics for his lifelong contribution to electron optics in 1986 [11].

## 1.2. Czech contribution to the development of electron optics

The year 1947 is considered to be the beginning of electron microscopy in Czechoslovakia. As part of post-war aid to Europe, the US UNRRA (United Nations Relief and Rehabilitation Administration) provided two RCA transmission electron microscopes to Czechoslovakia. One of them was given to Professor Wolf in Prague and the other to Professor Herčík in Brno at the Institute of Biology, Faculty of Medicine, Masaryk University. The delivery of the electron microscope to Brno was reckoned to be a great challenge. Professor Aleš Bláha from the Department of Theoretical and Experimental Electrical Engineering of Brno University of Technology set the goal to construct their own electron microscope. He put together a team, consisting of students prof. Ing. Armin Delong, DrSc., Ing. Ladislav Zobač, CSc., Prof. Ing. Vladimír Drahoš, DrSc. and designer J. Speciální, working under the his leadership [12].

The design of the first prototype did not take long and the microscope was ready for testing in 1949. This experimental device known as the "Tripod" was able to verify basic principles and it provided all necessary experiences to build the first real electron microscope with the name designated as Tesla BS241 [13]. Despite the fact that the microscope suffered from a significant manifestation of an axial astigmatism of the objective lens, the microscope was tuned to a competitive form [14]. Twenty-five of these instruments with an accelerating voltage of 50 kV and a resolution of approximately 2 nm were placed in laboratories across Czechoslovakia.

Everything seemed promising until 1953 when the Technical University was transformed into a Military Technical Academy, which was not interested in civilian projects. Professor Bláha, the leader of the research group of electron microscopy was fired and forced to move to Bratislava for political reasons. The rest of the team of the department of electron microscopy started to work for the newly established company Tesla Brno, which was also given the production of electron microscopes [15].

Another design goal of the research group from Brno was as simple a transmission electron microscope as possible. It had no ambition to compete with other available microscopes on the market by parameters, but it was supposed to be a device with low manufacturing requirements, made of more accessible materials, with affordable price and user-friendly controls.

The first one of this unique desktop instrument was built in 1954 and, after two years, the serial production was launched. This microscope designated Tesla BS 242 operated with an accelerating voltage of 60 kV and it reached a resolution of 15 – 25 Angstrom. It became popular very quickly with customers in many prestigious laboratories throughout the world, as its parameters were comparable to other microscopes on the market but the other ones could not compete on price.

The production of this instrument in Tesla Brno National Company lasted 20 years. Over 1300 instruments were manufactured, which were sold to more than 20 countries around the world. The high popularity of this product is demonstrated by the fact that it was awarded a gold medal at EXPO 58.

In the 1960s, new transmission and also scanning electron microscopes were designed for Tesla. There was a significant development of the field of electron optics thanks to the director of the Institute of Scientific Instruments, prof. Armin Delong, and the Head of the Department of Electron Optics, Prof. Ing. Vladimír Drahoš, DrSc. It is especially worth mentioning firstly the successful project of transmission microscopes TEM TESLA BS 413 with a resolution of up to 0.6 nm and an accelerating voltage of up to 100 kV and secondly the project of the scanning electron microscope TESLA BS 350 with a field-emission gun [13]. Tesla Brno was the world's biggest producer of electron microscopes in the early 1970s.

After Tesla dissolved, experienced former Tesla and Czechoslovak Academy of Sciences employees established four new companies: Tesla Elmi, TESCAN, Delmi and Delong Instruments.

### **1.3. Beginnings of scanning modes of electron microscopy**

The second development direction of electron microscopy is the scanning mode, pioneered by the German physicist and inventor Manfred von Ardenne. This mode does not work

with the idea of forming an image by irradiating a large area of the specimen and forming the image in the image plane after adequate magnification. On the contrary, his vision works with the idea of a small probe scanning the specimen and collecting a signal from each single point of the sample [16]. In the 1930s, Manfred von Ardenne was able to theoretically describe the scanning mode of a transmission electron microscopy and subsequently led the research to practical implementation [14].

The first scanning electron microscope in which secondary and backscattered electrons coming back from a thick sample are collected in order to form an image was developed by American scientist Vladimir Kosmich Zworykin in 1942.

Because of the inconvenient performance of the thermionic electron source, it was clear from a very early stage that the resolution of scanning electron microscopes could never compete with the resolving power of transmission mode [17]. High ambitions were given to new field emission guns developed by Albert Crewe in collaboration with Hitachi. This new kind of electron source was capable of forming a probe focused to the area with a diameter of a few angströms. In 1965, this progress, enabling much higher optical quality, led Crewe to create a concept of a scanning transmission electron microscope with the field emission gun. During the 1970s, a research group under his leadership developed an STEM instrument converted from SEM in which the observation of thorium and uranium single atoms on amorphous carbon film was reported [18]. During the same decade, Crewe worked also on the project of a hexapole corrector compensating the spherical aberration for a dedicated STEM [19][20].

## 1.4. Development of aberration correctors

At the time when classical optical microscopy approached its physical limitations given by the wavelength of light, the effort to reduce resolution moved to electron optics. Scientists had a clear ambition to achieve subatomic resolution when designing the first prototypes. The inventors of the first electron microscope, Ernst Ruska and Max Knoll, were not familiar with the new research and thesis of Louis de Broglie about the wave nature of matter [5].

Therefore, they did not have any reason to not consider an electron as an almost perfect probe with extremely small dimensions. The wave nature of elementary particles was an unwelcome finding to achieve their goals. However, they soon realized that the wavelength of the accelerated electrons in an electron microscope would be at least 5 orders of magnitude lower than the wavelength of light. According to the prognosis of Ernst Ruska, the expected resolution was 2.2 Angstroms. Ruska used Abbe's diffraction limit to obtain this estimate. He assumed the validity of the statement not only for electromagnetic waves but also for material waves of the electrons. He calculated with an accelerating voltage of 75 kV and aperture angle of  $2 \times 10^{-2}$  rad corresponding to his prototype. However, achieving such an exquisitely high resolution proved to be very difficult and required another 40 years of intense research.

In accordance with the prior design of light optical devices, it was assumed that the quality of electron optics imaging depended on the clever and advanced design of each part of the electron optical assembly, as in the case of light optics. Unfortunately, soon after the invention of the electron microscope, the first papers on the theoretical background

of charged particle optics appeared and it was clear that there is a different situation in the case of electron optics [21].

In 1936 Otto Scherzer published a statement about the unavoidability of the main axial aberrations [22]. This so-called Scherzer theorem, mainly related to the spherical and chromatic aberrations, proved that they could not be eliminated by an ingenious lens design. Scherzer derived positive definite expressions for corresponding aberration coefficients, meaning that typical rotationally symmetric electron optical lenses are always affected by severe aberrations.

This condition is very limiting. Even the assumed resolution derived from the electron wavelength was in practice at least 50 times worse [23].

Scherzer had made a number of entirely reasonable assumptions. The theorem is valid, namely for the static rotationally symmetric round lenses forming a real image of a real object, having no conductors on the axis, no discontinuities in the electrostatic potential distribution, and that the system is free of space charge and acts as a lens, not a mirror.

Scherzer's statement caused considerable skepticism in the scientific community because it was in a real contrast to their experiences with light optics dealing with this problem by using the correction elements with a negative aberration coefficient. Many leading scientists in the field of electron optics were not willing to accept Scherzer's theorem. They tried to find ways how to circumvent it. The great electron physicist of those years, Walter Glaser, spent many years finding a solution to overcome Scherzer's theorem. He found a field distribution eliminating the influence of spherical aberration [24]. However, it has been shown that such fields are not able to produce a real image of a real object [4].

In 1947, Otto Scherzer himself proposed several ways how to design an aberration-free electron optical system by abandoning one from the assumptions on which his statement reposed [3]. According to this article, the correcting actions could be achieved by several approaches. Many of these proposals were later used and refined during the designing of real correction systems [25].

Scherzer's paper studied cylindrical lenses for correction of chromatic aberration and discussed incorporation of octupoles very carefully in response to spherical aberration correction. The possibility to utilize space charge in the vicinity of the axis is also summarized, including introducing a charged foil. This idea was later developed by Scherzer and Gabor in other papers, presenting the concept of foil lenses (Scherzer) and placing an electrode on the axis of an electrostatic lens (Gabor). The last parts of the paper dealt with correcting action of the electron mirror and high-frequency lenses.

The first generation of correctors (called proof of principles) constructed up to the early 1990s, was not generally able to improve the optical properties of electron microscopes, because they were themselves the source of other significant aberrations. It was intended only to verify correction principles, but this valuable experience was used later in the development of modern functioning correctors.

The stigmator developed by James Hillier and Edward Ramberg in 1947 can be considered the first correcting element [26]. The real corrector based on multipole lenses was made by Scherzer's student Robert Seelinger only 4 years after Scherzer's revolutionary work. This first true experimental correction device, called the "astigmatic attachment," was able to clearly demonstrate the functionality of the electron beam correction principle, especially in the case of artificial enhancement of aberrations manifestation by wobbling [27].

After two years of hard work (1953), micrographs from a 25 kV microscope with a reduced spherical aberration were published by Seelinger. It showed a significant correction of spherical aberration, which was reduced to only 6 % of the original value. However, due to aberrations of the corrector itself, no resolution improvement was achieved with this device.

The corrected system with better resolution than the same uncorrected one was developed in 1956 by Gottfried Möllenstedt, who followed Seelinger's work. Thanks to the correction, seven times higher resolution was achieved than in case of uncorrected assembly. However, an aperture angle of an order of magnitude larger than a typical one had been used for increasing the influence of the spherical aberration and thus making correction easier and less sensitive [28].

During the following 50 years, there were several projects with the ambition to create a truly beneficial correcting system. It is especially worth mentioning the corrector for scanning electron microscopes consisting of quadrupole and octupole elements presented by J. H. M. Deltrap, which was capable of a correction of spherical and chromatic aberrations. However, Deltrap encountered complications in the form of difficulties with alignment due to the lack of automatic control procedures. Therefore, the corrector suffered from considerable instability, leading to a severe astigmatism [26].

Another important milestone was the work of Hardy in 1967, which described the design combining an electrostatic and electromagnetic corrector consisting of four quadrupoles and three octupoles. This solution has many similarities to currently used correctors for scanning electron microscopes.

Over the next few years, primarily technical solutions based on rotationally unsymmetrical fields of multipole lenses were developed. This was mainly due to the detailed study of Peter Hawkes published in 1965 on the issue of rotationally unsymmetrical lenses, more precisely multipole elements, and their aberrations.

Numerous experiments done up to the 1990s proved that aberration correction in electron optics is feasible. But it is a very complex issue requiring attention in many aspects. The most important groups working on this research were from Cambridge, Darmstadt, and Leningrad.

## 1.5. Aberration-corrected era

There were already several attempts and even successful projects to incorporate different types of correcting devices to microscope column in the first decade of new millennium. The detailed overview can be found in [29]. In fact, all the main electron microscope manufacturers had aberration-corrected systems in their portfolio. The following chapter will summarise an important attempts with various approaches of individual design groups. The projects especially worth mentioning are corrected microscopes developed by Hitachi [30], NION company [31][32], and FEI. On the other hand, none of them were optimized for operating with low voltage and therefore suitable for sensitive samples. The activities of CEOS company producing and developing different kinds of correctors for the world's leading producers of the microscopes will also be described.

### 1.5.1. CEOS

CEOS (Corrected Electron Optical Systems)]GmbH company was established by Max Haider and Joachim Zach in Heidelberg in 1996. The company was founded with the purpose of collaboration with the main microscope manufacturers as well as experimental projects such as the American project TEAM and the German projects SALVE and PICO. Their products were installed in various top-end TEM and STEM devices of many worldwide producers mentioned below. They participated in the development of the Sub-eV Sub-Angstrom Microscope (SESAM) and Sub-Angstrom Transmission Electron Microscope (SATEM) [33].

The brief review of CEOS correctors is listed in [34] with a summary of their parameters. Over time, CEOS developed four versions of hexapole corrector CETCOR, CESCOR, D-COR and the most advanced B-COR.

The basic CETCOR corrector is based on Rose's design. There is a transfer lens doublet transferring a coma-free plane of the objective lens, which is usually immersed in the objective field. The sequence continues by the system of two hexapoles separated by another transfer lens doublet. The correcting elements are attached to the rest of the microscope by the adaptor lens.

The CESCOR corrector is modified exclusively for STEM setup. It is possible to combine it with the basic CETCOR corrector to obtain a TEM/STEM versatile device [35].

For the needs of the TEAM project, many modifications were done resulting in a new version referred to as D-COR. The important improvement of the corrector compared to the previous one is the possibility of additional correction of the fifth-order spherical aberration and the six-fold astigmatism. On the other hand, even this semi-aplanatic corrector did not solve the problem of the off-axial anisotropic coma. The elimination of this influence is essential for obtaining a sufficiently large field of view [36].

To overcome the limitation of off-axial aberrations with the dominating effect of off-axial coma, CEOS developed a fully aplanatic B-COR with the sequence of three strong hexapoles separated by transfer doublets. The two weak hexapoles doublets are added to the above-mentioned hexapole triplet for correction of the azimuthal off-axial coma. This aplanatic hexapole-type CEOS  $C_S/B_3$ -corrector finally opened the door to a large aberration-free field of view. This novel corrector is able to eliminate the residual intrinsic six-fold astigmatism, correct for all parasitic fourth-order axial aberrations and, above all, solve generalized coma aberrations up to the third-order, including the azimuthal off-axial coma. A detailed description of the B-COR  $C_S/B_3$ -corrector and the experimental confirmation of feasibility of fully aplanatic imaging using conventional TEM has been demonstrated in [37].

### 1.5.2. Hitachi

Hitachi offered aberration-corrected microscopes called HD-2700 STEM and HF-3300 equipped by CEOS correctors to customers. Their instruments are exceptional due to the capabilities of the self-alignment system of the corrector based on continuous control of the corrector setting according to the Ronchigram pattern. This system is capable of very fast full-optics alignment of the  $C_S$  corrector [38].

### 1.5.3. NION

NION was founded by Ondrej Krivanek and Niklas Dellby in 1997 with the aim to become a developer of high-end scanning transmission electron microscopes (STEM) and other electron-optical instruments. In addition to participating in other R&D projects, they built and produce completely new aberration-corrected microscopes, Nion UltraSTEM™ 100 [32] and Nion UltraSTEM™ 200 equipped with an  $C_3/C_5$  aberration corrector [39][40].

Nion microscopes are able to operate with an accelerating voltage in the range of 40kV-200kV and even provide single-atom ultrahigh sub-angstrom resolution [41]. The above-mentioned corrector consists of 16 quadrupoles grouped into four quadruplets and three combined quadrupole-octupole elements. Despite the presence of the quadrupole-octupoles, Nion instruments are not designed for a correction of chromatic aberration. However, they are equipped with a monochromator primarily for analytical reasons.

### 1.5.4. JEOL

The company known as JEOL used a CEOS corrector, but they tried to do their own in-house research for some improvements. They pioneered the incorporation of two correctors to one microscope with the goal of obtaining a device corrected for both transmission modes i.e. TEM and STEM.

After a few years of development, JEOL managed to achieve a resolution of 47pm using the microscope R005 with built-in double asymmetric  $C_s$  correctors. The 47 pm-spaced dumbbell structure of germanium atomic rows was observed by this corrected electron microscope in HAADF-STEM regime. These correctors were based on CEOS design with some marginal modifications [42]. This impressive result was made possible due to a cold field emission source, electronically stabilized power supply and mechanically stabilized column.

From the perspective of this work, the endeavour to design a corrected microscope operating with an accelerating voltage of 30kV should be mentioned. The project was designated as Triple C, meaning  $C_s$  correction,  $C_c$  correction and expected applications in the investigation of carbon materials [43].

### 1.5.5. FEI

FEI, as well as other companies, incorporated an aberration corrector into their most advanced devices. Around the turn of the Millenium, there was an effort to develop an in-house corrector based on the combination of a crossed electrostatic and magnetic dipole field surrounded by two hexapoles. This corrector was intended to deal with both spherical and chromatic aberration.

In the end, FEI used  $C_s$  corrector manufactured by CEOS together with a monochromator [44]. This instrument clearly proved the advantages of the combination of spherical aberration correction and monochromatization.

In 2009, FEI delivered the first functional TEM device with the corrector of chromatic and spherical aberration to the University of California, Berkeley within a project called TEAM I. Unfortunately, the results did not meet expectations. It has shown that the improvement given by the correction of chromatic aberration resulting from theory was overestimated [45]. The reason for such behaviour was found by Uhlemann in parasitic

magnetic field noise<sup>1</sup> caused by thermally driven currents in the conductive materials used for manufacturing of electro-optical elements of the microscope and also the column itself [46].

Another FEI microscope, Titan, equipped by  $C_s/C_c$  corrector together with a monochromator was put into operation within the PICO project in Ernst-Ruska Centre in Jülich in 2011 [47]. This instrument was able to reach the resolution of 50pm with an accelerating voltage of 300kV in both TEM and STEM modes. The same resolution was achieved in TEM also for 200kV and, for a lowered accelerating voltage of 80 kV, it reached 80 pm [48].

### 1.5.6. Sub-Angstrom Low-Voltage Electron Microscope

The project of the Sub-Angstrom Low-Voltage Electron Microscope (SALVE) was launched at the University of Ulm in 2008 due to demand for a device enabling the study of radiation-sensitive samples due to the fact that the resolution in the micrographs is often limited by radiation damage rather than by the quality of the microscope itself. For this purpose, the research group led by Ute Kaiser developed an aberration-corrected electron microscope operating in the low-voltage range of 20–80 kV [9].

The first generation of the SALVE microscope was a Carl Zeiss Libra 200-based experimental platform corrected for spherical aberration (2009-2011) [49][45]. This initial phase of the SALVE project evaluated the feasibility of high-end low-voltage HRTEM. A great amount of attention was paid to the design of the accelerator and to the alignment of the field emission gun. Both were exclusively optimized for low voltage[50]. The SALVE I microscope itself was equipped with a hexapole  $C_s$ -corrector and a Schottky field emitter with an electrostatic omega monochromator. The limitations of the SALVE I microscope were thoroughly summarized in Uhlemann’s paper [51]. The first phase of the project proved that phase contrast imaging with an accelerating voltage of 20 kV is possible up to the limit given by the intrinsic six-fold astigmatism  $A_5 = 15$  nm.

The Salve I project was also intended to be a development phase for some advanced key components of the upcoming project SALVE II. Particularly, a new type of corrector based on quadrupoles and octupoles was designed. It allowed to extend the correction possibilities by chromatic aberration. It also led to the necessary redesigning of the microscope column.

The follow-up project SALVE II began in 2011 [52]. During this second development phase, the above-mentioned  $C_c/C_s$  - corrector was incorporated to the SALVE I microscope. The new corrector was based on the CEOS (Corrected Electron Optical Systems) TEAM corrector [53], which was originally optimized to provide ultra-high resolution and a large field of view at 300 kV [54]. Thus, the design modifications were necessary for optimal working at 20kV. The original TEAM corrector was shortened and simplified. The capabilities of the corrector were versatile. It corrected all axial aberrations, including up to the 5th order, with a remaining positive 5th order spherical aberration  $C_5$  for bright atom contrast. Off-axial aberrations, including up to the 3rd order, were also corrected. Both of these corrections were important for a large aberration-free field of view. Lastly, it corrected chromatic aberration  $C_C$  and related chromatic astigmatism. Furthermore, it was able to correct anisotropic magnification to eliminate any distortion [50].

---

<sup>1</sup>Johnson-Nyquist-noise

The SALVE II microscope had the ambition to be the first commercially available low-voltage corrected transmission electron microscope. But, due to a withdrawal of Carl Zeiss company from the TEM market, this goal was not fulfilled.

The SALVE II microscope started to deal with the less known phenomenon of the so-called Johnson-Nyquist-noise, which caused additional image spread. This problem of a high-end chromatically corrected microscope caused a substantial limitation of the atom contrast and required another modification of the corrector.

Despite incompletely fulfilled goals, the second phase of the SALVE project convincingly presented the fact that an aberration-corrected low-voltage transmission electron microscope was able to provide the images with a hitherto unseen resolution.

The basic platform was changed for the follow-up phase of the SALVE project. The third generation, SALVE III, was based on the FEI Titan Themis microscope equipped with a new quadrupole-octupole  $C_s/C_c$ -corrector developed and manufactured by CEOS for the SALVE II and was further improved for the needs of the latest SALVE generation.

## 2. LOW-VOLTAGE ELECTRON MICROSCOPY

*Hledat ty cesty to už samo o sobě je jaksi dobrodružství; nalézat je a realizovat to je další potěšení.*

— prof. Ing. Armin Delong

The following section is dedicated to a description of a low-voltage transmission electron microscope with special attention to its advantages and disadvantages. The special features of this instrument will be briefly summarized and compared with more common, conventional transmission electron microscopes.

The current market of scientific and laboratory instruments provides electron microscopes with extensively various instrumentation, capabilities, and accelerating energy. The most widespread transmission electron microscopes operate at an accelerating voltage of 50kV-300kV. This category is usually called conventional transmission electron microscopy. Such high beam energy gives specific properties to these devices that make them an uncommonly powerful investigative tool. But, on the contrary, it can also be very limiting for many possible applications, as will be described later.

The unique instruments with an accelerating voltage below 50kV are called Low Voltage Electron Microscopes (LVEM). The energy boundary is not strictly precise, but it is the result of the unofficial agreement, which is based on a relative influence of chromatic and spherical aberration. In addition, low particle energy technology can profit from its possibility of dimension reduction, because no bulky insulators are required.

This study pays special attention to low voltage microscopes, LVEM5 and LVEM25, produced by Delong Instruments co. These instruments are based on professor Delong's concept of an affordable, user-friendly low-voltage electron microscope that would equip every laboratory. The most important characteristics of both systems are listed below in the section (2.1).

LVEM5 is the only commercially produced benchtop electron microscope with astoundingly compact dimensions. LVEM5 operates with an accelerating voltage of approximately 5kV and it provides extraordinary versatility by integrating 4 imaging modes. Depending on the LVEM5 configuration, the user can easily alternate between operating the microscope as a Transmission Electron Microscope (TEM), Scanning Transmission Electron Microscope (STEM) and Scanning Electron Microscope (SEM). Additionally, it is even able to acquire Electron Diffraction data. Both surface and transmission images of the sample can be captured from the same area of interest. Despite having dimensions comparable to a light-optical microscope, it astonishes users with a resolution of 1,2nm in the TEM boost mode. The LVEM5 is primarily intended for imaging of nanoparticles, powders, nanotubes, bulk materials, unstained polymer sections, unstained biological sections, phages, and viruses. Low-beam energy is especially convenient for sensitive samples which would otherwise be damaged or even destroyed in a very short period of time.

LVEM25 is a design for slightly higher beam energy, ranging from 10keV to 25keV, depending on the activated mode. Its 3-in-1 investigative capabilities include 25keV transmission electron microscopy, scanning transmission electron microscopy in two beam energies 10keV and 15keV, and also electron diffraction. A higher accelerating voltage allows

one to investigate thicker samples, making sample preparation easier to process. The key application areas include pathology, virology, drug delivery research, and nanotechnology.

Its small dimensions allow for very easy installation of both devices in the laboratory with no special facilities requirements, no need for a dark room, or even a cooling water system. It is a design for a wide range of applications in material sciences, such as nanomaterials, polymers, as well as life sciences.

LVEM5 and LVEM25 instruments are shown below in the figure 2.1 to establish the idea of their dimensions.



Figure 2.1: The left side shows LVEM5. Its minimal dimensions are clear from the comparison with the operator's hand. The right picture is dedicated to complete workstation of LVEM25.

Both devices use a Schottky-type field emission gun with high brightness and spatial coherency. The small virtual source of this electron gun enables TEM and also STEM mode. The substantially lower accelerating voltage of both systems than the typical energy of conventional electron microscopes provides a significantly improved image contrast. This phenomenon is relevant especially for the samples composed of light elements. The relatively low energy of the particles used results in increased electron scattering and, therefore, enhanced image contrast. This makes low voltage systems particularly suitable for biological, organic and light materials samples with no need for additional contrast-enhancing procedures. The insufficient contrast of conventional systems is usually solved by selective staining by heavy metal atoms (Mo, W, Os, U) but this solution changes the original structure of the sample, which is then observed indirectly. Low accelerating energy enables the acquisition of high image contrast even with basically prepared samples without staining in their inherent natural conditions.

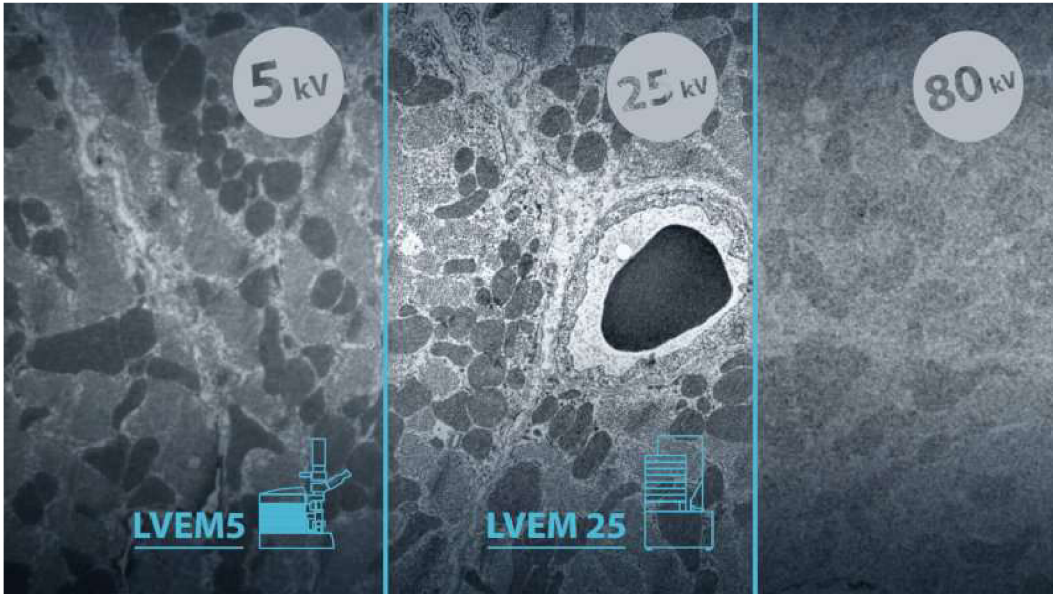


Figure 2.2: The comparison of contrast in the micrographs made by using different instruments of various accelerating energies. The contrast reduction due to the increase of electron energy is clearly visible, especially in the case of accelerating energy of 80keV (a typical energy for conventional transmission electron microscopes). The image is created to highlight the benefits of LVEM25. The contrast in micrographs prepared by LVEM5 is already effected by the thickness of the specimen.

The main columns of the common transmission electron microscopes are usually quite massive, due to the fact that they contain ordinary electromagnetic lenses made from coils that cannot be simply scaled down. All transmission electron microscopes developed by Delong Instruments are equipped with objective lens based on permanent magnet technology. This construction allows for a remarkably high level of miniaturization and enables operation without any cooling system, which is usually essential due to the considerable heat generated by the coils of electromagnetic lenses.

The first stage of LVEM5 and LVEM25 magnification is done by electron optics, which form the initial image on a fluorescent YAG screen. This scintillation crystal, processed to a flat surface plate with high optical homogeneity, converts the electron-optical image into the initial light image, which is further magnified by light optics with a selection of proper light objectives.

The volume of YAG activated by the electron passage is sufficiently small to take advantage of the resolving power of the following applied light magnifying optics. This high spatial resolution of the YAG screen is also a consequence of low electron energy. The higher energy of incident particles would lead to a bigger excite volume of YAG screen material and thus, lower spatial resolution.

Inline, two-stage optics of LVEMs begin by a Schottky-type electron source followed by a permanent magnet doublet. Its first gap is considered to be the condenser lens 1. Due to the inlens character of the immersion objective lens, the second gap, situated farther from the electron source, forms both condenser lens 2 by the pre-field and also objective lens by the part of the field following after the specimen.

Electrons then travel upwards through the projection system composed of one or two projection lens and continue towards to YAG screen.<sup>1</sup> The optical layout is presented in the following picture 2.3.

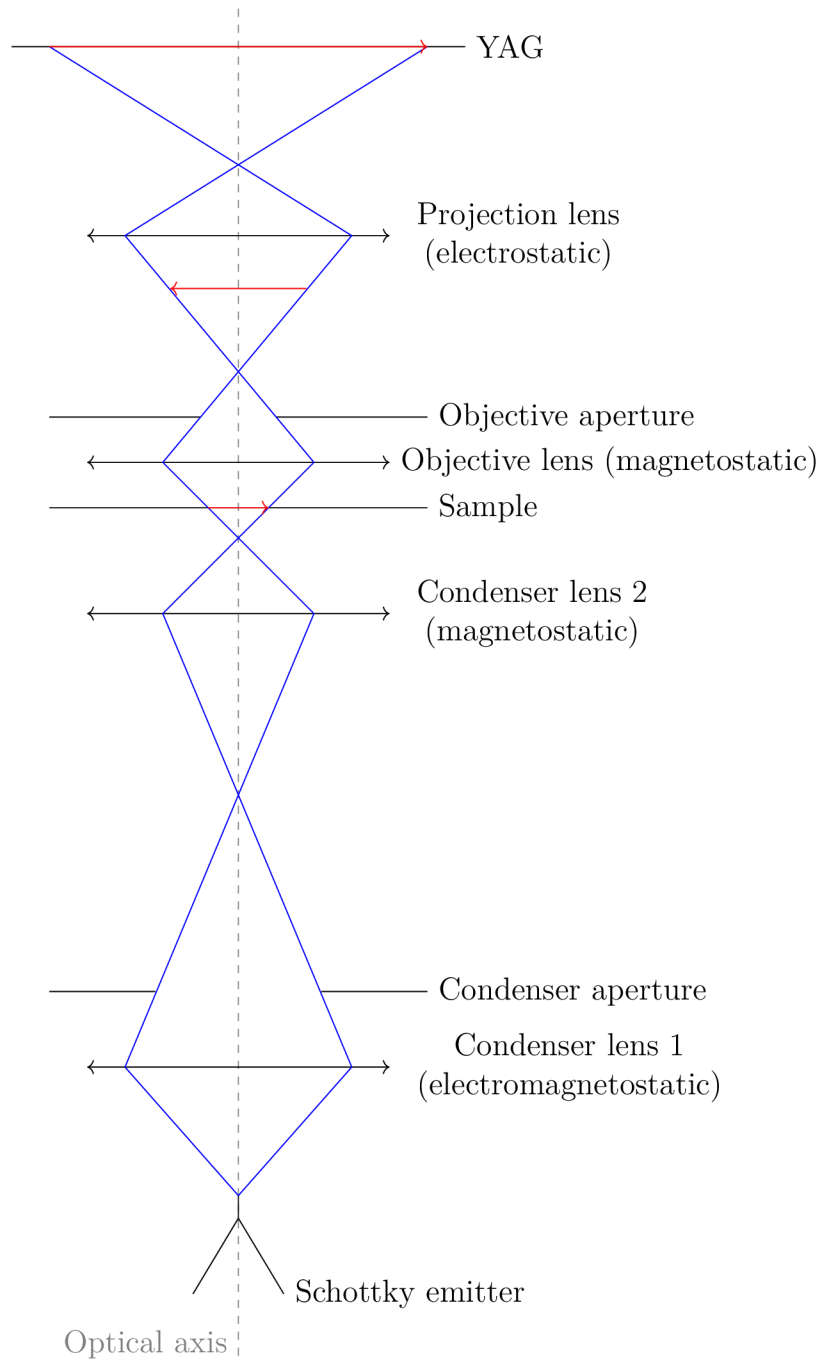


Figure 2.3: Schematic optical layout common to both devices, LVEM5 and LVEM25.

## 2.1. Parameters of current LVEM5 & LVEM25

The presented thesis pays special attention to the low voltage microscopes produced by Delong Instruments, co. The calculations were made using the parameters of devices

<sup>1</sup>One projection lens version is available only for LVEM5, TEM Basic

LVEM5 and LVEM25. For clarity, the important parameters, as specified by the manufacturer, are listed below.

Aberration coefficients of spherical and chromatic aberration, tabel 2.1, are especially relevant for the purpose of the feasibility study presented in the section 5. The aberration coefficients obtained by simulations were verified experimentally due to the resolution limits reached in practice.

Table 2.1: Relevant theoretically calculated spherical and chromatic aberration coefficients of the objective lenses belonging to the LVEM5 and LVEM25 [55] [56].

LVEM 5			
Mode	Accelerating voltage [kV]	$C_s$ [mm]	$C_c$ [mm]
TEM	5	0.64	0.89
STEM/SEM	5	0.64	0.89

LVEM 25			
Mode	Accelerating voltage [kV]	$C_s$ [mm]	$C_c$ [mm]
TEM	25	1.03	1.05
STEM	15	0.80	0.85
STEM	10	0.64	0.72

LVEMs offer to users different resolving power for each provided operating regime depending on accelerating voltage and/or hardware-based enhancement of TEM imaging mode in case of LVEM5.

Table 2.2: Declared experimental resolution limits of uncorrected LVEM5 and LVEM25 [55] [56].

LVEM 5	LVEM 5	LVEM 5	LVEM 25	LVEM 25	LVEM 25
5 keV	5 keV	5 keV	10 keV	15 keV	25 keV
TEM Basic	TEM Boost	STEM	STEM	STEM	TEM
2 [nm]	1.2 [nm]	2.5 [nm]	1 [nm]	1.3 [nm]	1[nm]

To complete the image of LVEM devices, the basic characteristics of every single electron optic elements are listed in the tables 2.3, 2.4 below. It can be seen that the main difference in the concept of both devices is in the additional electrostatic condenser lens in LVEM25 and its higher electron energy. This is enabled by larger dimensions of LVEM25, due to the fact that there is no space for this lens and unavoidably bulky insulators in miniaturized LVEM5. Thus the illumination is tuned exclusively by beam energy in the case of LVEM5.

Table 2.3: Summary of the most important features of a desktop transmission electron microscope LVEM5 [55].

Electron optics of LVEM5	
Condenser lens	magnetostatic
Condenser aperture	50 $\mu$ m, 30 $\mu$ m
Objective lens	magnetostatic
Objective aperture	50 $\mu$ m, 30 $\mu$ m
Electron source	Schottky cathode ZrO/W[100]

Table 2.4: Summary of the most important features of LVEM25 [56].

Electron optics of LVEM25	
Condenser lens	electrostatic & magnetostatic
Condenser aperture	50 $\mu$ m, 30 $\mu$ m
Objective lens	magnetostatic
Objective aperture	50 $\mu$ m, 30 $\mu$ m
Electron source	Schottky cathode ZrO/W[100]

# 3. METHODS OF ABERRATION CORRECTION

*Wird trotzdem eine Voraussage erwartet, so möchte ich rein gefühlmaßig den unrunder und den Hochfrequenzlinsen zutrauen, daß sie als erste eine Auflösung von einigen Angström erreichen, die für das Sichtbarwerden schwerer Atome genügen dürfte. Welches Verfahren jedoch als erstes an die durch die Wärmebewegung gegebene Grenze des nützlichen Auflösungsvermögens herzuführen wird, dürfte bei unsere heutigen Erfahrungen in keiner Weise zu prophezeien sein.*

— Otto Scherzer [3]

The aforementioned Scherzer theorem is valid for systems with rotationally symmetrical lenses, electrostatic or magnetic fields, and zero space charge. Violation of any of these parameters common to uncorrected electron optics can create an element with a negative spherical or chromatic aberration coefficient that is potentially usable as a corrector.

Otto Scherzer himself proposed several ways to perform correction of these unavoidable aberrations of rotationally symmetric electron lenses.

The following section is devoted to the brief description of the individual approaches to aberration correction. The basic technical solutions, advantages, and limitations of the main corrector types are summarized below.

To this day, the most successful and basically only commercially widely used correction systems are based on multipoles i.e. elements without rotational symmetry, whose aberration coefficients may be negative values, and thus serve to compensate the aberrations of other necessary rotationally symmetric electron lenses of the microscope.

Less common solutions such as electron mirror and potential on the axis will be mentioned only marginally.

This summary is not completely exhaustive but it contains the most interesting milestones according to the author's opinion.

Very detailed information about the relevant correction techniques is summarized in [57].

## 3.1. Multipole correctors

Multipole correctors can be defined as symmetric telescopic systems of multipoles and round lenses compensating for the aberrations of the commonly used round lenses. There are several multipole-based arrangements with different levels of complexity and capabilities. Individual technical solutions can be divided into two groups: hexapole and quadrupole-octupole correctors.

The first functional corrector compensating for spherical aberration of STEM was quadrupole-octupole based [58]. And, on the contrary, for the first TEM corrected imaging the hexapole type of a corrector was used [51].

Currently, multipole-based correctors are by far the most used type of correcting elements.

### 3.1.1. Hexapole corrector

As the title of this section suggests, employing hexapoles with an inherent negative spherical aberration is one of the possible technical solutions to design a spherical aberration corrector only. <sup>1</sup> Hexapoles, or in other words sextupoles, are optical elements with the arrangement of their pole pieces with sixfold symmetry, hence producing a field with threefold symmetry.

Before the advent of aberration correctors for electron microscopes, hexapoles had been used as stigmators for correction of a three-fold astigmatism.

The choice of this type of corrector is especially convenient due to its low complexity demands in comparison with the quadrupole-octupole corrector. The undoubted advantage is that the hexapole field does not alter paraxial trajectories in contrast to round lenses and quadrupoles, where the affection of a paraxial space is a natural feature. Hence, the paraxial trajectories are not affected by aberration contributions brought by the corrector itself and hexapoles do not even act as a focusing lens for them.

Another important technical aspect which was considered is the fact that, due to the absence of the axial field, hexapoles have significantly (2 orders) lower demands on power supply stability than octupoles.

For the correct interpretation of the principle of the hexapole action on the incoming electron, let us consider an electron moving parallel to the optical axis and entering the hexapole field at a distance of  $r_H$  from the axis. In case  $r_H$  is close to zero, i.e. electron traveling strictly in the very paraxial region, the electron does not experience any action given by the surrounding hexapole field and continues its journey unaffected. On the other hand, electrons with the initial distance from the axis significantly greater than zero  $|r_H| > 0$  are deflected from the original direction at a certain angle  $\alpha$ .

While in case of short hexapole there is only second-order deflection, if the extended hexapole field is employed, another third-order deviation appears. To explain and clear up the situation, let's consider two electrons. The first one enters the field in position  $r_H$  and the second one in position  $-r_H$ . One of them is driven into the area of a stronger hexapole field, while the second electron is deflected into the area of a weaker hexapole field. Hence, the Lorentz or electric force of one of them becomes stronger, while the force affecting the second one weakens. The longer the electrons are exposed to the hexapole field, the larger the difference between hexapole field action, which experiences each of them, is. This difference in the force action leads to the isotropic divergence corresponding to the negative spherical aberration [28]. The principles and comparison of short and thick hexapole actions are clear from the picture 3.1.

According to the proposals published by Crew and Kopf [59][60], using only one extended hexapole field is possible. But this minimal configuration is highly inconvenient. It does not provide the necessary flexibility to adjust the system in terms of side effects, such as manufacturing imperfections and mechanical misalignments. In addition, very strict conditions for a ray diagram need to be satisfied, because severe hexapole field aberrations have to be eliminated. If they are not satisfied while using a single hexapole setup, the desired effect of a negative spherical aberration comes at the expense of a large amount of mainly threefold astigmatism, which is the primary aberration induced by the hexapole field. Its impact would significantly deteriorate the image and cause the advantage of a spherical aberration correction to be completely irrelevant.

---

<sup>1</sup>Hexapole correctors are not capable of chromatic aberration correction.

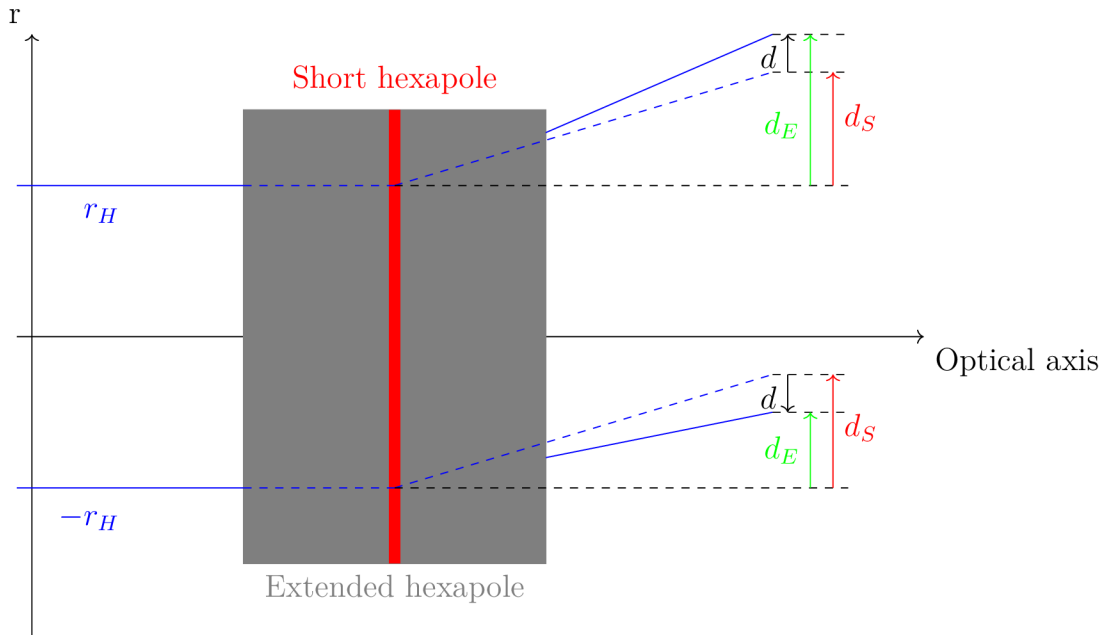


Figure 3.1: The comparison of effects of short (red) and extended (gray) hexapoles on two electrons with non-paraxial trajectories (Trajectories are colored by blue; dashed line belongs to the short hexapole and full line belongs to the extended hexapole.) entering the hexapole field at a distance from the optical axis  $r_H$  and  $-r_H$ . A third-order deviation  $d$  appears as a result of hexapole field variation along electron trajectories within the extended hexapole field. Electron trajectory deviation from the optical axis in case of a short hexapole is denoted  $d_S$  and in case of an extended hexapole field  $d_E$ .

Furthermore, besides the desired third-order spherical aberration, there are other secondary hexapole field aberrations, namely fourth-order three-lobe aberration and sixfold astigmatism, which have to be kept sufficiently small by the proper corrector setting. The detailed overview of aberrations belonging to the hexapole field is tabulated in the following table 4.1.

Table 3.1: The list of the geometrical aberrations up to the 5th order induced by hexapole field.

Important aberrations of a hexapole field				
Common name	Aberration coefficient	Multiplicity	Order n	
Threefold astigmatism	$A_2$	-3	2	
Third-order spherical aberration	$C_3$	0	3	
Third-order off-axial coma	$K_3$	0	3	
Third-order field curvature	$FC_3$	0	3	
Third-order field astigmatism	$FA_3$	0	3	
Third-order distortion	$D_3$	0	3	
Fourth-order three lobe aberration	$D_4$	$\pm 3$	4	
Off-axial star aberration	$C$	$\pm 3$	4	
Off-axial fourfold astigmatism	$C$	-3	4	
Fifth-order spherical aberration	$C_5$	0	5	
Fifth-order sixfold astigmatism	$A_5$	-6	5	

To annul the side effect of a primary hexapole aberration, a symmetry condition has to be introduced. In practice it means that a crossover must be formed in the symmetry center causing an inversion of magnification from  $M = 1$  to the opposite value  $M = -1$ . This setup guarantees that the action of the hexapole field is equal in two equivalent parts of the system with opposite magnification.

Due to the isotropic characteristic of the spherical aberration with azimuthal symmetry, its action does not change regardless of whether there is the inversion caused by crossover or not. On the contrary, threefold astigmatism with odd azimuthal symmetry is not invariant to the inversion and thus it can be fully compensated. Although the threefold astigmatism of the specific hexapole field remains the same along the whole hexapole field, in the second half of the corrector it alters the inverted triangularly distorted beam, thus annulling it. In other words, the triangular distortion which arises in the first half of the hexapole field can be fully compensated afterward by the astigmatism induced in the second half of the corrector. At the exit plane of the last hexapole field, the initially round beam is rotationally symmetric again and, furthermore, exhibits negative spherical aberration.

In case of the aforementioned single hexapole setup [59], the crossover has to be placed precisely in the middle of the extended hexapole field to satisfy this symmetry condition, which is hard to guarantee, thus different layouts are preferred [28].

The condition in which hexapoles have to be arranged to cancel out their primary axial second-order aberration, while the third-order effects are maintained, has led to various hexapole corrector designs. The simplest workable design of a hexapole-type corrector, which provides the above-mentioned characteristics, consisting of two hexapole stages separated by a pair of round lenses, creating a transfer lens doublet, is shown in the figure 3.2. This simple arrangement described in detail by Rose in 1990 [105] already guarantees that three-fold astigmatism is canceled out, whereas the negative contribution of a third-order spherical aberration of both hexapole units adds up. Furthermore, this concept involving a transfer lens doublet also warrants the disappearance of another aberration, specifically three-lobe aberration  $D_4$ , which is considered to be a secondary hexapole field aberration. Hence, the sixfold astigmatism  $A_5$ , i.e. ternary hexapole field aberration, does not vanish anymore.

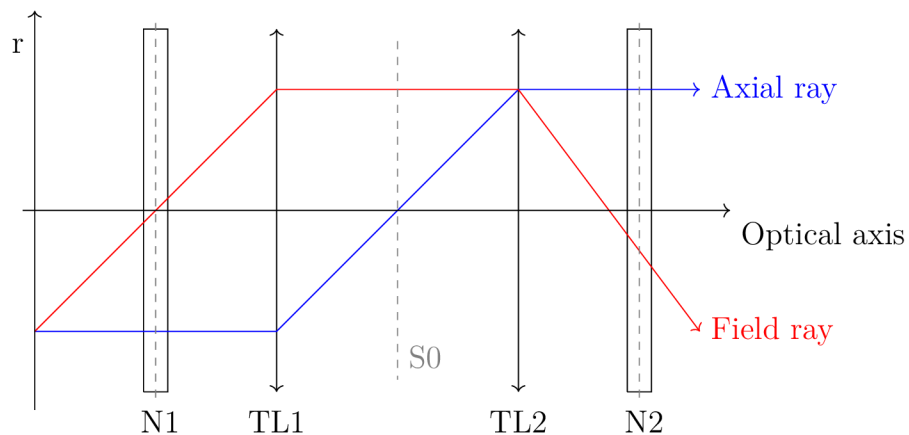


Figure 3.2: The arrangement of the optical element of the Rose hexapole corrector with depicted fundamental ray path. Minimal configuration consists of two transfer lenses TL1 and TL2 surrounded by hexapoles placed in planes N1 and N2.

The transfer lens doublet inserted between the hexapoles telescopically images the first hexapole to the position of the second one with a magnification of  $M = -1$  and thus ensures that threefold astigmatism vanishes. To meet this crucial condition the hexapoles must have the same azimuthal orientation.

Transfer lenses have to be excited in the opposite manner to deal with a beam rotation in their magnetic fields. The second transfer lens unrotates the parasitic rotation of the first one.

Within the optical arrangement of the entire microscope, the hexapole corrector is located according to the operation mode. Transmission electron mode (TEM) requires the presence of the corrector behind the objective lens. It is quite obvious that there is no need to correct the illumination beam, as it does not carry any information about the sample. On the contrary, scanning transmission mode (STEM) utilizes the corrector before the objective lens, due to the fact that the minimal spot size of the focused electron beam is crucial.

This aforementioned basic setup was later evolved by Rose in 1981 [61] and it has become the basis for all novel modifications of hexapole correctors [62].

In an extended modification, another transfer lens doublet can be additionally placed prior to the corrector itself to image a coma-free point of the objective into the center of the first hexapole. This full arrangement is shown in the figures (3.3), (3.4) for TEM and also in STEM configuration. However, the presented corrector concept consists of only one transfer lens doublet because it is intended to be for scanning transmission mode and thus the coma is not an issue, especially in LVEM5 and LVEM25.

To summarise the most important design aspects, the individual electron-optical components of the corrector must be placed according to clearly described rules. The two symmetric hexapole units (HEX1, HEX2) and telescopic 4f round-lens doublet in between are arranged in such way that the mid-plane of the first hexapole field has to be conjugated to the mid-plane of the second hexapole unit.

The hexapole doublet exhibits local double symmetry. The hexapole fields have to be symmetric with respect to the mid-plane between the transfer lenses S0 and also with respect to the mid-planes N1 and N2 of the hexapoles. While the transfer lens fields have to be anti-symmetric with respect to plane S0 [63].

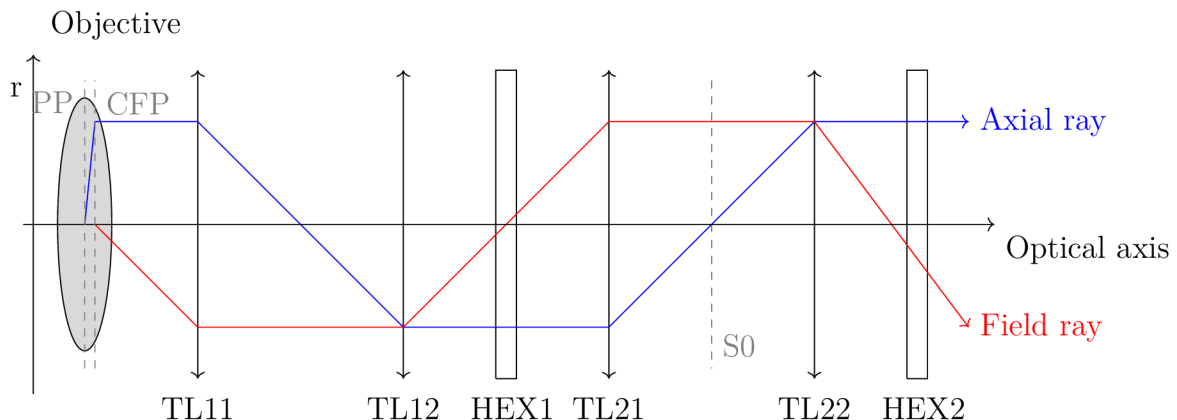


Figure 3.3: The full concept of TEM hexapole corrector situated behind the objective lens, consisting of two doublets of transfer lenses (TL11, TL12, TL21, TL22) and two hexapoles HEX1 and HEX2 [57].

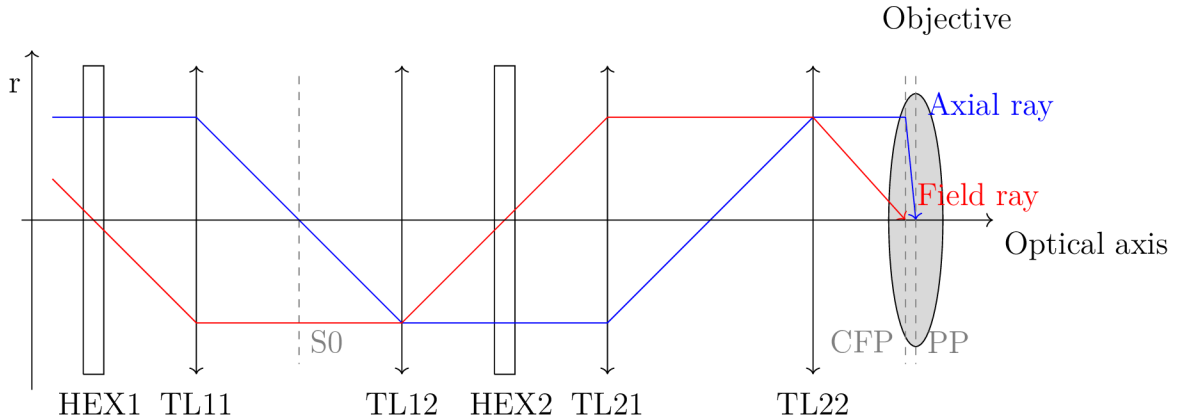


Figure 3.4: Full STEM (four transfer lenses and two hexapoles), concept dealing with coma is situated in front of the objective lens [28].

### 3.1.2. Quadrupole-octupole corrector

The more ambitious technical challenge is a corrector consisting of a combination of quadrupoles and octupoles. These designs often aim to construct achromatic aplanats. It is especially eye-catching due to the current trend in the development of instruments operating with low accelerating voltage. Decreasing of the electron energy leads to a heavy manifestation of chromatic aberration, which becomes a more serious problem. In this case, they have to employ a crossed magnetic and electric field, acting as a first-order Wien filter to deal with chromatic aberration.

The principle of the quadrupole-octupole corrector was invented by Deltrap in 1964. The quadrupole-octupole corrector of spherical and chromatic aberrations consists of 4 quadrupoles and 2 octupoles in a minimal configuration. However, arrangements with a different complexity have been published.

One of the possible arrangements published by Rose consists of at least 12 quadrupoles and 3 octupoles to compensate for spherical aberration and for the fourfold axial astigmatism introduced by the quadrupoles. This arrangement is organized to the two telescopic quadrupole sextuplets, each formed by two identical symmetric quadrupole triplets. Two octupoles are placed in the midplane of each quadrupole sextuplet. The third one compensating for fourfold axial astigmatism introduced by the quadrupoles is located behind the second adaptor lens [105].

Probably the most versatile corrector design to be published is a study of an ultracorrector presented by professor Harald Rose. This instrument is capable of compensating for the primary and secondary first-order chromatic aberrations, as well as all third-order geometrical aberrations. The ultracorrector is formed by two quadrupole septuplets, a total of 19 adjustable octupole fields, and twelve-pole elements for superposing quadrupole and octupole fields [64].

The double symmetry condition has to be employed to avoid twofold and fourfold third-order aberrations naturally introduced by the quadrupole-octupole corrector. The higher degree of symmetry is very convenient for cancelling out a higher number of aberrations. In general, the symmetric arrangements have more advantages because they can be more easily aligned precisely, more precisely than asymmetric ones.

The aforementioned concepts of quadrupole-octupole correctors clearly demonstrate the complexity of such instruments, which can be considered just for top-end state-of-art or experimental devices.

The vast majority of quadrupole-octupole corrector designs employ magnetic multipoles, due to the fact that they were intended for conventional or high-voltage electron microscopes, where an electrostatic solution is not feasible. Since the correction of low-voltage instruments was considered, the integration of the same electrostatic multipoles has become efficient.

The possibility of correction of chromatic aberration is an undisputed advantage of such systems, but the complexity of the multipole arrangement leads to some additional problems regarding mechanical alignment. Due to the higher number of multipole elements, the size of the complete device is inevitably significantly larger than in case of hexapole corrector. It would be negligible, though, when considering a conventional transmission microscope with a massive main column. It can, however, be important for smaller desktop LVEMs. The comparable size of the corrector and the main column can lead to some additional mechanical vibrations, which further deteriorate the final resolution. That is all due to the increase in the size of the microscope column.

## **3.2. Electron mirror**

An electrode with a sufficiently high negative potential placed in the path of an electron beam forms a so-called electron mirror. In this case of electrostatic mirrors, one of the basic conditions of Scherzer's theorem is violated. More precisely, mirrors change the sign of the velocity of the reference particle. Because of the fact that this condition is not exactly satisfied, it is possible to predict that the mirrors could have a correction ability.

In fact, mirrors are capable of correcting both spherical and chromatic aberration simultaneously. The resolution-limiting effect is therefore moved to the remaining higher-rank aberration. The equipotential planes of a negatively charged electrode create a potential barrier decelerating the electrons of the initial electron beam. The electron mirror causes a complete loss of kinetic energy of electrons in front of the negative electrode and their re-acceleration afterward to the reverse direction.

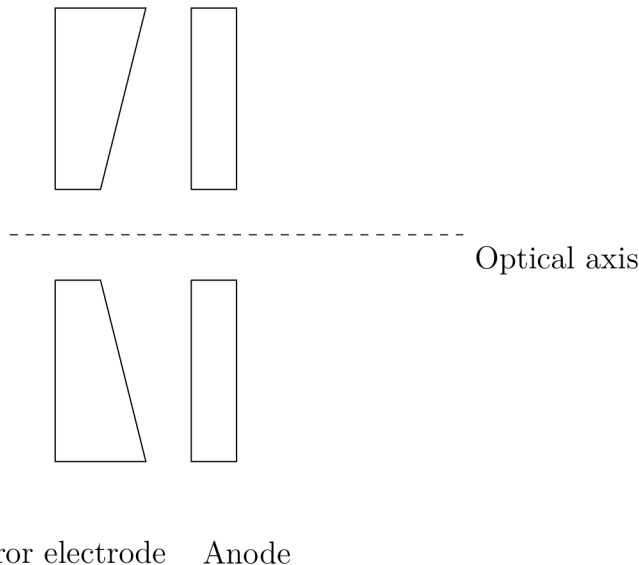


Figure 3.5: Electrodes arrangement of the electron mirror in the minimal configuration. Other electrodes can be placed between negative mirror electrode and anode i.e. negative mirror electrode and grounded anode. Extended configuration employing four electrodes in total (tetrode mirror) provides enough freedom to correct  $C_c$  and  $C_s$  at the same time.

Except negatively charged reflecting mirror electrode itself, the typical design of the electron mirror consists of a positive anode, typically at ground potential. There are openings on the optical axis in the both electrodes. The opening in the anode allows the electrons to enter and to leave the mirror field area between both electrodes. Another opening in the negative mirror electrode is used during an alignment procedure, when the electrons need to be allowed to pass through the mirror [65].

The electrodes of the mirrors suitable for aberration correction have to be shaped adequately with respect to the desired aberration coefficient with the opposite sign from those of objective lens. The converging hyperbolic mirrors pioneered by Rempfer are usually employed for this purpose [66]. In the minimal configuration called diode mirror, it consists of two above-mentioned electrodes. In this case all optical properties are fully determined by the mirror potential. In order to provide sufficient variability, the additional free parameters must be introduced. It can be done by the increasing number of electrodes. The tetrode mirror guarantees sufficient freedom to obtain independent adjustment of the optical properties in order to the simultaneous correction of spherical and chromatic aberration.

The physical principle of aberration correction taken by mirror corrector can be qualitatively explained by considering the fundamental difference between the focusing effect of transmission (electrostatic lens) and reflecting (electron mirror) optical element. At first, the attention will be paid to spherical aberration. In the case of well-known transmission mode the outer electrons traveling farther from the optical axis are under the influence of the focusing field for a longer time and also they encounter a higher part of the potential hill compared to electrons in the paraxial region. As a result, the lens focuses the electrons transiting the field in the outer parts of the beam to the shorter distance.

On the contrary, there is a different situation in the mirror mode. If the electrons can't surmount the potential barrier, the major source of positive spherical aberration resulting from the passage of the outer electrons through the higher potential barrier than the

paraxial electrons, disappears, because all the electrons of the beam are reflected from the same equipotential surface. In addition, outer electron spends less time in the field, because they travel a shorter distance to the specific equipotential surface than paraxial electrons. They are less affected by the focusing field and consequently the farther the rays are from the optical axis, the longer their focal distance. Such an optical behaviour leads to the opposite manifestation of spherical aberration and thus to its negative coefficient.

The behavior of the chromatic aberration can be explained in a similar way. The electrons with higher energy penetrate deeper into the mirror field and the focusing force acts longer time. The fact, that these electrons are under the influence of the field for a longer period of time, leads to a decrease in the focal distance with increasing energy. These optical properties refer to the the negative value of chromatic aberration coefficient.

The aberration correctors based on electron mirrors consist of three necessary important parts schematically depicted in the figure 3.6. Except for the above-mentioned electron mirror itself, there are magnetic beam separator and interface lens.

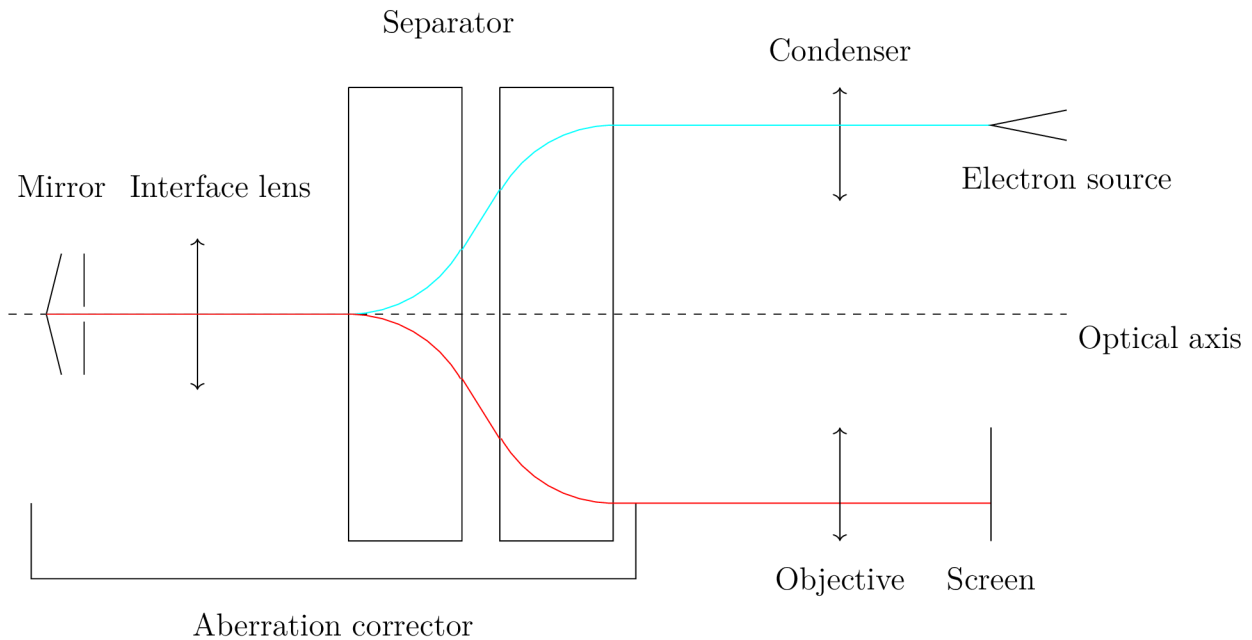


Figure 3.6: Schematic layout of the aberration-corrected optical assembly using the mirror corrector. Optical system capable to cancel both spherical and chromatic aberration consists of common optical elements of conventional electron microscope such as electron source, condenser and objective lens and projection system. Additionally, the assembly contains corrector with electron mirror, interface lens, and beam separator.

Despite the very promising optical properties, the practical realization of this kind of corrector was delayed because of problems with the design of necessary beam separator separating the beam heading toward the mirror and the beam returning back. Such a beam separator is unavoidable because the optical systems with electron mirror have not a single straight optical axis, but two collinear straight axes.

The separator has to be designed very carefully to avoid as much as possible the deteriorating effects of different kinds of electrical instabilities originating from current and voltage power supplies. Also, the intrinsic deflection aberrations of the separator have to be minimized.

The key component of the separator is the magnet with the direction of the magnetic field perpendicular to the plane defined by the optical axis of incoming and outgoing beams. Such an orientated magnetic field bending the beam to the one side with respect to the direction of the electron movement. It means that the trajectories of the electrons going through this magnetic field in approximately opposite directions are deflecting to the opposite sides. Thus the incident and returning beam are bending away from each other.

Another important element of the mirror corrected system is an interface lens located between a mirror and a beam separator. The interface lens has several different tasks. Its essential duty is to control and to create a balance between overcorrected aberrations introduced by the mirror and the undercorrected aberrations of the rest of the electron optical system. The aberration equilibrium is set by introducing its own aberrations together with its imaging and magnification action between the mirror and the objective lens. The interface lens is designed to have the desired value of chromatic aberration to create the proper balance. Typically chromatic aberration added by electron mirror is much greater compared to the chromatic aberration of the objective lens which is needed to be corrected. Such a case is referred in [65]. On the other hand, there are devices, such as photoelectron microscopes and other emission microscopes, where the rest of the optical system is responsible for a high chromatic aberration, the contribution of which is comparable to the chromatic aberration of the mirror. In these cases, the full correction action of the electron mirror is needed. Thus the interface lens must be tailored according to the special needs of every single device.

Although electron microscopes with aberration corrector based on electron mirrors have been proposed, but the need for a separator free of the significant deleterious resolution-limiting effect is still the major obstacle to the integration of this kind of correcting devices into real electron-optical systems.

The first ambitious effort to build a microscope equipped by a mirror corrector was an energy-filtered LEEM/PEEM instrument called SMART. The LEEM device seems to be a natural choice for the incorporation of this kind of corrector because separator is needed anyway.

Another novel design of  $C_C$  and  $C_3$  corrected low voltage electron microscope (LEEM) combined with a photoelectron emission microscope (PEEM) was presented by Tromp. His instrument with integral in-line energy filter and double dispersive prism reached the spatial resolution below 2 nm. The magnetic prism arrays deflect the beam to the perpendicular directions twice and then return the beam to the direction of the main optical column. The intrinsic symmetry of Tromp's design helped to develop a straightforward alignment procedure which makes this device user-friendly and highly reliable [67].

### 3.3. Potential on the axis

There is a broad group of techniques using electric potential on the axis to correct for spherical and chromatic aberration. Although insertion of an electric charge into the path of electron beam can be beneficial to compensate for above-mentioned aberrations of the common electron lenses, these techniques are not significantly widespread. There are several different concepts, some of them even exotic enough, of keeping and maintaining the electric charge in the right position. Thus only the most important attempts will

be summarized in the following section. Particularly correction abilities of space charge cloud, foil lenses and conductors on the axis are discussed.

### 3.3.1. Aberration correction by space charge cloud

Space charge cloud with appropriate distribution can be considered as another possible correction technique. The most convenient space charge potential for this purpose is created by electron density increasing quadratically with off-axial distance. Although it seems to be very promising principle allowing to design spherical aberration free lenses, there are severe problems with maintaining a space charge cloud in the required position. Only stationary state can guarantee to prevent the frosted-glass effect blurring out some parts of the image.

A Challenging task how to create suitable radial space charge distribution was thoroughly investigated by Gabor [68] and Scherzer [3] himself very early after publishing already-mentioned Scherzer's theorem. Also experimental studies were done by Ash [70], Ash & Gabor [69]. It is also worth mentioning the experiments performed by Haufe [71] and Le Poole [72]. Haufe designed a special short lens which produced a thin and rotationally symmetric space charge area perpendicular to the axis with sufficient stability. Haufe achieved the partial correction of electron lenses placed beyond his corrector, but the areas outside the central zone suffered by insufficient variation of density distribution preventing complete correction of the of the entire cross-section of the beam.

Le Poole chose a completely different approach. Very slow electrons were injected into axial area of the long magnetic lens, where they precess along the field and thus they generate space charge cloud used to aberration correction.

Detailed theoretical studies about aberrations in presence of space charge cloud were published in 1950s and 1960s especially by Typke, who derived expression for corresponding spherical aberration coefficient.

### 3.3.2. Foil lenses

The question of holding the electric charge in required regions has to be answered before we consider the aberrations themselves. Natural solution of maintenance of electric charge in required region seems to be insertion of a very thin charged foil into the beam path. Despite the fact that this method provides a very convenient way how to guarantee necessary spatial distribution, the additional beam deteriorations may be created by the presence of the foil itself. The undesirable interaction between electrons and foil can cause much more harm than good.

Due to the absence of suitable non-scattering foils, the attention was focused on fine gauze instead. Although the fine gauze causes unavoidable discontinuities and thus, the detailed calculations showed that these perturbations can be tolerated and reduced by ingenious design. This field perturbation can be approximated by the microlens set created by meshes of the gauze. It was proved that better results can be obtained by placing several gauzes in a row or single superconducting gauze.

Thorough fundamental works were presented by Bernard [73] [74] [75], Seman [76], Verster [77] and Rus [78].

According to the research at University in Nagoya done by Maruse and Inchihashi, the supporting conducting grid or specimen itself can be used to avoid undesirable effects

of scattering in the additional foil. Especially the articles [79], [80], [81] worth to be mentioned.

### 3.3.3. Axial Conductors

The conductors located in the axial region of the corrected lens are another obvious and natural choice how to preserve an electric charge in specific areas to compensate for spherical and chromatic aberration. In contrast to the above-mentioned concepts, there is an evident disadvantage that the axial area is blocked by the conductors. The paraxial electrons are shaded and thereby excluded from the image-forming process hence the electron beam is shaped to a hollow cone.

The different designs with single or multiple conductors carrying an electric current were analyzed in detail. Early proposals had many disadvantages, they involved the use of special off-axis lenses or required the insertion of a corrector directly into the objective gap.

Khursheed and Ang presented a theoretical study of the on-axis electrode corrector capable of correcting spherical and chromatic aberration in 2015 [83]. Compared to the previous proposals their design was exceptional because it required only minimal modifications of the microscope column. Especially the most critical parts of the microscope did not need to be changed. Their design is intended to be for helium ion microscope, focused ion beam columns, high voltage electron beam lithography instruments, and last but not least scanning transmission electron microscopes.

Corrector consists of two units replacing conventional scanning electron or ion microscope's final hole-aperture. Both individual units had different purposes. The first one correcting for a spherical aberration can be based on both electric or magnetic field. In case of electric field, the unit has a similar structure as a coaxial cable with a central wire-electrode on a zero potential. The magnetic alternative using on-axis conductor carrying electric current and thus generating magnetic field according to the Amper's law.

The following unit responsible for chromatic aberration correction superimposes electric and magnetic. The direction of the electric force component is radially outwards while magnetic force component points inwards. Such an arrangement guarantees exactly opposite action on electrons with different energies than it is common for conventional electron lenses. The electrons with higher energy are more attracted inwards and on the other hand, the less energetic electrons will be affected by radial outwards force.

Although this concept seems to be promising it should be pointed out that reaching necessary excitation for chromatic aberration correction will be difficult in practice to avoid overheating of the central wire and it must be compensated by the elongation of the entire corrector.

Another concept was introduced by Tadahiro Kawasaki and his coworkers.[84] They proposed novel simple  $C_s$  corrector with an axially symmetric electrostatic field between annular and circular electrodes called ACE corrector (annular and circular electrodes corrector). The electrostatic field created by ACE corrector behaves like a combination of convex and concave lenses, hence the spherical aberration coefficient of such a compound lens is negative and it can compensate for spherical aberration of the following objective lens.

The circular electrode was fabricated in a standard way by photolithography as it is common for conventional apertures. Due to very fine structure of connecting bridges be-

tween the central obstacle disk and the outer base plate focused ion beam (FIB) technique had to be employed for manufacturing of annular electrode. Fig.3.7

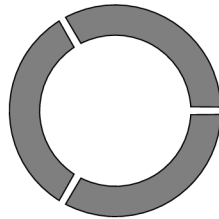


Figure 3.7: The chart of an annular electrode which is used in ACE corrector. The achieved width and thickness of three tiny connecting bridges were  $1.5 \mu\text{m}$  and less than  $3 \mu\text{m}$ . The aperture hole is represented by the gray areas.

### 3.4. High-Frequency Lenses

The possibility of solving an aberration problem by the time-varying field was examined firstly by Nesslinger in 1939. He studied the behaviour of a simple einzel lens with a central electrode connected to a high-frequency power supply. The principle of spherical aberration correction done by high-frequency lenses is based on illuminating the lens with time-varying field by the chopped electron beam and synchronizing these pulses with the phase of the lens potential.

The outer electrons travel a little bit longer time than paraxial electrons and the phase of the lens field has to be synchronized in such a way that the electrons encounter with decreased focusing field in the adequate phase of the cycle. The frequency required to modify the potential of the central electrode has to be in the gigahertz range.

The most complete study of high-frequency lenses was provided by Oldfield (1976) [82].

# 4. ABERRATIONS

*Life is like riding a bicycle. To keep your balance, you must keep moving.*  
— Albert Einstein

The following chapter is dedicated to the description of the basic types of aberrations with a crucial impact on the final image on the screen and resolution of the electron microscope. Aberration correctors are usually able to compensate only some of the primary aberrations, rarely secondary aberrations. Therefore the emphasis will be stressed on aberrations of lower order with a dominant effect.

Aberration theory is a very complex part of the charged particle optics. Therefore only the brief summing up is presented in this thesis. A more detailed comprehensive aberration description and derivation of aberration coefficients can be found, for example, in [16] and [27] or in fundamental articles [85] and [86].

The action of common electron-optics elements on electron's trajectories performs linear behaviour described by Gaussian optics. Any perturbations from this linear behaviour are geometric aberrations. In other words, aberrations can be understood as a deviation of a real electron trajectory from its paraxial approximation. Their effects are characterized by aberration coefficients.

The dominant linear behavior may be perturbed also by other effects except for the aforementioned geometric aberrations. The focusing power of deflecting elements is sensitive to any energy variation. The optical consequences of this energy distribution of electrons in the incident beam are described by the chromatic aberration.

Other defects associated with mechanical and electrical imperfections, inhomogeneity of magnetic material of pole pieces, inaccurate alignment of the lens arrangement are collectively referred to as parasitic or mechanical aberrations. Parasitic aberrations can be also characterized by coefficients, but these defects are usually not considered in aberrations evaluation, because they are different for every single piece of manufactured instrument and they are not even constant with time.

The situation with the aberration coefficient notation is often confusing. Many forms of classification systems have been evolved. To clarify and avoid obfuscation the overview table of the most important aberrations is attached.

Table 4.1: The list of the most important aberrations with corresponding coefficients according to the different notations [87] [88].

Aberration coefficient notation			
Aberration name	Krivanek	Uhlemann & Haider	Sawada
Image shift	$C_{0,1}$	$A_0$	
Two fold astigmatism	$C_{1,2}$	$A_1$	$A_2$
Defocus	$C_{1,0}$	$C_1$	$O_2$
Three fold astigmatism	$C_{2,3}$	$A_2$	$A_3$
(Second-order) Axial coma	$\frac{1}{3}C_{2,1}$	$B_2$	$P_3$
Four fold astigmatism	$C_{3,4}$	$A_3$	$A_4$
(Third-order) Axial star aberration	$\frac{1}{4}C_{3,2}$	$S_3$	$Q_4$
Spherical aberration	$C_{3,0}$	$C_3 = C_S$	$O_4$
Five fold astigmatism	$C_{4,5}$	$A_4$	$A_5$
Fourth order axial coma	$\frac{1}{5}C_{4,1}$	$B_4$	$P_5$
Four-order three lobe aberration	$\frac{1}{5}C_{4,3}$	$D_4$	$R_5$
Six fold astigmatism	$C_{5,6}$	$A_5$	$A_6$
Fifth order rosette aberration	$\frac{1}{6}C_{5,4}$	$R_5$	
Fifth order axial star aberration	$\frac{1}{6}C_{5,2}$	$S_5$	$Q_6$
Fifth order spherical aberration	$C_{5,0}$	$C_5$	$O_6$
Seven fold astigmatism	$C_{6,7}$	$A_6$	$A_7$
Sixth order axial coma	$\frac{1}{7}C_{6,1}$	$B_6$	$P_7$
Sixth order three lobe aberration	$\frac{1}{7}C_{6,3}$	$D_6$	$R_7$
Sixth order pentacle aberration	$\frac{1}{7}C_{6,5}$	$F_6$	
Eight fold astigmatism	$C_{7,8}$	$A_7$	$A_8$
Seventh order hexagon (chaplet) aberration	$\frac{1}{8}C_{7,6}$	$G_7$	
Seventh order rosette aberration	$\frac{1}{8}C_{7,4}$	$R_7$	
Seventh order star aberration	$\frac{1}{8}C_{7,2}$	$S_7$	$Q_8$
Seventh order spherical aberration	$C_{7,0}$	$C_7$	$O_8$

Although aberrations can be derived for a general electron-optical system, only some special cases are relevant in practice. The most important particular case are aberrations of a round lenses, because rotationally symmetric lenses are the elementary building blocks of a standard electron microscope.

There are five cardinal isotropic aberrations of third order in lenses with rotational symmetry: spherical aberration, astigmatism, field curvature, distortion and coma. And furthermore there are another three anisotropic aberrations: anisotropic coma, anisotropic astigmatism, and anisotropic distortion.

The total deviation  $\Delta u_i$  of the paraxial trajectory from the real trajectory, i.e. trajectory affected by geometric aberrations of third order, is: [27]

$$\begin{aligned}
 \Delta u_i = & Cr_a^2 u_a \text{ (Spherical aberration)} \\
 & + 2(K + ik)r_a^2 u_0 + (K + ik)u_a^2 u_0^* \text{ (Coma)} \\
 & + (A + ia)u_0^2 u_a^* \text{ (Astigmatism)} \\
 & + Fr_0^2 u_a \text{ (Field curvature)} \\
 & + (D + id)r_0^2 u_0 \text{ (Distortion)}
 \end{aligned} \tag{4.0.1}$$

The primary third-order spherical aberration and primary chromatic aberration are the most crucial aberrations severely determining the resolution of electron microscope. Thus these aberrations will be discussed in more detail.

## 4.1. Spherical aberration

A spherical aberration can be understood as a consequence of the fact that the lenses differently affect the trajectories of electrons at different radial distances from the optical axis. It is the aberration of the greatest importance for objective lens and thus also for the whole optical assembly of a conventional transmission electron microscope itself.

Considering the ideal aberration-free system, the image of a point source would be a point in the image plane. In reality, if the beam is confined by an aperture, every single Gaussian image point is blurred into an aberration figure due to spherical aberration. Furthermore, if the beam is confined by a circular aperture typical for electron microscopes, an aberration figure is an aberration disc of a circular shape respecting the shape of the aperture.

The spherical aberration coefficient  $C_S$  is routinely used to description of primary spherical aberration. Its typical value, in case of an objective lens, is in range of 0.5–2mm [89]. For the optimized microscope designs, it is usually in a good agreement that the value of the objective  $C_S$  coefficient is approximately equal to the focal length of the objective lens itself.

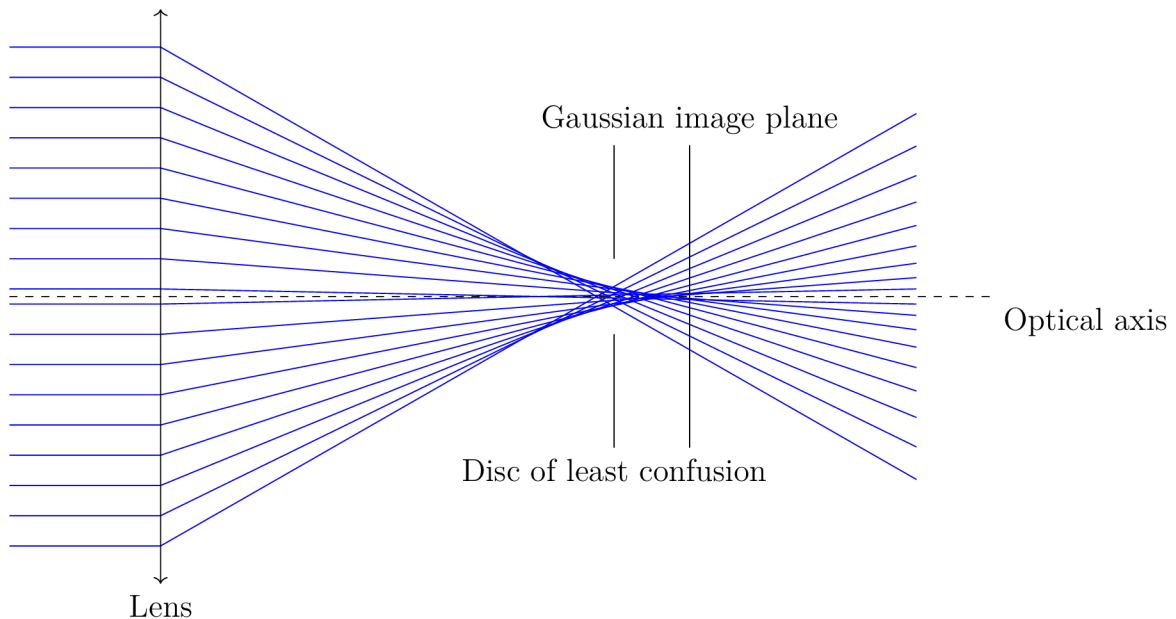


Figure 4.1: The pencil of rays affected by the spherical aberration. Rays with different radial distance from the axis in the aperture plane are refracted to the different focal points corresponding to every single ray with the particular distance of the ray in the aperture plane. The aperture plane is associated with the lens in this figure.

To give an exact and clear interpretation of the principle of spherical aberration origin, it is necessary to employ mathematical description of an object point source imaging. The

pencil of rays from some object point with coordinates  $(x_o, y_o)$  intersects the image plane at points  $(x_i, y_i)$ :

$$\begin{aligned} x_i &= M[x_o + Cx_a(x_a^2 + y_a^2)] \\ y_i &= M[y_o + Cy_a(x_a^2 + y_a^2)]. \end{aligned} \quad (4.1.1)$$

This set of points replace Gaussian projection from  $(x_o, y_o)$  to the single point  $(Mx_o, My_o)$ , where M is magnification, and hence it forms aberration figure, where  $(x_a, y_a)$  are coordinates of the ray in the aperture plane [16]. In case of circular aperture with radius  $R_A^2$ , defined as:

$$x_a^2 + y_a^2 \leq R_A^2, \quad (4.1.2)$$

a circular aberration figure is created as mentioned before.

The deviation of electrons from one object point from the paraxial trajectory can be compactly expressed by a complex number:

$$\Delta u_s = \Delta x_i + i\Delta y_i = MCx_a(x_a^2 + y_a^2) + MCy_a(x_a^2 + y_a^2)i, \quad (4.1.3)$$

The size of the aberration disc created by considered electron beam is obviously given by the absolute value of this complex number  $u_s$

$$\begin{aligned} |\Delta u_s| &= \sqrt{\Delta x_i^2 + \Delta y_i^2} \\ &= \sqrt{M^2C^2x_a^2(x_a^2 + y_a^2)^2 + M^2C^2y_a^2(x_a^2 + y_a^2)^2} \\ &= MCr_a^2\sqrt{(x_a^2 + y_a^2)^2}. \end{aligned} \quad (4.1.4)$$

From the last formula, it is clear that the rays passing furthest from the optical axis as allowed by the aperture determine the radius of the spherical aberration disc. Considering the most extreme marginal trajectories coming from an axial object, which intersect the aperture plane at the edge of the circular aperture, they form the image with radius  $|\Delta u_{si}|$ :

$$|\Delta u_{si}| = MCr_A^3. \quad (4.1.5)$$

It is usually more convenient to modify these equations in the sense of the expressions depending on coordinates of the object point and the angle between trajectory and optical axis in the object plane. Two distinctive paraxial trajectories  $s(z)$  and  $t(z)$ , given by coordinates in object and aperture planes, will be employed to specify the points of an arbitrary trajectory.

$$\begin{aligned} s(z_o) &= 1, & s(z_a) &= 0 \\ t(z_o) &= 0, & t(z_a) &= 1 \end{aligned} \quad (4.1.6)$$

Any other electron trajectory can be written as a linear combination of above-mentioned base trajectories.

$$\begin{aligned} x &= x_o s(z) + x_a t(z) \\ y &= y_o s(z) + y_a t(z) \end{aligned} \quad (4.1.7)$$

The angle between electron trajectory and optical axis is characterized by the slope of trajectory tangent line in the object plane.

$$\begin{aligned}x'_o &= x_o s'_o + x_a t'_o \\ y'_o &= y_o s'_o + y_a t'_o\end{aligned}\tag{4.1.8}$$

From the equation (4.1.3), the components of the spherical aberration can be written in the form:

$$\begin{aligned}\Delta x_i &= \frac{C}{t'_o{}^3} x'_o (x'^2_o + y'^2_o) + \dots = C_s x'_o (x'^2_o + y'^2_o) + \dots \\ \Delta y_i &= \frac{C}{t'_o{}^3} y'_o (x'^2_o + y'^2_o) + \dots = C_s y'_o (x'^2_o + y'^2_o) + \dots\end{aligned}\tag{4.1.9}$$

Thus the routinely used coefficient  $C_s$  of the primary third-order spherical aberration is established.[16]

#### 4.1.1. Plane with minimal spherical aberration disc

From point of view of optimization of a real instrument for minimal spherical aberration, there is undoubtedly an interesting question, where the plane with the smallest caustic radius can be found. In this section, the system affected exclusively by spherical aberration will be considered.

It is clear that the aforementioned plane of interest will be located somewhere between the Gauss image plane and the plane of intersection of the most extreme marginal rays. This plane is usually called the plane of marginal focus. Due to the axial symmetry of the electron optics, the whole task can be simplified to a planar problem, let's say in the plane  $xz$

The ray coordinate in general plane  $x(z_i - \Delta z)$  at distance  $\Delta z$  from the Gaussian image plane located in  $z_i$ , can be written:

$$x(z_i - \Delta z) = x_a t(z_i - \Delta z) + MC x_a r_a^2 \approx -x_a t'_i \Delta z + MC x_a r_a^2\tag{4.1.10}$$

In case of marginal trajectory<sup>1</sup>:

$$x_A(z_i - \Delta z) = -x_A t'_i \Delta z + MC x_A r_A^2\tag{4.1.11}$$

These two rays are equidistant from the axis in some plane, leading to the equation:

$$-x_a t'_i \Delta z + MC x_a r_a^2 = -x_A t'_i \Delta z + MC x_A r_A^2.\tag{4.1.12}$$

Due to the transformation to the planar problem,  $x_a$  resp.  $x_A$  can be written instead of  $r_a$  resp.  $r_A$ . Therefore the distance from the Gaussian image plane can be expressed by simplification:

$$\Delta z = \frac{MC(x_A^2 + x_a x_A + x_a^2)}{t'_i}.\tag{4.1.13}$$

---

<sup>1</sup>Marginal ray is the outermost ray in the aperture plane. It touches the edge of the aperture stop of the system.

Going back to the expression for a position in the general plane (4.1.10) and using the result (4.1.13), the following equation will be obtained:

$$x(z_i - \Delta z) = -MC(x_a + x_A)x_ax_A = -MCx_A - MCx_A^2x_a. \quad (4.1.14)$$

To reveal a plane with minimal size of aberration disc, the minimum of the previous function has to be found.

$$\frac{dx(z_i - \Delta z)}{dx_a} = 0 \quad (4.1.15)$$

$$\begin{aligned} -2MCx_ax_A - MCx_A^2 &= 0 \\ x_a &= -\frac{x_A}{2} \end{aligned} \quad (4.1.16)$$

To investigate the function minimum the derivation has to be performed and the relevant equation has to be solved. The second ray forms the envelope of the caustic in the plane of the minimal aberration disc is defined by the coordinates  $x_a = -\frac{x_A}{2}$  in the aperture plane. The minus sign indicates the fact that the marginal ray has already crossed the optical axis and its x-coordinate has the opposite sign than the ray found above.

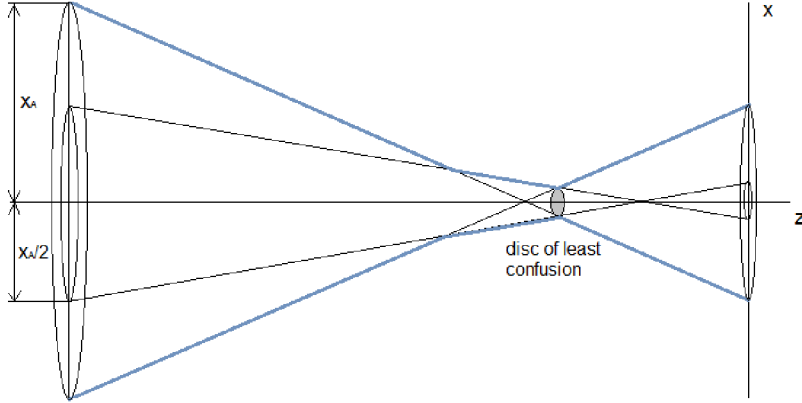


Figure 4.2: Diagram of two considered rays with maximal and half distance from the optical axis to the aperture in the aperture plane. The double cone shape of the beam envelope is marked by blue color. In reality all trajectories with the initial distance from the optical axis in the aperture plane  $r < r_A$  form smooth beam envelope with minimal radius given by the equation (4.1.17).

The smallest radius of an image of a point object, considering exclusively the effect of spherical aberration, will be found by using previous result in combination with the equation (4.1.13):

$$\Delta z_{min} = MC \frac{(x_A^2 + \frac{x_A^2}{2} + \frac{x_A^2}{4})}{t'_i} = \frac{3}{4} \frac{MC}{t'_i} x_A^2 \quad (4.1.17)$$

Thus the plane with minimal spherical aberration disc has been found at distance  $\Delta z_{min}$  from the Gaussian image plane. The radius of aberration disc is than written as:

$$|\Delta u_{s,min}| = x(z_i - \Delta z_{min}) = \frac{1}{4} MC x_A^3. \quad (4.1.18)$$

Considering exclusively the effect of the spherical aberration, it corresponds to the smallest spot achievable by electron beam focusing through the entire optical projection done by the investigated lens. This area is called *disc of least confusion* associating with the smallest image blurring possible. Its position relative to the distance between the Gaussian image plane and the plane of marginal focus  $\Delta z = z_G$  is given by the equation:

$$\Delta z_{min} = \frac{3}{4}z_G. \quad (4.1.19)$$

It can be summarized, that the disc of least confusion is located in a plane three-quarters of the distance from the Gaussian image plane to the marginal focus [16].

It should be noted that optimum strictly neglects other influences. In real systems, the best image will not be created in the plane found by equation (4.1.19), but rather closer to the Gaussian image plane.

The spatial distribution of electron beam density plays a decisive role in this issue. Due to the fact that the electron beam density is the highest in the paraxial region focused near the Gaussian image plane, the image will be the sharpest just near this plane. Unfortunately, the image contrast will be low in this plane due to the electrons with non-paraxial trajectories, which may generally have a high spherical aberration.

On the other hand, the high contrast can be observed in the plane defined by the disc of least confusion. However the majority of paraxial rays is not focused perfectly in this plane and they occupy a larger area, hence the resolution provided in this plane would be worse.

#### 4.1.2. Dependence of the spherical aberration on aperture

For practical calculations, it is usually useful to express the spherical aberration as a function of the aperture angle  $\alpha$ . Under the term aperture angle we will consider the angle between the marginal ray and optical axis of the system as it is shown in the figure 4.3. This angle is often referred to as the semi-aperture angle. Such terminology is reasonable because, from a physical point of view, the important parameter is the angular deviation of the ray from the optical axis, due to the proper definition of the paraxial space.

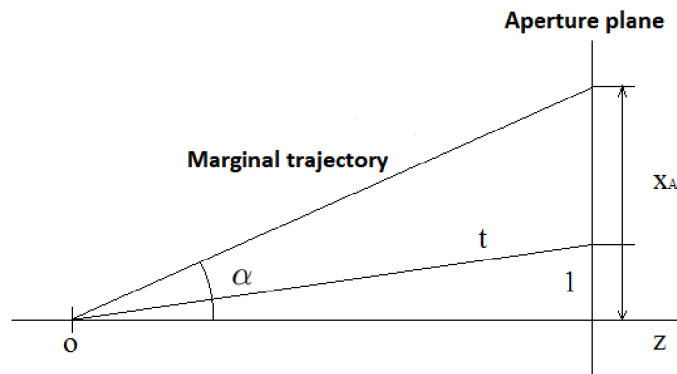


Figure 4.3: The electron beam of axial symmetric system is limited by aperture with radius  $x_A$  defining marginal ray originating from the object  $o$ . Paraxial ray  $t$  is defined by the coordinates in the object plane  $t(z_o) = 0$  and aperture plane  $t(z_a) = 1$ .

The aim of the following paragraph is the transformation from the dependence on coordinates of the ray in the aperture plane to the dependence on aperture angle. From the equation 4.1.9 the definition formula of spherical aberration coefficient  $C_s$  is :

$$C_s = \frac{C}{t_o^3} \quad (4.1.20)$$

The lower index  $o$  refers to object plane and index  $a$  will denote parameters valid for an aperture plane. Using previous formula in the equation (4.1.18) the minimal radius of aberration disc  $\Delta u_{s,min}$  will be obtained in the form:

$$|\Delta u_{s,min}| = \frac{1}{4} M C_s t_o^3 x_A^3. \quad (4.1.21)$$

The slope of paraxial ray  $t$  with a unit distance from the optical axis  $z$  in the aperture plane has appeared in the formula. The lower index  $o$  refers to object plane and index  $a$  to aperture plane. The value of  $t$  ray slope in the object plane is inversely proportional to the distance between object and aperture plane  $z_{oa}$

$$t_o' = \frac{1}{z_{oa}} \quad (4.1.22)$$

The value of the slope of marginal ray is directly proportional to the slope of considered paraxial ray hence aperture angle can be written as:

$$\text{tg } \alpha = \frac{1}{z_{oa}} x_A = t_o' x_A \approx \alpha \quad (4.1.23)$$

The aperture angle in conventional systems is small enough that a linear approximation of the tangent function can be used. The combination of the equations (4.1.21) and (4.1.23) leads to desired dependence of  $\Delta u_{s,min}$  on aperture angle:

$$|\Delta u_{s,min}| = \frac{1}{4} M C_s \alpha^3. \quad (4.1.24)$$

More general approach considering different plane than the plane where disc of least confusion is located provides the equation form:

$$|\Delta u_s| = k_1 M C_s \alpha^3, \quad (4.1.25)$$

where coefficient  $k_1$ , for reasons clarified in the chapter (4.1.1), defines the location of the plane of interest, where the spherical aberration disc is investigated. Relevant values of constant  $k_1$  are  $k_1 = 1$  specifying Gaussian image plane and  $k_1 = \frac{1}{4}$  corresponding to the plane of disc of least confusion.

## 4.2. Chromatic aberration

Despite the continuous effort to develop electron sources the incident beam is not strictly monochromatic, but the electrons have slight variations in nominal energy. The reasons for broadening of energy spectrum can be found in intrinsic properties of electron source, instabilities of electric power supplies and last but not least the energy spread is further

broadened by electron-electron interaction and by the interaction of electrons with the specimen [90].

As a consequence of such an energy distribution, the resulting image is blurred by the chromatic aberration.

The initial energy spread of electrons leaving the cathode surface  $\Delta E$  is typically few electronvolts for thermionic emitters. More advanced Schottky cathode reduces energy spread to approximately  $\Delta E = 0.6$  eV [91][92] and cold field emission guns provides even  $0.1 - 0.3$  eV [93]. Due to the interactions of the electrons with the sample, the additional energy losses can significantly broaden the energy distribution by tens of electronvolts for the samples of standard thickness [94].

The deviation in Gaussian image plane of the paraxial trajectory of the electron beam with a nominal energy  $E$  from the real trajectory affected by chromatic aberration is given by the formula:

$$\begin{aligned}\frac{\Delta x(z)}{M} &= -(C_c x'_0 + C_D x_0 - C_\phi y_0) \left( \frac{\Delta \Phi}{\Phi_0} - \frac{2\Delta B_{max}}{B_{max}} \right) \\ \frac{\Delta y(z)}{M} &= -(C_c y'_0 + C_D y_0 - C_\phi x_0) \left( \frac{\Delta \Phi}{\Phi_0} - \frac{2\Delta B_{max}}{B_{max}} \right),\end{aligned}\tag{4.2.1}$$

where  $x_0, y_0$  are coordinates in the object plane,  $\Phi$  electric potential,  $B$  magnetic flux density,  $M$  magnification and  $\Delta$  deviation of relevant physical quantity. Not all terms are non-zero in every possible conditions. Coefficient of anisotropic chromatic distortion equals to zero  $C_\phi = 0$  for electrostatic lens and the highlighted term has to be taken into account just in case of magnetic lens [95].

Chromatic aberration is characterized by the similar set of coefficients as it is used in case of geometric aberrations. There are two kinds of chromatic aberration with various importance for the different electron-optical elements: An aperture chromatic aberration  $C_c$  and chromatic distortion characterized by another two coefficients  $C_D$  and  $C_\phi$ . The chromatic aberration  $C_c$  is the most severe for objective lens, while both components of chromatic distortion i.e. chromatic aberration of magnification  $C_D$  and  $C_\phi$  anisotropic chromatic distortion mainly affects the projective lenses. Due to the fact that a major influence on the resolution of the transmission electron microscope have the aberrations of the objective lens, only the aperture chromatic aberration  $C_c$  will be considered.

The image of a point source affected by an axial chromatic aberration has, similarly to a spherical aberration, the form of a circular disk. The radius depends on the ratio of the energy width, the nominal energy of the primary beam and the aperture angle.

Common widespread methods used to eliminate chromatic aberration are in principle based on reducing the energy spread of the electron spectrum made by monochromator or employ an electron source with a lower energy width or the chromatic aberration can be corrected using an quadrupole-octupole corrector with the combination of magnetic and electrostatic fields.

# 5. BENEFIT ANALYSIS OF THE ABERRATION CORRECTION

*Knoll and I simply hoped for extremely low dimensions of the electrons. As engineers we did not know yet the thesis of the “material wave” of the French physicist de Broglie that had been put forward several years earlier (1925). Even physicists only reluctantly accepted this new thesis. When I first heard of it in summer 1931, I was very much disappointed that now even at the electron microscope the resolution should be limited again by a wavelength (of the “Materiestrahlung”). I was immediately heartened, though, when with the aid of the de Broglie equation I became satisfied that these waves must be around five orders of magnitude shorter in length than light waves.*

— Ernst Ruska [96]

In the very beginning the most important questions about the level of potential benefits or on the other hand inefficiency of aberration correction had to be answered. The following part is intended to be the feasibility study of aberration correction for the desktop low voltage systems. The conclusions arising from the arguments set out in this section played a key role in the decision-making of which concept of low voltage corrected transmission electron microscope is beneficial. This section is based on article ‘Aberration correction for low voltage optimized transmission electron microscopy’ published in MethodsX, 2018 [97].

## 5.1. Estimated resolution of corrected LVEM

The total resolution is determined by the combination of all aberrations, but it is necessary to use only the most important ones to arrive at a relevant estimate. In the case of an uncorrected system the following contributions have to be considered: the primary spherical aberration .

$$d_s = k_1 C_s \alpha_i^3, \quad (5.1.1)$$

the chromatic aberration

$$d_c = k_2 \frac{\Delta E}{E_0} C_c \alpha_i, \quad (5.1.2)$$

and the diffraction limit

$$d_d = 0,61 \frac{\lambda}{\alpha_i}, \quad (5.1.3)$$

where standard notation is used [27]. The meaning of the constants  $k_1$ ,  $k_2$  is mainly to define the position of the image plane, as it is discussed for the spherical aberration in sections 4.1.1 and 4.1.2 or in detail for example in [16].

The contributions of the partial aberration discs  $d_s$ ,  $d_c$  and  $d_d$  can be summarized to a total aberration disc  $d$ :

$$d = \sqrt{d_s^2 + d_c^2 + d_d^2}. \quad (5.1.4)$$

It can be specified in more detail:

$$d = \sqrt{(k_1 C_s \alpha_i^3)^2 + \left(k_2 \frac{\Delta E}{E_0} C_c \alpha_i\right)^2 + \left(0.61 \frac{\lambda}{\alpha_i}\right)^2}. \quad (5.1.5)$$

The experimental spatial resolutions of the current LVEM 5 and LVEM 25 are given in table 2.2. The declared values are in good agreement with theoretical models using the standard evaluation method.

From equation 5.1.4 it is obvious that the optimal solution of a corrected system should not be significantly limited by one major contribution, but all primary contributions should be comparable. The degree of importance of each aberration has been thoroughly studied in various system conditions to determine which aberration is limiting and thus should be corrected.

The most manifesting aberrations of common electron optical devices are the chromatic and the geometric (especially the primary third-order spherical aberration) ones, their influences on the size of the paraxial space (determined by aperture angle) are competing with the influence of the diffraction limit. An optimal aperture angle therefore exists. The correct choice of the aperture angle is necessary to maintain the best possible resolution.

Optimal aperture angles  $\alpha_{optim}$  have been calculated in the range of LVEM accelerating voltage. From fig. 5.1 it can be seen that for a specific set of aberration coefficients there is preferred accelerating energy. This conclusion can also be obtained directly from the aberration integrals, where the integrands are dependent on the accelerating voltage.

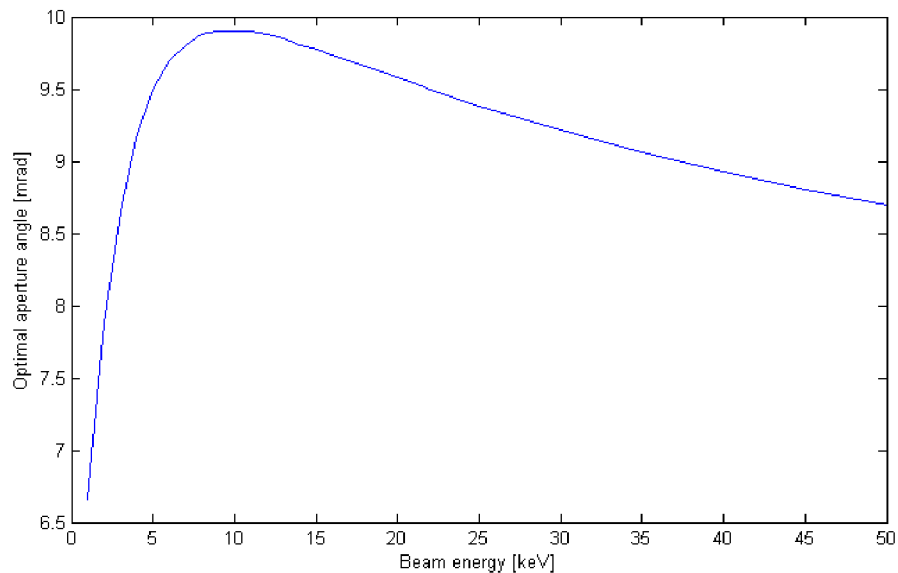


Figure 5.1: Optimal accelerating energy for a specific set of aberration coefficients (LVEM 5)  $C_s = 0.64$  mm,  $C_c = 0.89$  mm,  $\Delta E = 0.6$  eV.

The results for all above mentioned modes of interest with a typical energy spread  $\Delta E$  of Schottky and CFE cathodes and relevant aberration coefficients (tab.2.2) are presented in table 5.1. The change of the optimal aperture angle for typical energy spreads of Schottky and CFE cathodes is 0.2 – 1.5 mrad.

Table 5.1: Optimal setting of aperture angles obtained by minimisation of the integral aberration disc.

$\Delta E [eV]$	LVEM 5 5 keV	LVEM 25 10 keV	LVEM 25 15 keV	LVEM 25 25 keV
0.6 (Schottky)	9.5 [mrad]	10.2 [mrad]	9.4 [mrad]	8.3 [mrad]
0.3 (CFE)	11.0 [mrad]	10.6 [mrad]	9.6 [mrad]	8.5 [mrad]

The change between Schottky and CFE is significantly bigger considering the lower electron energy, all because of higher importance of the chromatic aberration. The effect of the monochromatisation degree is continuously demonstrated in figure 5.2. It can be clearly observed that the lower energy spread leads to a larger  $\alpha_{optim}$  and thus to a larger paraxial space.

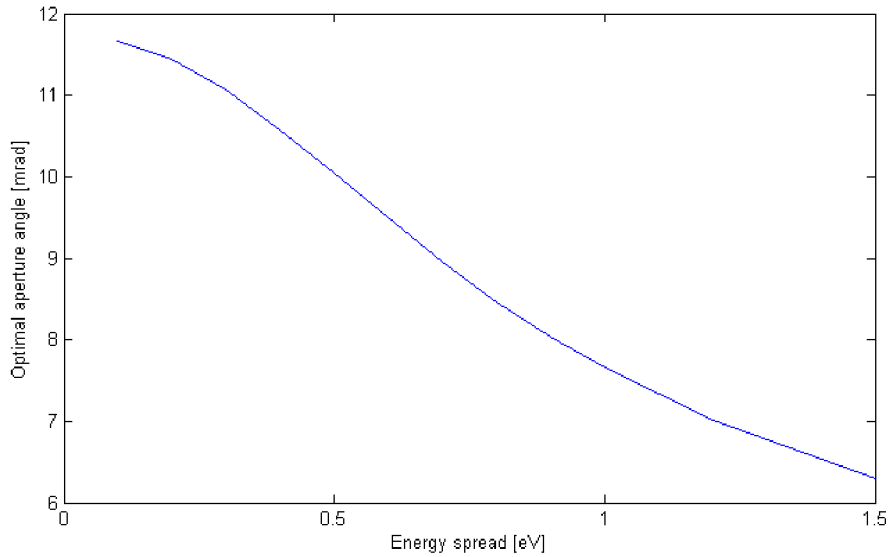


Figure 5.2: Model parameters  $C_s = 0.64$  mm,  $C_c = 0.89$  mm,  $E = 5$  keV.

The integral aberration discs were calculated with  $\alpha_{optim}$  according to equation 9.0.1. It can be considered to be the resolution limit of an uncorrected system. The calculations were done for a Gaussian image plane (i.e.  $k_1 = 1$ ,  $k_2 = 1$ ), where the screen is placed approximately tab. 5.2.

Table 5.2: Integral aberration discs for  $\alpha_{optim}$  in the Gaussian imaging plane.  $\Delta E = 0.6$  eV

	LVEM 5 5 keV	LVEM 25 10 keV	LVEM 25 15 keV	LVEM 25 25 keV
d [nm]	1.5	0.92	0.79	0.67

A closer look at the partial aberration discs is helpful in order to understand the behavior of the resolution limit. The data prove that the decrease in the accelerating voltage

makes the chromatic aberration more severe. The diameter of the integral aberration disc for the 5kV LVEM is reduced by CFE to app. 80% when using Schottky cathode. In the case of 25kV using CFE cathode the radius of the integral aberration disc became smaller by only 4% (tab.5.3).

Table 5.3: The aberration discs for energy spread typical for Schottky and CFE cathods (0.6 eV, 0.3 eV). Aberration coefficients were used from LVEM5 and LVEM25. [55][56]

	5 keV		25 keV	
$\Delta E_0$	0.6 eV	0.3 eV	0.6 eV	0.3 eV
$d_s$ [nm]	0.27	0.43	0.30	0.31
$d_c$ [nm]	1.01	0.59	0.21	0.10
$d_d$ [nm]	1.11	0.95	0.56	0.55
$d$ [nm]	1.52	1.20	0.67	0.64

An interesting question would certainly be how crucial is the correction of individual aberrations. The primary spherical and chromatic aberration were considered to evaluate the profit resulting from their full correction. Aberration correction in calculations is realized by nullifying an adequate aberration coefficient. Results are clearly summarized in the following tables 5.4, 5.5.

The separate correction of spherical aberration is not beneficial at all in case of very low beam energy 5keV. On the contrary, undesirable defects introduced by corrector itself would cause deterioration of resolution. Certain resolution improvement should be achieved by dealing with chromatic aberration, but incorporation of necessary equipment able to do so would turn over the whole concept of desktop LVEM5 microscope.

However, very similar results, as the separate correction of chromatic aberration would provide, are expected in case of combination of spherical aberration correction together with reduced energy spread by using of cold field emission electron source.

The impact of chromatic aberration weakens with increasing accelerating voltage as mentioned above, thus the situation reverses, tab.5.5. Separate correction of chromatic aberration is almost pointless and dominant effect is taken over by spherical aberration. Accelerating voltage 25kV is already mainly sensitive to spherical aberration correction with expected resolution improvement about 28%. The combination of spherical aberration elimination with reduced energy spread by CFE to one-half brings a very promising outcome, when resolution can be reduced by 43%. Such a potential for resolution improvement is already worth the effort to deal with development troubles caused by the incorporation of a corrector to the optical column. It is important to emphasize that the chromatic contribution of the sample is not considered.

In addition, separate correction of spherical aberration can be made by less complicated and more compact hexapole type corrector.

Table 5.4: Tabulated efficiency analysis of particular aberration correction types for an accelerating voltages 5kV.

Type of correction	$\Delta E$ [eV]	$\alpha_{optim}$ [rad]	Tot. aber. disc $d$ [nm]	Percentage dec.
Uncorrected	0.6	0.0096	1.53	-
Corrected for $C_C$	0.6	0.012	1.04	32%
Corrected for $C_S$	0.6	0.010	1.50	2%
Corrected for $C_S$	0.3	0.014	1.06	31%

Table 5.5: Tabulated efficiency analysis of particular aberration correction types for an accelerating voltages 25kV.

Type of correction	$\Delta E$ [eV]	$\alpha_{optim}$ [rad]	Tot. aber. disc $d$ [nm]	Percentage dec.
Uncorrected	0.6	0.008	0.67	-
Corrected for $C_C$	0.6	0.008	0.63	6%
Corrected for $C_S$	0.6	0.014	0.48	28%
Corrected for $C_S$	0.3	0.019	0.38	43%

The decision about the prospective corrector development direction has been made, based on this analysis. Because of the results presented in this chapter and also reasons later discussed in detail in the section 7, the goal was set to built a hexapole corrector exclusively designed for low voltage electron microscope similar to LVEM25 concept.

## 5.2. Wave aberration theory

The aberrations can be also treated through the wave aberration function  $\chi(\alpha)$ . An undisputable advantage of this approach is the fact that it provides direct insight into the optics principles, because first-order optical properties are calculated at first and the deviations are investigated later [27].

This concept is based on the idea that every object point sends out spherical wave with concentric wavefronts with equal phase. The perfect lens influence this wave in such manner that the spherical wave converging to single image point is also created after the lens focusing action. The rays of geometrical optics used in previous sections are orthogonal to the wavefront [89].

Real lenses introduce aberrations and thus they modify the shape of the wavefront. Krivanek defines the aberration function in case of STEM configuration as a physical distance between the actual wavefront converging on the sample, and an ideal wavefront that would be produced by the Gaussian optical elements in the absence of all aberrations. The theory is also valid for TEM arrangement, but direction of the electron movement has to be reversed thus the aberration function diverge from the sample instead of converging on it [27].

The phase shift is given by aberration function  $\chi(\omega)$ :

$$\begin{aligned}
\chi(\omega) = \frac{2\pi}{\lambda} \operatorname{Re}\{ & \frac{1}{2}\omega\bar{\omega}C_1 + \frac{1}{2}\bar{\omega}^2A_1 + A_2 + \omega^2\bar{\omega}B_2 \\
& + \frac{1}{4}(\omega\bar{\omega})^2C_3 + \frac{1}{4}\bar{\omega}^4A_3 + \omega^3\bar{\omega}S_3 + \frac{1}{5}\bar{\omega}^5A_4 \\
& + \omega^3\bar{\omega}^2B_4 + \omega^4\bar{\omega}D_4 + \frac{1}{6}(\omega\bar{\omega})^3C_5 + \frac{1}{6}\bar{\omega}^6A_5 \\
& + \omega^5\bar{\omega}R_5 + \omega^4\bar{\omega}^2S_5 + \frac{1}{7}\bar{\omega}^7A_6 + \omega^4\bar{\omega}^3B_6 \\
& + \omega^5\bar{\omega}^2D_6 + \omega^6\bar{\omega}F_6 + \frac{1}{8}(\omega\bar{\omega})^4C_7 \\
& + \frac{1}{8}\bar{\omega}^8A_7 + \omega^7\bar{\omega}G_7 + \omega^6\bar{\omega}^2R_7 + \omega^5\bar{\omega}^3S_7 + \dots\}
\end{aligned} \tag{5.2.1}$$

where  $\omega$  is complex-valued scattering angle.

For the purpose of this thesis the polynomial will be reduced, because of the correction ability of the hexapole corrector, which is able to achieve active correction of the 3th order and the partial compensation of the 5th order. Furthermore quadrupole-octupole corrector is able to correction up to 5th order spherical aberration (system limited by the  $C_7$ ). Thus only spherical aberration up to the 7th order is considered. A phase shift can be also expressed in the form related to aperture angle  $\alpha$ , thus the aforementioned formula can be modified to:

$$\chi(\alpha) = \frac{2\pi}{\lambda} \left( -\frac{1}{2}\Delta f\alpha^2 + \frac{1}{4}C_3\alpha^4 + \frac{1}{6}C_5\alpha^6 + \frac{1}{8}C_7\alpha^8 + \dots \right). \tag{5.2.2}$$

It is also important to stress that only spherical aberration is included in this wave aberration analysis. The influence of chromatic aberration is neglected for this section.

To achieve the best possible resolution, it is necessary to find a compromise between the geometrical aberrations and the diffraction limit. To maintain the required image quality, the phase shift has to be below a certain value. The Rayleigh criterion is used as a commonly accepted phase shift.  $\chi = \frac{\pi}{2}$  i.e. P-V (peak to valley) is equal  $\frac{\lambda}{4}$ . A higher phase shift causes low intensity of the 0th order maximum of the diffraction pattern. It results in an increase of the intensity of the higher order maximums and de facto to a loss of the image contrast.

A quantitative evaluation of the image quality was done by Strehl ratio:

$$S = e^{-(2\pi RMS)^2}, \tag{5.2.3}$$

where  $RMS$  Root-Mean-Square, a parametre which describes the wavefront, is defined:

$$RMS = \frac{P-V}{4.5}. \tag{5.2.4}$$

Although the definition of the spatial resolution itself is a tricky task and different approaches are described in literature and used by different manufacturers, the generally accepted value of Strehl ratio to maintain reasonable image quality is  $S \geq 0.8$  [98][99]. For the purpose of this study the value is set to  $S = 0.88$ .

The goal of eliminating the undesirable effect of aberrations is to achieve a given limit of a phase shift at the greatest possible aperture angle. The general form and resulting

behaviour of the polynomial function 5.2.2 determines the existence of local extremes. The required form of the polynomial, which means oscillating phase shift below a certain predefined limit until the last local extreme appears, can be created by the proper choice of coefficients. (fig. 5.3)

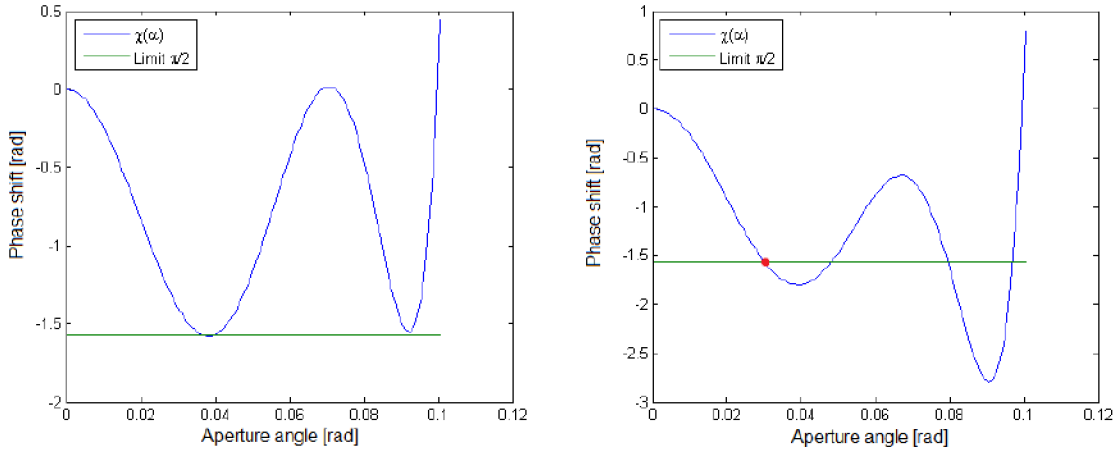


Figure 5.3: *left*: The phase shift behaviour with an appropriate choice of a coefficient (corrected system).  $\chi(\alpha)$  stays below a certain limit in the biggest possible interval of aperture angle. *right*: In case of improperly selected coefficients or uncorrected system, the phase shift will exceed (red dot) the limit already with lower  $\alpha$ .

Formulas for the most appropriate spherical aberration coefficients  $C_3$  and  $C_5$ , defocus, the corresponding resolution and the aperture angle in different conditions were derived analytically (tab. 5.6) by Intaraprasong et al. [100] and Chang et al. [101]. It should be emphasized that it is not optimal to set coefficients to zero, because the aberrations of a lower order are capable of reducing the influence of the higher order aberrations, which cannot be principally corrected by the chosen type of corrector.

In other words, according to the specific value of the coefficient of higher-order spherical aberration given by properties of instrument itself, there is an optimal value of lower-order spherical aberration coefficient, which should be set by the corrector. Such a choice of a lower-order aberration provides better resolution than if the aberration would be perfectly corrected in terms of setting the lower-order aberration coefficient to zero.

Table 5.6: Formulas for an optimal setting of the aberration coefficients by the corrector and parameters of systems corrected for the primary (limited by the 5th order) spherical aberration resp. corrected for the secondary (limited by the 7th order) spherical aberration. Term  $\frac{1}{b}$  means limiting fraction of wavelength  $\lambda$  with tolerable effect on the image quality [100].

Order of correction	3	5
Optimal $C_3$	$-4\left(\frac{3}{2b}\lambda C_5^2\right)^{\frac{1}{3}}$	$10\left(\frac{2\lambda C_7}{b}\right)^{\frac{1}{2}}$
Optimal $C_5$	-	$-6\left(\frac{2\lambda C_7^3}{b}\right)^{\frac{1}{4}}$
$\Delta f$	$-3\left(\frac{9}{4b^2}\lambda^2 C_5\right)^{\frac{1}{3}}$	$4\left(\frac{8\lambda^3 C_7}{b^3}\right)^{\frac{1}{4}}$
$\alpha_{max}$	$\left(\frac{96\lambda}{bC_5}\right)^{\frac{1}{6}}$	$2\left(\frac{2\lambda}{bC_7}\right)^{\frac{1}{8}}$
Resolution	$0.61\left(\frac{b}{96}C_5\lambda^5\right)^{\frac{1}{6}}$	$\frac{0.61}{2}\left(\frac{b}{2}C_7\lambda^7\right)^{\frac{1}{8}}$

According to the optimal setting of coefficients, the significance of different order correction of the spherical aberration is shown in the figure 5.4. The new calculated resolution limits, depending on the value of the coefficient of limiting aberration, can be clearly seen.

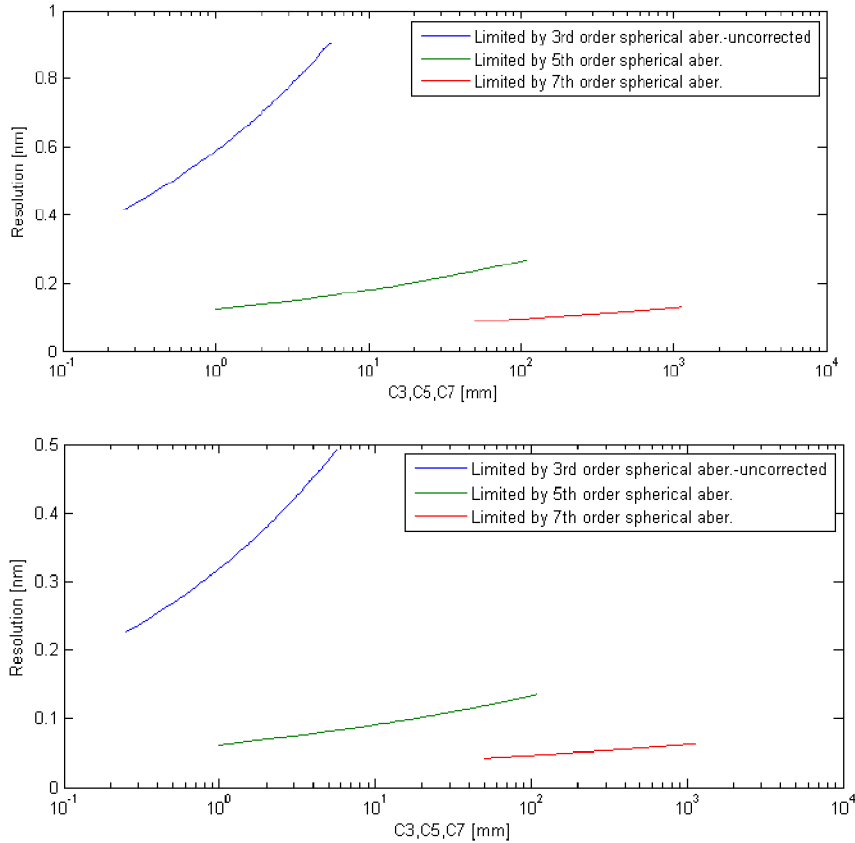


Figure 5.4: The image shows the dependence of an expected resolution limit on the aberration coefficient of a limiting order of the spherical aberration for a different order of an aberration correction. Non-corrected system limited by the primary spherical aberration (green), correction of the 3rd order spherical aberration i.e. limited by the 5th order of spherical aberration (green) and correction of the 5th order spherical aberration i.e. limited by the 7th order of spherical aberration (red).  $E_0 = 5$  kV (upper fig.),  $E_0 = 25$  kV (lower fig.)

The significant effect of active correction of the primary spherical aberration can be observed. The influence of the additional correction of the secondary spherical aberration (the 5th order) theoretically improves the attainable resolution, but requirements for stability of the corrector's power supplies can be too high. In addition, it is necessary to take into account the influence of the chromatic aberration, which will be discussed later.

The discussed model is able to find the optimal setting of the aberration coefficients by a corrector to reach the biggest aperture angle, meeting the chosen requirements of the phase shift. The proper choice of coefficients enables to extension of the aperture angle to the interval after the last local phase shift minimum, as is shown in fig. 5.3.

Optimal aperture angles of all LVEM5 and LVEM25 imaging modes were calculated for a system limited by the 3rd and the 5th order spherical aberration (tab. 5.7). The aperture angles would clearly enlarge due to the correction. The aperture angles of an uncorrected microscopes are 0.01 rad [55] [56]. A correction of the primary spherical aberration promises to improve this value by at least three times and with the correction of the 5th order spherical aberration, it would be possible to use an aperture angle approximately eight times higher as compared with the current systems.

Table 5.7: Optimal aperture angles of the corrected system: correction up to the 3rd order  $\alpha_3$  ( $C_5 = 100$  mm), correction up to the 5th order  $\alpha_5$  ( $C_7 = 1000$  mm).  $S = 0.88$ .

	5 keV	10 keV	15 keV	25 keV
$\alpha_3$ [rad]	0.040	0.038	0.037	0.035
$\alpha_5$ [rad]	0.083	0.079	0.077	0.075

These results are relevant especially in the case of the instruments with eliminated deterioration caused by chromatic aberration. Systems with unsolved chromatic defect have to be designed with smaller aperture angles according to the table 5.1.

The resolution of the spherical aberration corrected system was calculated with the aperture angles from the table above tab. 5.7. The results are shown in the following table 5.8.

Table 5.8: The resolution of the system with a correction of the 3rd order  $d_3$  ( $C_5 = 100$  mm) and the 5th order spherical aberration  $d_5$  ( $C_7 = 1000$  mm) neglecting the influence of the chromatic aberration and other geometrical aberrations.  $S = 0.88$ .

	5 keV	10 keV	15 keV	25 keV
$d_3$ [nm]	0.26	0.20	0.17	0.13
$d_5$ [nm]	0.13	0.09	0.08	0.06

Due to the unconsidered effect of chromatic and other geometrical aberrations except spherical aberrations, the aforementioned calculated resolution  $d_3$  and  $d_5$  can be understood rather as the residual aberration discs of the higher order spherical aberration.

Because of significant enlargement of the optimal aperture angle, the chromatic aberration disc is also bigger. To maintain the diameter of the chromatic aberration disc comparable with the spherical one and therefore take full advantage of the correction potential of the spherical aberration, it is necessary to increase the degree of monochromatisation. Using a new aperture angle and keeping the energy spread without any reduction leads to crucial enlargement of the chromatic aberration disc to  $d_{c5} = 8.8$  nm in case of LVEM5 with correction of the 5th order spherical aberration. It has been proved that, in order to achieve some meaningful values of  $d_c$  comparable with  $d_s$  (particularly  $d_3$  and  $d_5$ ), it is necessary to reduce the energy spread to  $\Delta E = 0.08$  eV for LVEM 25 and  $\Delta E = 0.04$  eV for LVEM 5 (correction of the 3rd order spherical aberration). The energy spread requirements for the 5th order correction are even higher. In this case, it should not exceed the value  $\Delta E = 0.02$  eV.

The available technology of monochromators is currently capable of fulfilling these conditions in a very limited way, because the energy spread below  $\Delta E = 0.1$  eV with reasonable signal-to-noise ratio is very difficult to achieve [102]. The chromatic aberration thus still poses a very serious problem.

The estimated resolution of the  $C_s$  ( $C_3$ ) corrected systems with a monochromator and a CFE gun is shown in the table 5.9.

Table 5.9: Computed resolution for systems with reduced energy spread and accordingly optimized aperture angles. The typical energy spread of  $\Delta E = 0.1$  eV is used in case of monochromated system ( $d_{monochrom}$ ) and  $\Delta E = 0.3$  for cold-field emission gun  $d_{CFE}$ .

	5 keV	10 keV	15 keV	25 keV
$d_{CFE}$ [nm]	1.06	0.56	0.45	0.34
$d_{monochrom}$ [nm]	0.61	0.32	0.26	0.20

# 6. ENHANCEMENT OF CHROMATIC ABERRATION BY A HEXAPOLE CORRECTOR

The previous part of this thesis dealt especially with the problem of a spherical aberration correction. There is, however, also a chromatic aberration that can be significantly severe for LVEM, as is shown in the section 5.1. Unfortunately as was mentioned in the section 3, chromatic aberration is correctable only by a more intricate quadrupole-octupole corrector. A hexapole corrector is not able to correct or even improve the manifestation of this aberration. On the contrary, rotationally symmetric elements, which are part and parcel of a hexapole corrector, add their own contributions to the chromatic aberration of the whole electron-optical system [103][104]. The minimum configuration of the sextupole corrector consists of a telescopic round lens doublet (transfer lens) and two sextupoles placed in front of and behind the doublet, according to the Rose arrangement [105].

In order to create an aplanat, it is necessary to transfer the coma-free nodal point  $N_1$  to the coma-free point of the objective. For this purpose another doublet of the transfer lens has to be used.

From the chromatic aberration point of view, only the transfer lenses have to be investigated. The separate contribution of a every single transfer round lens will be derived then.

The chromatic aberration is usually described by a coefficient  $C_c$  defined, in case of a magnetic rotationally symmetric lens, by integral [106][16]:

$$C_c = \frac{\eta^2}{4U} \int_{z_o}^{z_i} B(z)^2 h^2 dz. \quad (6.0.1)$$

$$\eta = \sqrt{\frac{e}{2m_0}} \quad (6.0.2)$$

In case of a thin lens approximation, the integral can be modified to the form:

$$C_c = \frac{\eta^2}{4U} \int_{-\infty}^{\infty} B(z)^2 h^2 dz. \quad (6.0.3)$$

The integration boundaries  $(-\infty; \infty)$  can be used, because the out-of-field parts have zero contribution to the total  $C_c$ . Due to the same approximation concentrating the field into a tiny space, the change of axial ray distance from the axis  $h$  inside the lens can also be neglected and replaced by a constant equal to the object distance  $z_o$ :

$$h(0) = z_o. \quad (6.0.4)$$

This equality relation is determined from definition of an axial ray specified by its position in the object plane  $h(z_o) = 0$  and the unit slope in the same plane. The situation is more clearly seen when observing the figure 6.1.

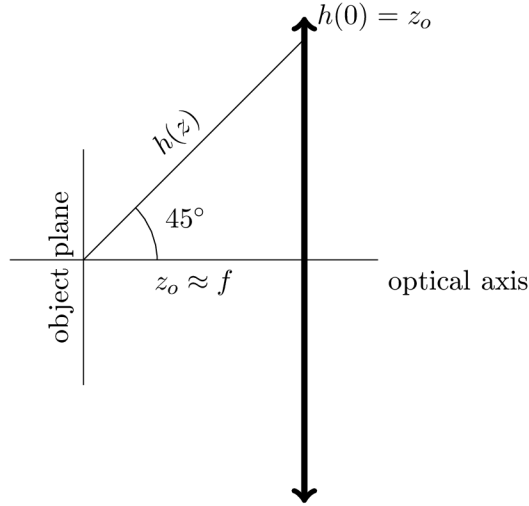


Figure 6.1: Scheme of the axial ray trajectory through a thin lens placed in the origin of coordinate system. The object is placed on a focal plane ( $z_o \approx f$ ) of an arbitrary lens ("arrow notation"). This scheme corresponds to the situation of the usage of the lens as an objective.

Because the distance of the axial ray from the axis is constant in a non-zero magnetic field space of the thin lens, it can be moved in front of the integral:

$$C_c = \frac{\eta^2}{4U} z_o^2 \int_{-\infty}^{\infty} B_z^2 dz. \quad (6.0.5)$$

The integral is replaced with consideration to the equation for focal length of the magnetic lens  $f$ :

$$\frac{1}{f} = \frac{e^2}{8m_0 E_0} \int B_z^2 dz. \quad (6.0.6)$$

Putting eq.(6.0.6) and eq.(6.0.5) together:

$$C_c = \frac{\eta^2}{4U} \frac{8m_0 U}{e} z_o^2 \frac{1}{f} \quad (6.0.7)$$

simplifying the algebraic expression, the final dependance is obtained:

$$C_c = \frac{z_o^2}{f}, \quad (6.0.8)$$

This dependence seems to be in a direct contradiction with the generally accepted rule for the design of an electron optical system. According to well-known guidelines for electron-optical lens design, the chromatic aberration coefficient is approximately equal to the focal length of the lens:

$$C_c \approx f, \quad (6.0.9)$$

This rule applies especially to magnetic lenses ( $C_c[mm] = f[mm]$ ). In the case of the electrostatic lenses, there is still a direct variation between  $C_c$  and  $f$  but the coefficient is several times higher due to the difficulties in achieving high gradients. This apparent paradox can be explained by considering the imaging conditions. Usually the chromatic aberration of an objective lens is critical for the resolution of the entire microscope. In

this common configuration, the object is located very near the object focus of the lens to reach high magnification and indeed the eq. (6.0.8) can be transformed to the form (6.0.9), because the object is close to the focus and therefore the distance of the axial ray from the axis in the lens region is equal to the focal length of the lens. In case of the different object positioning along the optical axis, the above-mentioned transformation of eq. (6.0.8) is not possible and the dependence is clearly inversely proportional.

The comparison of both situations is given in figure 6.2, which can be helpful for correct understanding of the behaviour.

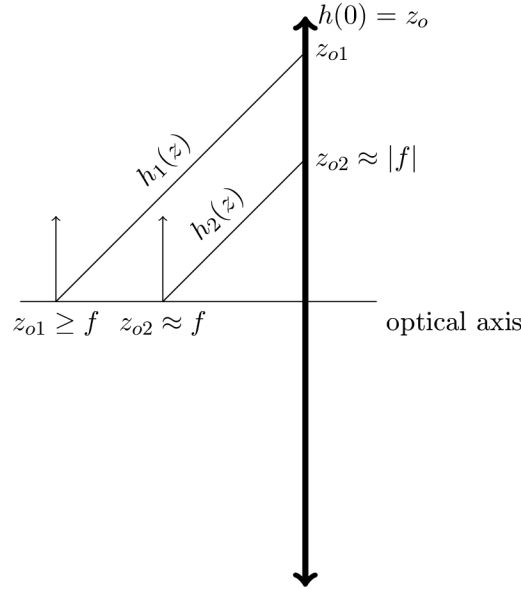


Figure 6.2: The situation denoted by mark 1 represents a general position of the object out of the lens focus (object distance  $z_{o1}$ ). This situation corresponds to the corrector doublet usage. Label 2 denotes the discussed situation of using the lens as an objective (object distance  $z_{o2}$ ) leading to a direct proportionality between  $C_c$  and  $f$  (6.0.9).

The conclusions resulting from the equation (6.0.8) are very important to the corrector concept. According to the above-mentioned guidelines for the optimal lens design (6.0.9), a lens with the short focal length could be mistakenly preferred. In case of the presence of a transfer lens in the corrector set-up, the contribution of a single transfer lens to the  $C_c$  can be derived based on the equation (6.0.8). The distance from the axis of the above-mentioned ray in the transfer lens  $h_{TL}$  is dependent on the position of the same ray on objective  $h_{ol}$  through magnification  $M_{TL}$  between these two planes:

$$h_{TL} = M_{TL}h_{ol}. \quad (6.0.10)$$

In case of an objective lens, the object is situated near the focus (coordinates  $f_{ol}$ ), thus it is possible to transform the previous equation to the form:

$$h_{TL} = M_{TL}f_{ol} \quad (6.0.11)$$

and the contribution of a single transfer lens can be expressed in terms of the objective focal length [63]:

$$C_c = M_{TL}^2 \frac{f_{ol}^2}{f_{TL}} \quad (6.0.12)$$

According to this result, weak transfer lenses are recommended to reduce the chromatic aberration of the whole system. These theoretical conclusions were confirmed by computer simulations. Electrostatic and magnetic transfer lenses were investigated. The electrostatic lenses were used for a short focal length because of their possible miniaturisation, where the magnetic lenses were unfeasible due to obligatory construction parameters of the microscope.

The contribution to the total chromatic aberration depending on the focal length of a single transfer lens is shown in figure (6.3). The electrostatic lenses turned out to be inappropriate (fig. 6.3), because they deteriorate the chromatic aberration much more than the magnetic ones. This critical deterioration by electrostatic doublets can be proved by comparison with results of  $C_c$  calculation for a magnetic doublet with the same focal length. This behaviour is demonstrated on the example of a two-doublets configuration with a 10mm focal length, which leads to an increase of the  $C_c$  of 288% in the electrostatic case and only 166% in the magnetic case.

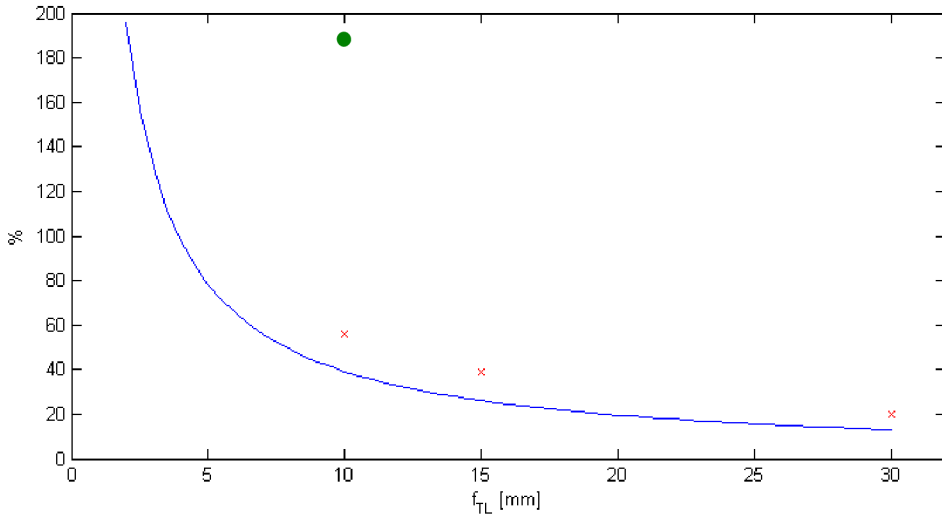


Figure 6.3: The Percentage increase of the chromatic aberration of the hexapole corrector relative to uncorrected system. The computer simulation of the magnetic transfer lenses in two-doublets configuration is denoted by red crosses (permanent magnet transfer lenses), green dot represents electrostatic case and blue curve is an analytical dependence.

The consequences for the concept of a desktop corrected LVEM are very fundamental. The size of the corrector body with the appropriate weak transfer lenses would be comparable to the main body of the microscope column. It undoubtedly increases mechanical vibrations and thus increases requirements for vibration damping.

It should be emphasized that the chromatic aberration will still be a limiting factor despite the correction of the spherical aberration. A hexapole corrector is therefore suitable mostly for a low-voltage STEM application, in contrast to the TEM, where the energy spread is additionally broadened by the passage of the beam through the sample [112]. It should be noted that to guarantee all of the presented results the transfer lenses has to be optimized for the given focal length, in the sense of the bore diameter and the gap dimension.

The combination of a hexapole corrector with the proper monochromator could be the solution, with obvious advantages for spectroscopy. Because of the available degree

of monochromatisation and the size of the instrument, it would be suitable only for LVEM25. The size of the column would be extended by approximately 100mm by the monochromator, so the monochromator size is comparable with the LVEM5 column.

# 7. OUTLINE OF THE CORRECTOR

*It would be better for the true physics if there were no mathematicians on earth.*

— Daniel Bernoulli

The following section is dedicated to the description of the design of the corrector exclusively developed for the needs of low voltage transmission electron microscopes. The detailed layout of the corrector with its built-in compensation elements will be introduced and the basics of the employed technology of permanent magnet lenses will be presented. Sections 7, 8, 9 are based on the slightly modified and extended text of the article [113], which thoroughly presented results of this research in Ultramicroscopy in 2020.

An extended hexapole field with negative spherical aberration can not be used advantageously in a single setup, because other hexapole field aberrations have to be eliminated and the sufficient flexibility of the adjustment has to be guaranteed. Especially threefold astigmatism, which is primary aberration induced by hexapole field, would significantly deteriorate the image, although it is unnecessary for the hexapole correction action. Furthermore, second-order hexapole field aberration (fourth-order three-lobe aberration) has to be canceled out by proper corrector setup.

The simplest design of a corrector, which provides the above-mentioned characteristics, consists of two hexapole elements separated by a round-lens doublet. This configuration has been chosen for the intended LVEM corrector. The reason for such a choice was to maintain all the benefits of a low voltage system. Low complexity is especially important for miniaturization, which is essential for integration to a desktop LVEM systems.

The incorporated hexapoles are electrostatic, due to the low-voltage character of proposed corrected system.

Because low voltage electron microscopy is limited mainly by chromatic aberration, we decided to propose a corrector only for STEM mode, which is not affected by broadening of energy spread by a sample. In spite of the fact that the contribution of spherical and chromatic aberration are comparable in size, the use of hexapole corrector (capable of spherical aberration correction only) is still beneficial. Because of all mentioned weaknesses, it is intended to be the first developing step leading to a combination of the hexapole corrector with CFE cathode or monochromator.

The considered corrector setup contains two electrostatic hexapoles separated by a magnetic round-lens doublet. The design of these two transfer lenses is critical for the correct function of the system. The configuration based on one set of permanent magnets (2 or more pieces of permanent magnets) with magnetization direction perpendicular to the optical axis has been proposed to ensure the maximum possible symmetry.

Utilized kind of a magnetic lenses with magnetisation of permanent magnets perpendicular to the optical axis is described in detail in [106]. This lens technology follows the philosophical concept of low voltage microscopes manufactured by Delong Instruments company.

The most convenient arrangement of the transfer lens doublet contains 4 permanent magnets stuck on the walls of the inner cuboid-shaped polepiece. Both pole pieces are

made of a soft iron with high magnetic conductivity. It guarantees a rotationally symmetric axial field of the permanent magnet lenses. The positioning of the permanent magnets between the inner and outer polepiece is shown in the figure (7.1). The number of magnets can vary without any significant influence on the axial field quality. It was decided for four-fold symmetry due to the fact that a high number of magnets causes demagnetization of separate magnetic elements. The higher Fourier components of the magnetic field depend only on the deviation of the rotational symmetry of the bore, not on the spatial distribution of the magnetic charge.

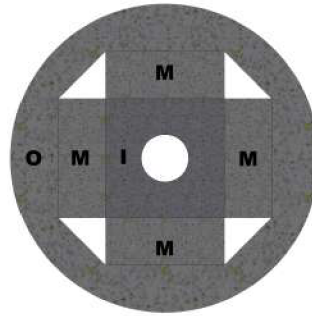


Figure 7.1: The case of 4 permanent magnets (M) arrangement, where magnets fill the space between the inner (I) and outer (O) polepieces.

The absence or respectively minor importance of the higher-order Fourier components of the magnetic field is proved by the FFT image of the micrograph made by the LVEM5 with condensor-objective double lens based on permanent magnet technology. The image capturing thin carbon foil is intentionally slightly out of focus for easier verification of the FFT's circular shape.

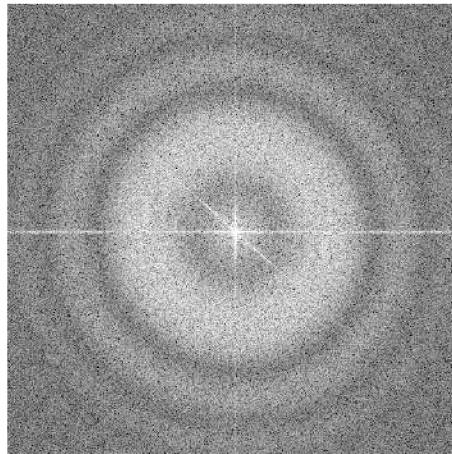


Figure 7.2: FFT image of thin carbon foil. The circular shape of the fringes indicates rotational symmetry of the axial magnetic field.

Electrostatic and conventional magnetic lenses were also considered for the purpose of the transfer lenses [107]. An electrostatic solution has proved to be unacceptable because of a crucial increase in chromatic aberration, much higher than in the case of magnetic lenses. According to our calculations, the contribution of an electrostatic doublet to

the chromatic aberration of the microscope is almost 3 times higher than in the case of magnetic lenses.

Conventional magnetic lenses were excluded due to the strictly limited space requirements. The basic configuration of the LVEM produced by DeLong Instruments is based on the desktop concept, therefore it was highly desirable to maintain approximate dimensions of the original microscope. The coils of conventional magnetic lenses would be too massive [108]. The significant changes in the proportions of the main microscope column could cause additional vibrations and mechanical instabilities, thus require further modifications.

This main idea of permanent magnet concept is derived from well-proven LVEM5 and LVEM25 technology developed by DeLong Instruments [55][56].

If we use the same permanent magnet concept, we can design a compact corrector that fits the microscope column. This technical solution allows to avoid a huge electromagnetic windings, which can be substituted by small permanent magnets supported by weak electromagnetic windings situated directly in gap regions of lens doublet. The total size of the corrector column is dependent mainly on the focal length of the transfer lens. However, the shortening of their focal length leads to an increase in the undesirable effect of the chromatic aberration [63]. Therefore, the overall dimension of the corrector is a compromise between mechanical requirements and the focal length of the transfer lenses. A focal length of a transfer lens approximately 30 mm seems to be an acceptable choice between chromatic deterioration and column extension. Such a focal length of a single transfer lens leads to the total length of the corrector to be about 150 mm and radius 17 mm, not including vacuum chamber.

The basic concept is shown in figure (7.3). It consists of outer and inner pole pieces, permanent magnets with magnetization perpendicular to the optical axes and two hexapoles. The described rotationally symmetrical magnetic lenses using permanent magnets always creates an inseparable couple with a common magnetic circuit. The transfer doublet of the corrector benefits from the above-mentioned physically inevitable coupling of the lenses. Both lenses of the doublet have a common source of magnetic fields, therefore identical fields excitation, and consequently maximal symmetry, is theoretically guaranteed.

Parallel beam leaving the corrector is ideal entrance for following condensor-objective double-lens. Due to the fact, that permanent magnets can not be switched off, corrected STEM mode with uncorrected TEM mode was proposed to alternate, where chromatic aberration of illumination beam added by transfer lens doublet is not important.

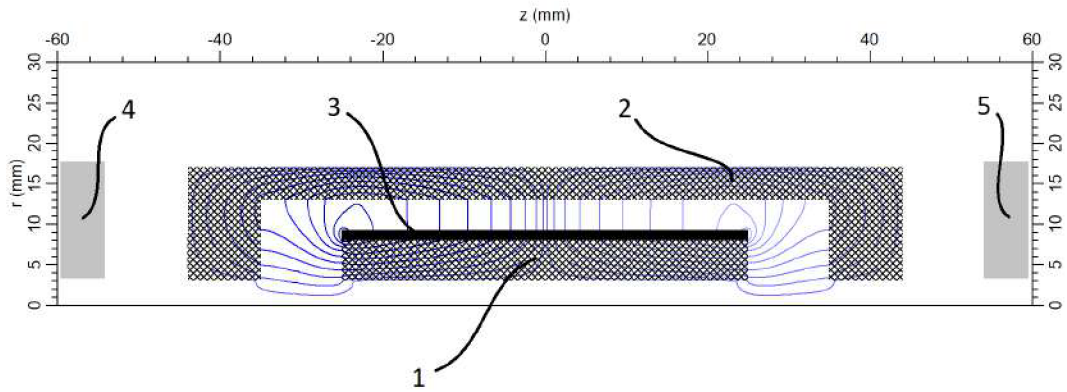


Figure 7.3: The basic concept of the developed hexapole corrector consists of inner (1) and outer (2) shared pole-pieces of the transfer lenses, permanent magnets (3) and two hexapoles (4) (5).

Due to the location of the magnets in the central part of the doublet, the magnetic field of a single lens isn't perfectly shaped. There is, however, excellent symmetry with respect to the center of the doublet.

The above-described corrector is encapsulated in the main vacuum chamber of the microscope. The positioning and mechanical stability of permanent magnets is ensured by magnetic forces of the magnets themselves and additionally secured by non-magnetic fixation cage. Such magnet fixation guarantees a sufficient precision because the position of the magnets is not a very critical parameter.

# 8. ADJUSTMENT OF THE CORRECTOR

The transfer lens doublet needs to be adjusted very precisely, otherwise there is a severe deterioration of the correcting action [109]. Above all, the arrangement of the individual optical elements with respect to each other must be strictly kept. Despite accurate manufacturing, the presence of compensation coils will be necessary, mainly due to manufacturing and material limitations of the permanent magnets. Three adjusting systems were used in our proposal: *Compensation coils* able to set a focusing power of the transfer lenses, *asymmetry elimination coils* solving the problem of precise specification of the symmetry center and output beam parallelism, a *solenoid* capable of counter-rotating the residual beam rotation.

## 8.1. Compensation coils

The windings of the two independent asymmetry elimination coils and two compensation coils in series are situated in the gap region of each lens of the doublet, and/or around the inner shared pole-piece. According to our calculations, their position is not a critical parameter, therefore one particular solution can be chosen based on technical and design requirements.

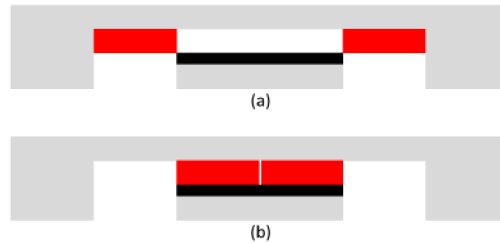


Figure 8.1: The corrector draught with the highlighted two possible positions of the compensation coils (denoted by red color).

Although both concepts are capable of sufficient compensation, we prefer the solution denoted (a) because the crosstalk between the fields created by individual coils is minimal and therefore the asymmetry elimination effect is higher, comparing with design (b). Thus the action of individual coils is more independent, making a doublet alignment easier. The crosstalk of the coil magnetic fields for both designs is shown in Fig. 8.2. It is clearly visible that a crosstalk is much smaller in the case of spatially separated coils.

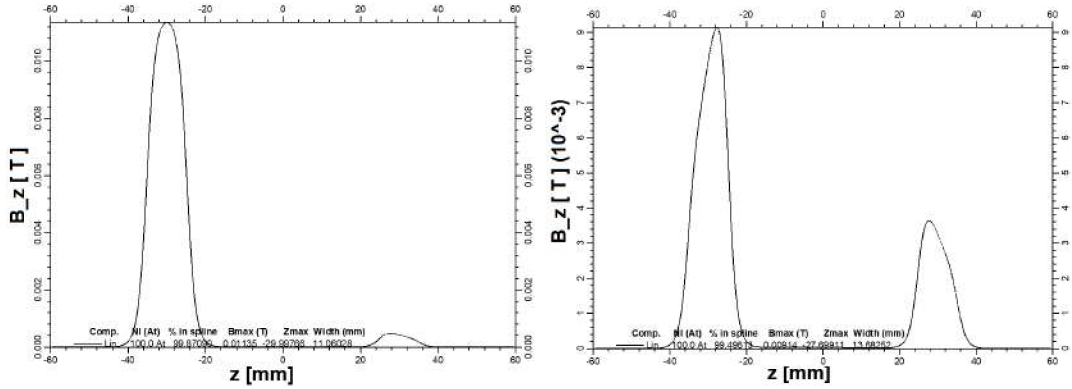


Figure 8.2: A comparison of the coils interaction with themselves. Only the left coil of both concepts (figure 8.1 (a) and (b)) is excited. The left figure corresponds to the design (a) with more spatially separated compensation coils and thus the minimized crosstalk. The right figure illustrates significant field crosstalk in case of design (b).

Both designs still provide enough space to add other correcting octupoles to the unoccupied gap region, if needed. The preferred concept with more spatially separated compensation coils is detailed in the picture below (8.3).

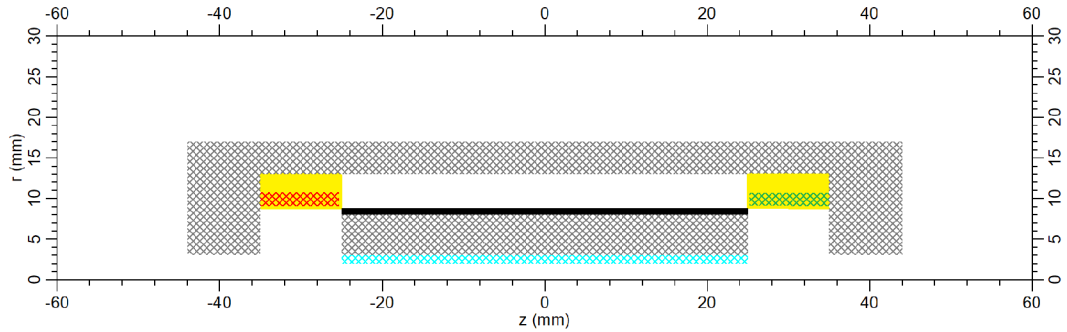


Figure 8.3: The design of the transfer lens doublet. Individual parts are marked with colors: Compensation coils - yellow, asymmetry elimination coils - red and green, permanent magnets - black, rotation correction (solenoid) - blue.

## 8.2. Required manufacturing accuracy

The major violation of the symmetry of the transfer lens doublet is caused by the imperfect amount of a permanent magnet's mass. Despite the high manufacturing accuracy, it is still a very critical parameter, especially because it is an untunable parameter. Therefore, the above-mentioned additional correction elements are necessary.

The adjustability of the transfer lens doublet had to be proved for the range of permanent magnet dimensions according to reasonable tolerances. Verification has been done for magnet thickness  $\pm 0.03$  mm from an ideal dimension, which corresponds to a  $\pm 4.2\%$  change in volume of the magnets. Such a manufacturing accuracy is commonly achievable.

Three basic parameters have been studied: Residual beam rotation behind the magnetic field of the second transfer lens, position of the middle crossover between the transfer lenses and parallelism of the beam after passing the corrector.

Residual beam rotation caused by the inaccuracy of magnet thickness has appeared to be completely negligible because doublet design is rotation-free, in principle. It is

also proved by calculation, the results of which are shown in figure (8.4). The above-mentioned rotation is several orders of magnitude smaller in value than the effect of the rotation correcting solenoid.

The position of the central crossover seems to be a more crucial parameter. Considering the above-mentioned manufacturing accuracy of  $\pm 0.03$  mm of the magnets, the crossover can move approximately  $\pm 0.02$  mm along the z-axis from an ideal central position in the middle of the transfer doublet. Naturally, it severely damages the essential symmetry of the corrector.

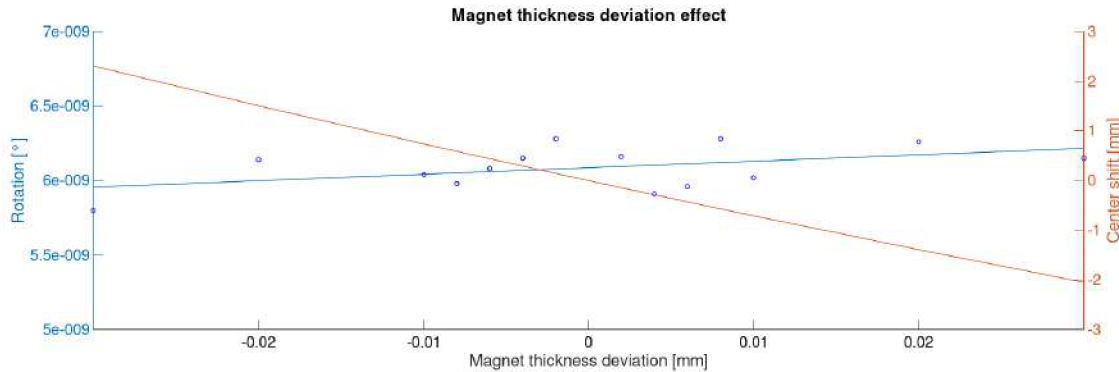


Figure 8.4: Magnet resizing effect on residual beam rotation and position of the middle crossover between transfer lenses. The spread of rotation values is caused by calculation error. Magnet size change  $\pm 0.03$  mm.

Symmetry disruption leads to a fatal effect on the objective focus beam size. The above-mentioned tolerance of the permanent magnet mass can cause an enlargement of the focus beam diameter 5 times in the worst case, even for the best-found hexapole excitation.

### 8.2.1. Correction for the amount of magnetic charge

The transfer lens doublet is designed for one particular electron energy, but it is not feasible to guarantee proper doublet adjustment just by the manufacturing process for several reasons.

An inaccurate amount of the permanent magnet mass causes a shift of the middle crossover between transfer lenses. The precise amount of magnetic charge is unknown not only because of manufacturing imperfections, but also because we don't know the exact material properties of the magnets which are used. So even in case of perfect manufacturing and magnetic field measurement during the manufacturing process, it would not be possible to achieve optimal magnet assembly for the correct doublet adjustments. In addition, the compensation system is able to optimize the doublet for precise beam energy, which can be slightly modified by the user for focusing. The compensation system is therefore a necessity.

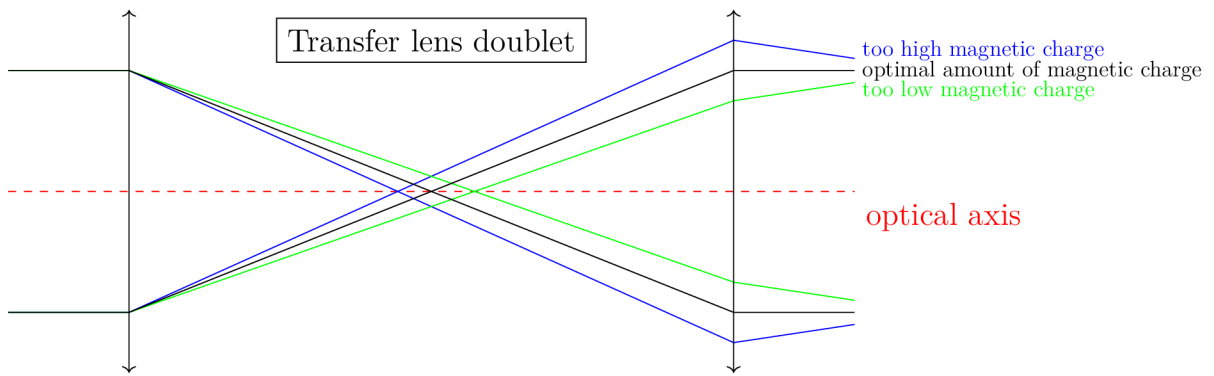


Figure 8.5: Ray diagram of transfer lens doublet with too low and too high amount of magnetic charge. The resultant change of the optical powers of the lenses caused a nonparallel output beam, creating inappropriate input for the second hexapole.

The compensation of this mid-plane symmetry disruption is based on appropriate excitation of compensation coils, where coils have to be excited to the same level, but in the opposite manner. This is the first step of transfer lens doublet alignment. The identical excitation of the individual compensation coils guarantees the same gain or damping for both transfer lenses simultaneously. Both compensation coils have to be connected in series to a single electric current power supply to eliminate mutual instability of multiple separate power supplies.

The simulated range of the center shift is chosen with respect to the expected asymmetry caused by manufacturing inaccuracy. The consequences of the technical tolerances have been already discussed in detail. The excitation of the compensation coils necessary to fix a particular magnet size deviation is shown in the figure 8.6.

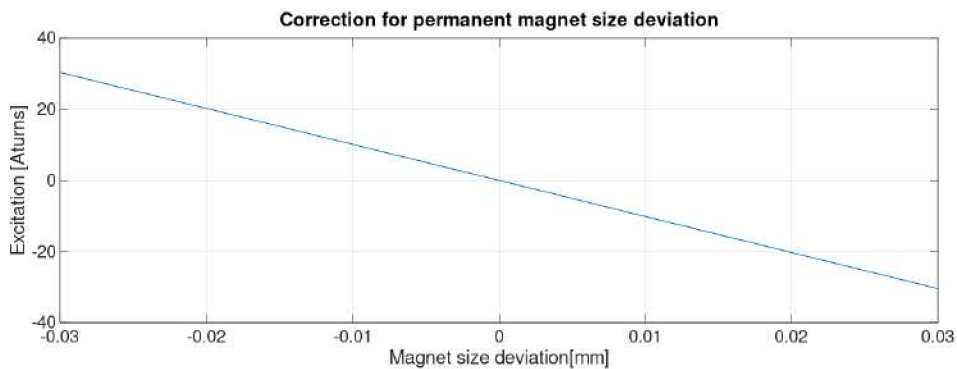


Figure 8.6: Necessary compensation coils excitation able to compensate a manufacturing size deviation of the magnets. The coils are excited in the opposite sense of electric current.

The limits of excitation in the graph consider the cross-sectional area of these coils to prevent heating caused by electric current in wires of the coils. Otherwise, the thermal stability of the system, and hence the remanence of the permanent magnets, may be affected. It could cause a change in the focal length of the lenses and therefore influence the adjustment of the doublet.

In the previous section, the monochromatic invariable electron energy has been considered, but for practical usage of the corrected microscope, high voltage will need to be changed within the range close to the ideal operational high voltage. It will also require

reconfiguration of transfer lens optical power by compensation coils to guarantee proper doublet function for particular electron energy.

### 8.2.2. Balancing of doublet asymmetry

Despite the compensation of the primary imperfection of the transfer lenses optical power described in the previous section, it may be necessary to use other auxiliary windings separately in an unbalanced regime to solve doublet asymmetry. These additional asymmetry elimination coils will be incorporated to the main compensation coils to have another free parameter to control for ideal beam parallelity behind the transfer lens doublet. Excitation of such a single-coil affects almost exclusively one transfer lens with very limited crosstalk to the other side of the doublet, Fig. (8.2).

According to the specific needs of the particular regime, asymmetry elimination coils can be used independently with different excitation of each coil. The position of middle crossover is affected almost exclusively by excitation of the first asymmetry elimination coil, located in the gap region of the first transfer lens. The second asymmetry elimination coil in the gap of the second transfer lens has the main task of fixing the output beam parallelism. Its effect on the middle crossover position is minimal, although it is non-zero due to the limited crosstalk of the fields.

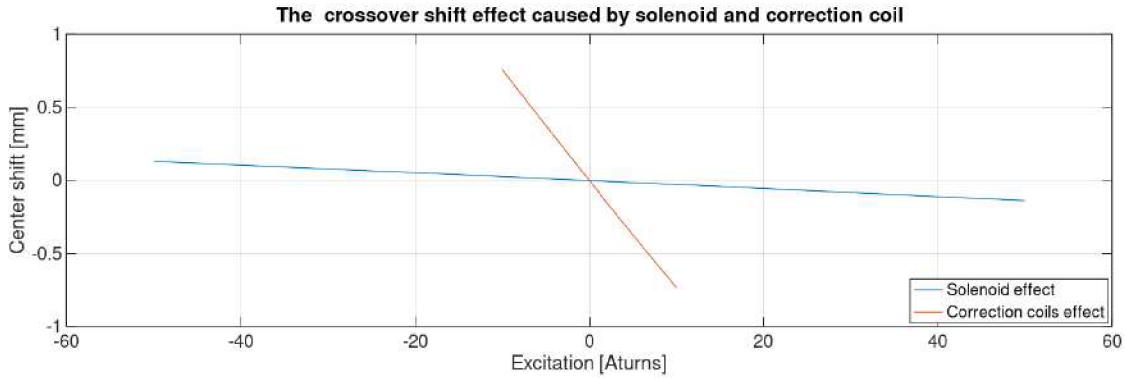


Figure 8.7: The comparison of crossover shift effect caused by doublet alignment elements. The undesirable crossover shift effect of the solenoid is almost negligible and easily reparable by compensation coils. The final setting is obtained by iteration method solving the problem of field crosstalks.

Doublet asymmetry is caused mainly by mechanical manufacturing, material inhomogeneities or magnetic defects. Another effect needs to be investigated is also optical power of solenoid lens, because there is a minor effect of auxiliary solenoid creating optical asymmetry. However its optical power is almost negligible and this source of asymmetry can be easily reduced by asymmetry elimination coils.

## 8.3. Residual beam rotation caused by compensation and asymmetry elimination coils

Although beam rotation should be zero in an ideal case, because of doublet symmetry, the residual beam rotation that needs to be dealt with is still present. This rotation exists primarily due to the activation of the compensation and asymmetry elimination coils. But

rotation correction is also necessary due to the precise orientation of the hexapoles, which can not be mechanically oriented with sufficient precision. In fact, identical orientation of the beam in front of and behind the doublet is required only due to the dependent action of hexapoles. Other parts of the imaging microscopy system are not sensitive to beam rotation.

It was necessary to integrate a component with minimum influence on adjustment of the doublet symmetry but with high rotation effect. The correction of the beam rotation is realized by a long solenoid placed in the bore region of the inner pole piece, blue color in figure 8.3. Such a correcting element has almost negligible influence on the position of the middle cross-section between transfer lenses. However, it is able to sufficiently eliminate residual rotation. The rotational ability of the solenoid is compared with the rotational side effect of the coils in the figure 8.8. The limits of excitation are also chosen with respect to the cross-sectional area of the solenoid winding and expected working conditions of the compensation coils.

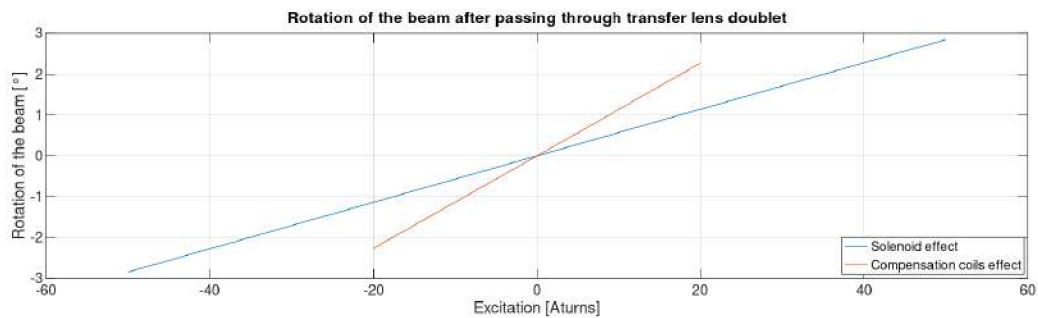


Figure 8.8: The comparison of the beam rotation caused by compensation coils versus rotation effect of the solenoid. Although solenoid rotates the beam less than compensation or correction coils for the same excitation, according to the figure 8.7, the solenoid can be excited to a sufficient level with minimal consequences for the doublet symmetry.

The rotation effect of the compensation coils is stronger than the rotation effect of the solenoid for the same excitation. However, solenoid still can be excited to a sufficient level to compensate residual rotation without the destruction of symmetry set by compensation and asymmetry elimination coils. It should be emphasized that the optical power of the solenoid is weaker than the optical power of common coil.

The comparison of graphs 8.8 and 8.6 proves adjustability of such a system. The whole corrector is a highly interacting unit, where the change of one subunit might alter the properties of the others, but important issue is that crosstalk is always weaker than the main correcting signal. This fact enables to iterate step-by-step up to the ideal setting. Because of the linear behavior of particular correction systems (particular magnetic fields are added or subtracted to each other), the optimal coil settings should be easily findable.

## 8.4. Parameters of Extended Hexapoles

The proper choice of mechanical dimensions of the particular segments of the corrector has a significant effect on the corrector properties and especially operating values.

The important parameters of the corrector design are without any doubt a length and bore diameter of the hexapole units. Theoretical interpretation of a hexapole length impact on a correcting power can be found in the section 3.1.1.

Therefore, in these calculations we defined goal to find the optimal hexapole parameters in terms of dimensions and thus keep the necessary voltage of the hexapoles at a reasonable level. Due to these reasons, the calculations with a different hexapole length and bore diameter has been performed.

For these simulations, we used model of ordinary electromagnetic objective lens with the gap of 5 mm and the bore radius of 2 mm, together with the electron beam confined by a circular aperture with radius of 0.025 mm.

The default dimensions have been derived in accordance with the current, practically proven, design of LVEM25. The results of the calculations found clear support for the hexapole dimensions of the presented concept.

The optimal configuration seems to be the hexapole with its bore diameter of 4 mm and 20 mm in length. In this case, the required voltage of 298 V was found, which is acceptable from technical point of view. To get an idea about behaviour of hexapole parameters, it can be mentioned that the elongation to 26 mm causes a decrease of necessary voltage to 90 V. On the contrary, shortening to 14 mm is responsible for increase of required voltage to 490 V, while maintaining the other parameters.

The comparison of different hexapole bore diameter revealed that optimum is 4 mm. Slightly bigger diameter (i.e. 6 mm) results in a significant increase of the necessary high tension applied on the hexapoles (950 V).

Precise values of required voltage are, indeed, highly dependant on the lens, which should be corrected, but all investigated models, corresponding to assumed parameters of corrected LVEM25 objective, would require a technically acceptable hexapole voltage lower than 500V.

The found range of required hexapole voltage is in a good agreement with previous studies and designs wherein multipoles of the similar construction have been used. The following picture 8.9 summarizes final corrector design with entire adjusting system. The total size of the corrector assembly is pointed out to emphasize the minimal dimension fitting to benchtop low-voltage electron microscopes.

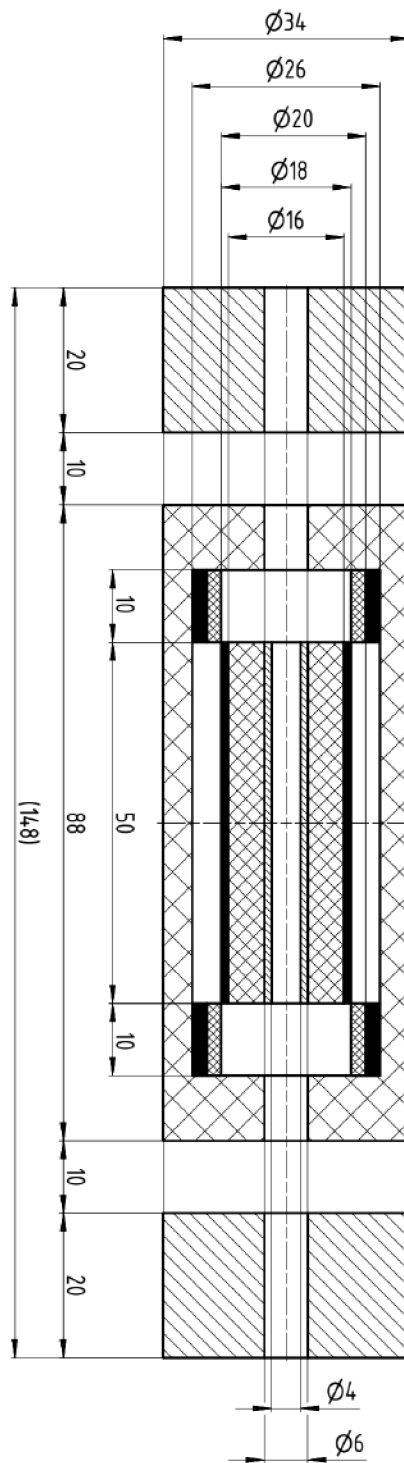


Figure 8.9: Mechanical drawing of presented novel hexapole corrector with all components of adjusting system.

# 9. CORRECTION POWER OF THE HEXAPOLE CORRECTOR

In order to perform the simulation of particle tracing and to calculate the aberration coefficient EOD software was used [110]. The above-described corrector is intended for STEM mode, therefore the success of the correction has been evaluated according to the radius of a disc of least confusion. The value was deduced from the trajectory diagram in fig. 9.1. The optical model used for computational testing of the correction ability consisted of a hexapole corrector and a simple magnetic objective lens with a long focal length of 9 mm, and thus a high spherical aberration  $C_s = 32$  mm (the value calculated by EOD). The idea of used experimental optical assembly is similar to Möllenstedt's approach mentioned in the section 1.4.

The radius of a disc of least confusion for the uncorrected (hexapoles turned off) and corrected setup (with the best-found hexapole excitation) has been calculated. The disc of least confusion of the magnetic lens in the above-mentioned assembly has a radius of approximately 100 nm with turned-off hexapoles. An extremely wide initial beam with a 0.4 mm diameter was used. Considering the above-mentioned focal length of the magnetic lens, the aperture angle is  $\alpha = 22$  mrad. Such an unrealistic extreme example of poor quality lens has been chosen as a model because of a strong manifestation of the primary spherical aberration.

Optimal hexapole excitation was found for a perfectly symmetrical corrector without the necessity of additional correction by compensation coils. The radius of the disc of least confusion was at least 20 times smaller. The radius deduced from the trajectory diagram was 5 nm in this case. The residual dimension of the disc of least confusion was not the result of the remaining primary spherical aberration, but rather associated with numerical noise. Further refining of the calculation made no sense in this basic case of a low-quality lens. The comparison of the trajectory diagrams of the crossover area of corrected and uncorrected mode is shown in figure 9.1. All calculations were done for electron energy 25 keV, considering a major influence of spherical aberration and minor effects of other axial geometrical aberrations. The limiting effect of diffraction and chromatic aberration is not considered in all mentioned electron tracing simulations. Their influence on low voltage electron microscopy was discussed in detail in [97].

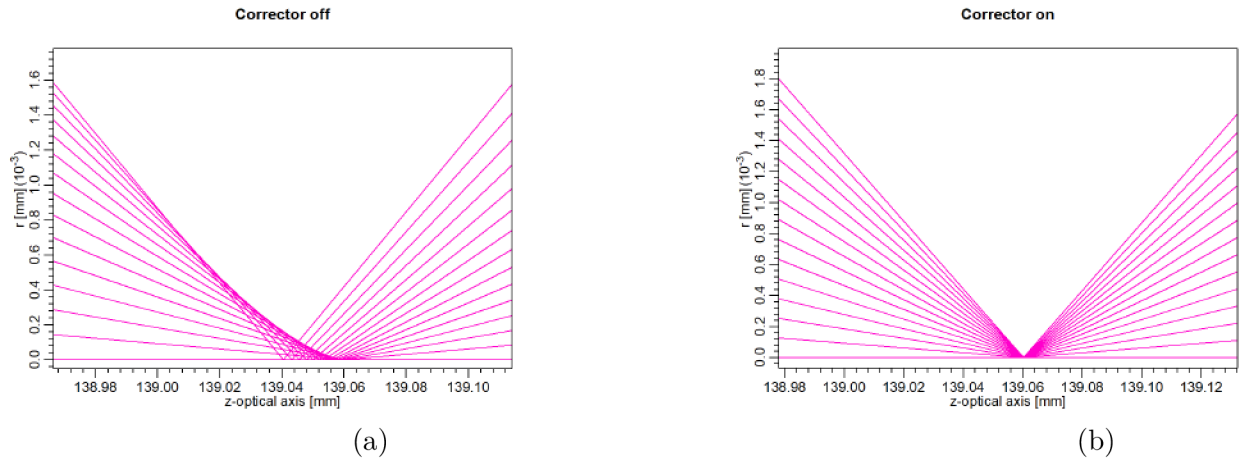


Figure 9.1: The details of the area near the focus of the rays behind a simple magnetic lens. The axis denoted  $r$  represents the distance from the optical axis. Figure (a) shows the situation with hexapoles turned off. The activation of hexapoles with proper excitation is responsible for aberration correction. The correcting ability is clearly visible by the size of the intersection, figure (b).

Small deviations from an ideal situation were also calculated. The permanent magnet volume was changed according to the tolerance defined in section ["Required manufacturing accuracy"](#) and optimal hexapoles excitations have been found through this interval. The radius of the disc of least confusion for a maximal investigated magnet thickness deviation of 0.03 mm is reduced only 10 times from the uncorrected state.

The attainable radius of the disc of least confusion for different precision of the doublet center positioning with an optimal correction voltage on hexapoles is presented in figure [9.2](#).

The optimal hexapoles excitation of approximately 107 V has been found for the considered examples. The precise values of optimal excitation have to be fine-tuned for every particular situation. Particularly the length of the hexapoles and doublet center setting are determining parameters for the required voltage on the hexapoles. However, adjustments are not unfeasibly sensitive as it is clear from the simulations. Our corrector design takes account of hexapoles with a length of 20 mm. The sufficient length is an important parameter of hexapoles used in correctors because too short hexapoles induced only threefold astigmatism and their third-order effect can not be fully developed. However, the length of 20 mm seems to be long enough to have a sufficient correcting effect on the hexapoles.

The optimal hexapole excitation values are characteristics of the particular system. But it can be assumed that required voltages are in reasonable range with consideration of technical design conditions.

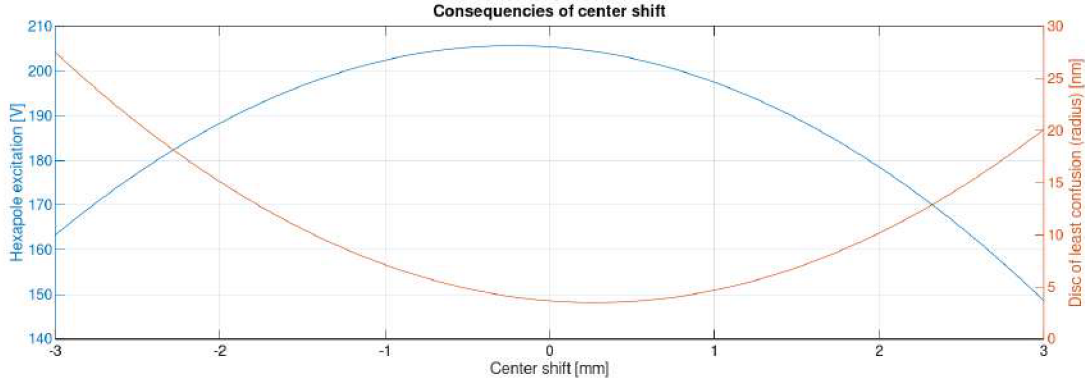


Figure 9.2: The optimal hexapole excitation necessary for the best possible correction is changing with precision of corrector adjustment. The highest excitation is expected to be needed for ideal alignment and it decreases with the higher level of misalignment. The correlation with the attainable radius of the disc of least confusion is also clear from the graph. However, the importance of the deterioration is significant, especially for very high misalignment. The expected precision of the corrector adjustments should guarantee minimal influence of the central crossover position.

The correction power of the hexapole corrector also has been investigated for energy spread  $\pm 1$  eV. The disc of least confusion has enlarged approximately twice in size in comparison with a perfect beam conditions reached by 25 keV electrons. Thus the correction power has been preserved but its efficiency is significantly lower.

Although the mechanical assembling can be done very precisely, it is still a limiting factor. Due to such a high demands on required manufacturing mechanical accuracy, it is very important create a sufficiently adjustable system. Therefore dodecapoles are likely to be used instead of a simple hexapoles in terms of providing extra opportunities and flexibility to proper adjustment and alignment of the corrector.

The twelvepole element is naturally able to excite the hexapole field just like hexapoles themselves. Except for this hexapole component, essential for spherical aberration correction, it can excite additional dipole and/or general quadrupole fields available for lateral positioning and correction of astigmatism.

All of these alignment capabilities are necessary because manufacturing imperfections and unavoidable material inhomogeneities do not allow us to create the ideal hexapole field by a simple sixpole element. Also due to assembling accuracy limitations, the symmetry axis of the multipoles does not generally coincide with the optical axis of the rest of the device. Undesirable combination of a resulting weak parasitic quadrupole misalignment field with a strong main hexapole field of the corrector can result in axial coma, star aberration and three-fold astigmatism.

To guarantee all the above-mentioned conditions we decided to incorporate rather dodecapoles, that are able to center the hexapole component of the multipole field about the common optical axis.

To verify the ability to correct the spherical aberration of the objective lens of the electron microscope with parameters of LVEM25 the appropriate model of the optical arrangement has been proposed. A simple magnetic lens with adequate geometry to achieve 1 nm resolution or better and also in general agreement with LVEM has been used. The objective model lens has a 5 mm gap and a bore diameter of 4 mm. The design

together with the result of the magnetic field simulation of this lens is shown in the figure (9.3).

### Magnetic lens design (objective)

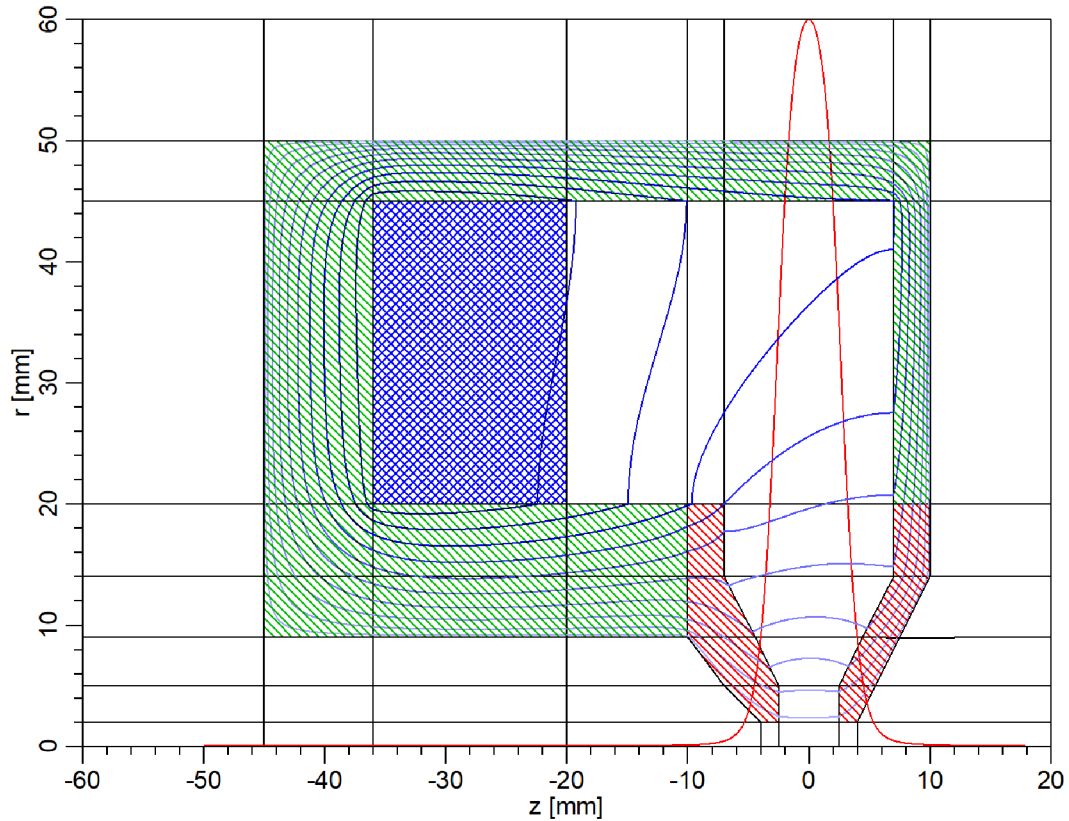


Figure 9.3: Model of the objective lens with desired optical properties. This model lens has been created to simulate properties of LVEM25 objective by lens with conventional design. Gap 5 mm, bore-diameter 4 mm.

The above-mentioned model objective lens capable of high-resolution imaging was combined with the same transfer lens doublet fig. 8.3 with focal lengths 30mm of each transfer lens. The permanent magnets placed on the inner pole piece are able to create an appropriate magnetic field fig. 9.5, which is easily adjustable by a compensation system for precise doublet setting, fig. 9.4.

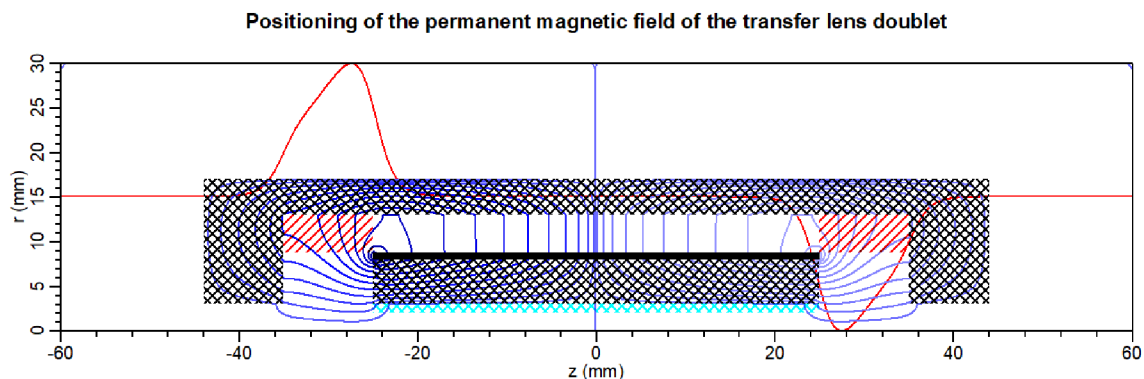


Figure 9.4: Magnetic field isolines and axial magnetic field of the transfer lens doublet (red line). Compensation system - red hatched array, permanent magnets - full black array, rotation correction (solenoid) - blue.

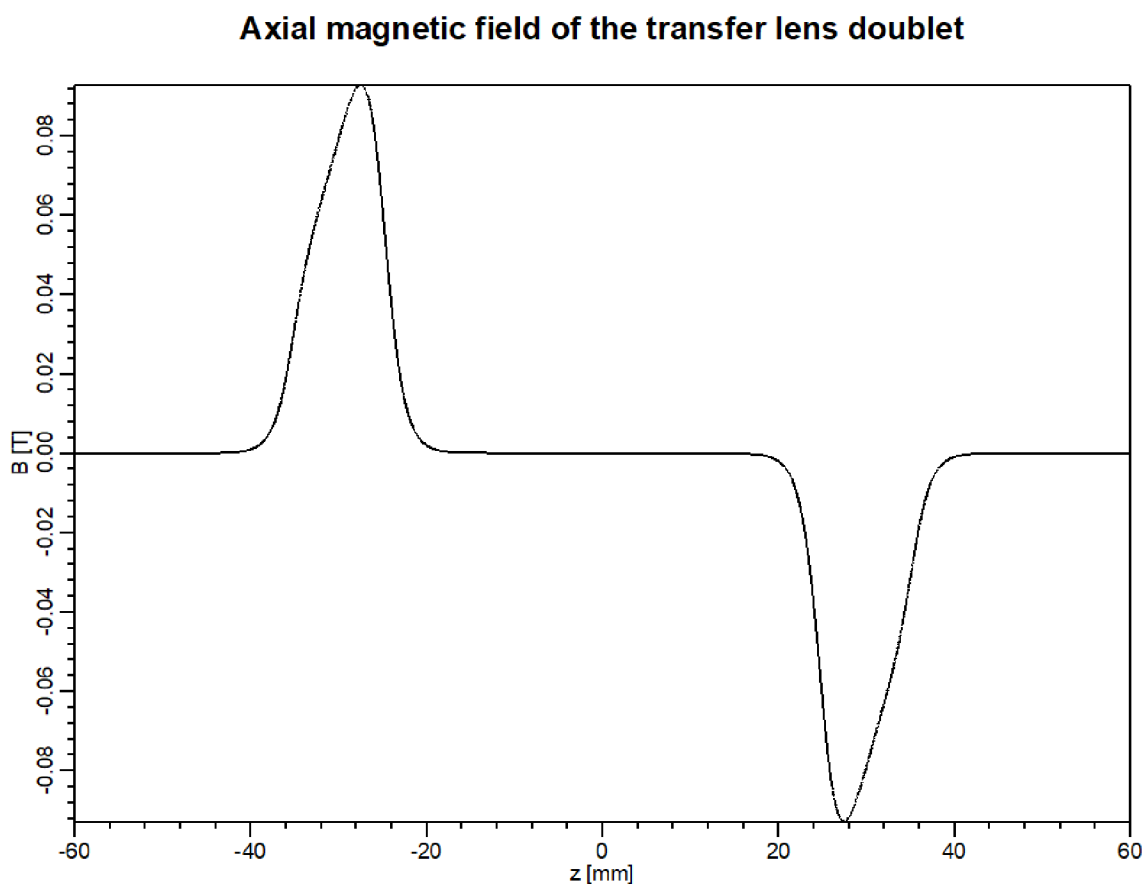


Figure 9.5: Axial magnetic field of the transfer lens doublet based on permanent magnet technology calculated for the design shown in the previous picture (9.4).

The form of zoomed crossover area in figure 9.6 with no visible manifestation of primary spherical aberration proves the correcting ability of the presented hexapole corrector even for system with high-resolution potential. The dimension of the above-mentioned crossover area (shown in the figure 9.6 is determined especially by numerical noise of chosen calculation accuracy. The real spatial resolution of such a system would be limited mainly by chromatic aberration. The effect of chromatic aberration and diffraction on aperture severely increases the dimension of the total disc of least confusion. In such a

case more close to reality, considering Schotky cathode with energy spread of 0.6 eV, lens with  $C_c = 1$  mm and optimal aperture angle (14 mrad), the expected spatial resolution of described system corrected for spherical aberration would be approximately 0.47 nm. Using standard formula:

$$d = \sqrt{(k_1 C_s \alpha_i^3)^2 + \left(k_2 \frac{\Delta E}{E_0} C_c \alpha_i\right)^2 + \left(0.61 \frac{\lambda}{\alpha_i}\right)^2}, \quad (9.0.1)$$

where standard notation is used [27].

The calculation was done for electron energy 25 keV. The required voltage on hexapoles in the presented setup is 493 V. The optimal voltage is in a reasonable and feasible range.

#### Crossover area of the model objective lens

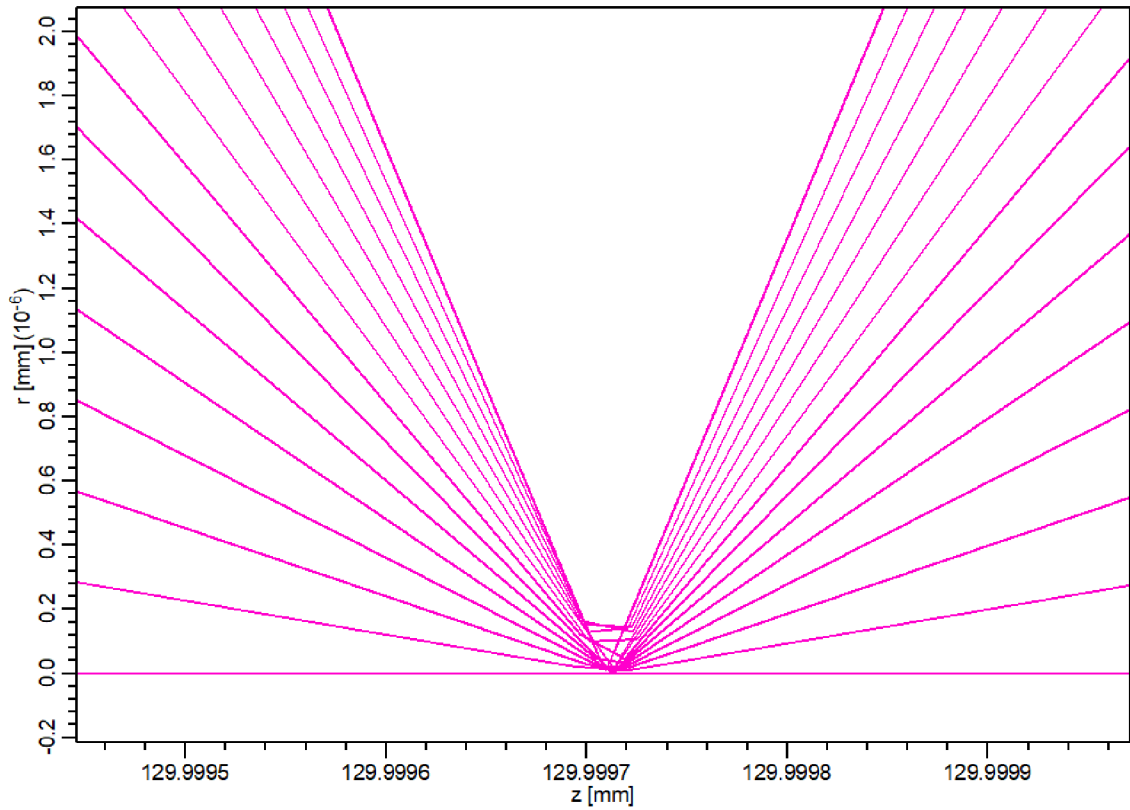


Figure 9.6: Picture shows corrected crossover area. Objective lens parameter of the presented model: gap 5 mm, bore-diameter 4 mm. Hexapole length 20 mm. The optimal hexapole voltage 493 V has been applied.

# 10. MANUFACTURING NOTES

Besides the theoretical principles of design, there is also the aspect of practical realisation which has to be discussed. The introduced hexapole corrector consists of four individual subassemblies with different manufacturing needs: magnets, magnetic circuit, hexapoles, and compensating coils. Therefore they will be discussed separately.

## Permanent magnets

As a source of a magnetic field used in the presented unique concept of the transfer lens doublet, permanent magnets are employed. The market offers a broad range of magnets with various parameters and the most suitable candidate must be carefully selected. The magnets denoted VMM7UH-N42H offering high performance have been chosen due to their optimal properties. This grade of magnets produces a sufficient magnetic field together with the necessary temperature resistance. This is especially important during the assembly process, when the vacuum chamber usually has to be baked several times to reach a sufficiently high level of vacuum inside the chamber.

Blocks of magnetic material are firstly modified to the required dimensions and equipped by a protective nickel layer afterward. In order to provide appropriate magnetic properties they firstly have to be completely demagnetized during the manufacturing procedure and then magnetized again until the full saturation.

## Magnetic circuit

The magnetic circuit is designed to be made of magnetically soft iron with carbon content less than 0.01%. This material is not sensitive to external stresses causing variation in magnetic properties. Compared to the usual conventions, soft iron for the magnetic circuit is not annealed to prevent the creation of bigger grains in the material structure and thus the magnetic homogeneity of the material is guaranteed. The absence of large domains with specific magnetic orientation helps to eliminate another potential source of an astigmatism.

The magnetic circuit is treated with a chemical nickel plating to prevent corrosion. The thickness of the nickel layer is approximately  $7\mu m$ , thin enough so that nickel does not affect the magnetic properties.

The whole body of magnetic circuit should additionally be magnetically shielded, because soft iron with its low permeability has an inefficient shielding effect for a small magnetic field. A suitable material for this purpose with a high permeability is alloy 78.

## Hexapoles

Hexapoles should be manufactured from the nonmagnetic material. Precisely titan grade 2 is preferred for this purpose. This widely commercially available titan grade was chosen because it possesses good weldability, sufficient strength, ductility and plasticity. The manufacturing cutting process is performed by electric discharge machining (EDM) and

the surface of the semi-finished product is treated by physical vapor deposition by titan or molybdenum. Thanks to this ingenious design, it is guaranteed that nonconductive parts of the hexapole are not visible from the optical axis. Thus it is possible to apply a layer on the polepieces of the hexapole by a wire placed on the optical axis.

## Coils

The last components for the brief manufacturing notes is the system of auxiliary coils, namely compensation coils, asymmetry elimination coils and long solenoid. They have to be winded by the wire with vacuum compatible isolation. The temperature resistance must also be taken into account because the whole system will be baked, hence the wire isolation should be able to withstand the temperature  $120^{\circ}C$ .

# 11. CONCLUSIONS AND FUTURE DIRECTIONS

*The mountains are calling and I must go.*

— John Muir

The presented thesis deals with the issue of aberration correction in case of low-voltage electron microscopes. The whole text began with an introduction into the historical context. The groundbreaking cornerstones of electron microscopy are chronologically summarized with special attention paid to the work of professor Armin Delong's research group in Brno and to the projects leading to aberration corrected system.

Then, the particular systems LVEM5 and LVEM25 are also briefly introduced together with the description of unique features and benefits of low-voltage electron microscopes. Finally, several basic correction principles and particular systems are mentioned and thoroughly clarified according to their importance for understanding this research or their promise of use.

The aberration corrected LVEM is a very promising technology, suitable for imaging of sensitive samples. In contrast to the conventional TEMs, it provides more enhanced contrast, especially when observing samples containing light atoms, where achieving sufficient contrast is often challenging. The current development of these devices focuses on the integration of the aberration corrector optimized for low-voltage systems.

In the beginning, the logically raised question, whether this principle can be advantageously applied also to the special case of low-voltage instruments, had to be answered. Thus, the initial analysis of feasibility and consideration of the potential benefits has been done. Overall, the presented findings about aberration effects confirm the indisputable improvement of the spatial resolution where aberration correction of low-voltage electron microscopes is concerned, compared to uncorrected systems. However, there are still plenty of factors to be considered.

A new solution of a hexapole corrector tailored to the needs of STEM mode of desktop low-voltage transmission electron microscopy has been presented. Attention has been paid to low complexity and the possibility of miniaturization, which are the key aspects to integrate it to the desktop low voltage microscope column.

The next subject of discussion was the issue of chromatic aberration contribution. According to our findings, consistent with theoretical research, the influence of chromatic aberration appears to be crucial. In addition, the unavoidable transfer lenses of a hexapole corrector itself increase the total chromatic aberration of the whole system. Magnetic lenses need to be used for this purpose due to their lower deterioration of chromatic aberration, as opposed to using electrostatic ones, which deteriorate chromatic aberration severely. Our calculations indicate that the contribution of an electrostatic doublet to the chromatic aberration is almost 3 times higher. Due to this dramatic deterioration, we concentrated on magnetic doublets, more specifically those designed with permanent magnets because of the dimension parameters of the desktop LVEM.

The contribution of transfer lenses to the total chromatic aberration is more significant for lenses with a short focal length. A compromise between an acceptable size of the corrector and the influence of chromatic aberration was set at 15 – 30 mm as the focal

length of a single transfer lens. According to all of these conditions, the main column of the corrector should be less than an acceptable 150 mm in length.

Magnetic lenses used for this purpose would require a special design based on the permanent magnets, because conventional magnetic lenses (even weak enough) that are suitable in terms of chromatic aberration, would be too massive and therefore they are not dimensionally compatible with the corrector for the desktop LVEM.

An additional unwanted contribution of the unnecessary transfer lens doublet to the chromatic aberration can be only reduced by the above-mentioned proper system design. In principle it can not, however, be corrected by a hexapole corrector. To deal with the deterioration caused by the chromatic aberration, the energy spread has to be eliminated. To keep the influence of the chromatic aberration below or at least comparable with the spherical aberration, it is necessary to reduce all possible unwanted contributions to chromatic aberration. The reported maximum value of the energy spread is at the limit of attainability by current monochromatization [102] [111]. For these reasons, it is more convenient to use the corrector for STEM application, because there is no additional broadening of the energy spread caused by an interaction with a sample.

The concept based on high-quality permanent magnet lens doublet has been supplemented with correction elements suitable for proper alignment. A significant part of the text is devoted to the validation of the functionality of the adjusting system, which was carefully designed for the specific needs of a miniaturized hexapole corrector.

The primary doublet adjustment is realized by equally excited compensation coils. It deals with the issue of permanent magnet manufacturing imperfections, which leads to an inappropriate focusing power of the doublet lenses. The second stage of alignment corrects doublet asymmetry. It is done by additional windings called asymmetry elimination coils, which are incorporated into the compensation coils. Their excitations can be chosen according to the specific needs of a particular system to guarantee the position of the doublet center and beam parallelism behind the second transfer lens. The requirements for power supply stability and mechanical manufacturing are feasible with the current technology.

The contribution of aberration correction has been investigated for different conditions and level of adjustment. The model optical systems, consisting of the corrector and magnetic objective lens are sensitive for any considered parameter. However, our results provide evidence for sufficient efficiency of the correction elements to solve all manufacturing imperfections.

The last part of this thesis was devoted to the few manufacturing hints providing a practical view of the instrument design.

The aforementioned thesis casts a new light on the possibility to realize an aberration-corrected LVEM with compact dimensions. We expect that the described corrector incorporated to LVEM25 will improve the resolution by 20%. The reported aberration-corrected LV-STEM will provide substantially enhanced contrast for light element samples making it convenient for biological sciences with no need for additional contrast-enhancing staining. The key application areas considered for this instrument are in virology, pathology, and drug delivery research.

Based on the presented research, two articles were published. The first one: *Aberration correction for low voltage optimized transmission electron microscopy* [97]; published in MethodsX in 2018, can be considered as a feasibility study of using corrector with LVEMs.

The second article: *Hexapole corrector for LVEM* [113]; introduced in Ultramicroscopy in 2020, presented the novel concept of the hexapole corrector in detail.

The unique features of the corrector concept were included in the Czech patent assigned a number 308174:

*Korektor sférické vady v zařízení se svazkem nabitých částic a způsob korigování sférické vady další čočky, typicky objektivové čočky, tímto korektorem*

*EN: A spherical defect corrector in a charged particle beam device and a method for correcting the spherical defect of another lens, typically an objective lens, by this corrector.*

# Bibliography

- [1] DELONG, A. *Elektronový mikroskop dnes a zítra*. Československý časopis pro fyziku 3, 2005.
- [2] KRIVANEK, O. L., LOVEJOY, T. C. and DELLBY, N. *Aberration-corrected STEM for atomic-resolution imaging and analysis*. Journal of Microscopy. 2015, 259(3), 165-172. DOI: 10.1111/jmi.12254. ISSN 00222720. Available from: <http://doi.wiley.com/10.1111/jmi.12254>
- [3] SCHERZER, O. *Sphärische und chromatische Korrektur von Elektronen-Linsen*. Optik, 1947.
- [4] HAWKES, P. W. *Aberration correction past and present*. Philosophical Transactions of the Royal Society A: Mathematical, Physical and Engineering Sciences, 367(1903), 3637-3664, 2009. DOI: 10.1098/rsta.2009.0004. ISSN 1364-503X. Available from: <https://royalsocietypublishing.org/doi/10.1098/rsta.2009.0004>
- [5] DE BROGLIE, L. *Recherches sur la theorie des Quanta*. Paris, 1924.
- [6] GILMORE, Ch. M. *Materials science and engineering properties*. Stamford, CT: Cengage Learning, 2015. ISBN 1111988609.
- [7] SMOLYANINOV, I. I. *Optical microscopy beyond the diffraction limit*. HFSP Journal. 2(3), 129-131, 2010. DOI: 10.2976/1.2912559. ISSN 1955-2068. Available from: <https://www.tandfonline.com/doi/full/10.2976/1.2912559>
- [8] HAWKES P.W. *Electron optics and electron microscopy: a personal retrospective*. Microscopy and Analysis, 25th Anniversary Issue September, 2012.
- [9] HAWKES, P.W. *The correction of electron lens aberrations*. Ultramicroscopy. 156, A1-A64, 2015. DOI: 10.1016/j.ultramic.2015.03.007. ISSN 03043991. Available from: <https://linkinghub.elsevier.com/retrieve/pii/S0304399115000509>
- [10] BUSCH, H. *Über die Wirkungsweise der Konzentrierungsspule bei der Braunschen*. Archiv für Elektrotechnik. 18, pp. 583-594, 1927.
- [11] HAWKES, P. *Recent advances in electron optics and electron microscopy*. Annales de la Fondation Louis de Broglie, Volume 29, Hors série 1, 2004.
- [12] ZOBAČ, L. Elektronový mikroskop v Č(SS)R očima pamětníka.
- [13] Institute of Scientific Instruments of the CAS [online] ISI CAS. Museum of the department of electron optics.[cit. 15.3.2020] Available from: <http://www.isibrno.cz/mih/muzeum/muzeumen.htm>
- [14] HAWKES, P. W. *The Beginnings of electron microscopy*. Orlando: Academic Press, 1985. ISBN 0-12-014578-2.
- [15] KOLAŘÍK, V. *Poznámky k historii elektronové mikroskopie v Brně*. Československý časopis pro fyziku 70, č.3, 2020.

- [16] HAWKES, P. W., KASPER, E. *Principles of electron optics*. Second edition. London: Elsevier/AP, Academic Press, an imprint of Elsevier, 2018. ISBN 9780081022566.
- [17] CREWE, A. V. *Limits of electron probe formation*. *Journal of Microscopy*. 178(2), 93-100, 1995. DOI: 10.1111/j.1365-2818.1995.tb03584.x. ISSN 00222720. Available from: <http://doi.wiley.com/10.1111/j.1365-2818.1995.tb03584.x>
- [18] CREWE, A. V., WALL, J., LANGMORE, J. *Visibility of Single Atoms*. *Science*. 168(3937), 1338-1340, 1970. DOI: 10.1126/science.168.3937.1338. ISSN 0036-8075. Available from: <https://www.sciencemag.org/lookup/doi/10.1126/science.168.3937.1338>
- [19] CREWE, A. V. *An Introduction to the STEM*. *Journal of Ultrastructure Research* 88, 94-104, 1984.
- [20] BECK, V.D. *Chicago aberration correction work*. *Ultramicroscopy*. 123, 22-27, 2012. DOI: 10.1016/j.ultramic.2012.06.005. ISSN 03043991. Available from: <https://linkinghub.elsevier.com/retrieve/pii/S0304399112001271>
- [21] HAIDER, M., HARTEL, P., MÜLLER, H., UHLEMANN, S, et al. *Current and future aberration correctors for the improvement of resolution in electron microscopy*. *Philosophical Transactions of the Royal Society A: Mathematical, Physical and Engineering Sciences*. 367(1903), 3665-3682, 2009. DOI: 10.1098/rsta.2009.0121. ISSN 1364-503X. Available from: <https://royalsocietypublishing.org/doi/10.1098/rsta.2009.0121>
- [22] SCHERZER, O. *Über einige Fehler von Elektronenlinsen*. *Zeitschrift für Physik*. 101, pp. 593-603, 1936.
- [23] HAWKES, P. W. *The Long Road to spherical aberration correction*. *Biology of the Cell*. 93, pp. 432-433, 2001.
- [24] GLASER, W. G. *Über ein von sphärischer Aberration freies Magnetfeld*. Prague, 1940.
- [25] MARKO, M., ROSE H. *The Contributions of Otto Scherzer (1909–1982) to the Development of the Electron Microscope*. *Microscopy and Microanalysis*. 16(4), 366-374, 2010. DOI: 10.1017/S143192761000019X. ISSN 1431-9276. Available from: [https://www.cambridge.org/core/product/identifier/S143192761000019X/type/journal\\_article](https://www.cambridge.org/core/product/identifier/S143192761000019X/type/journal_article)
- [26] SCHATTEN, H., PAWLEY, J. B. *Biological low voltage scanning electron microscopy*. London: Springer, 2008. ISBN 978-0-387-72970-1.
- [27] ORLOFF, J. *Handbook of charged particle optics*. 2nd ed. Boca Raton: CRC Press/Taylor & Francis, 2009. ISBN 978-1-4200-4554-3.
- [28] ERNI, R. *Aberration-corrected imaging in transmission electron microscopy: an introduction*. Hackensack, NJ: Distributed by World Scientific Pub. Co., 2010. ISBN 978-1-84816-536-6.

- [29] BATSON, P. E. *The First Years of the Aberration-Corrected Electron Microscopy Century*. Microscopy and Microanalysis. 18(4), 652-655, 2012. DOI: 10.1017/S1431927612001250. ISSN 1431-9276. Available from: [https://www.cambridge.org/core/product/identifier/S1431927612001250/type/journal\\_article](https://www.cambridge.org/core/product/identifier/S1431927612001250/type/journal_article)
- [30] INADA, H., ZHU, Y., WALL, J., et al. *The newly installed aberration corrected dedicated STEM (Hitachi HD2700C) at Brookhaven National Laboratory*. LUYSBERG, Martina, Karsten TILLMANN a Thomas WEIRICH, ed. EMC 2008 14th European Microscopy Congress 1–5 September 2008, Aachen, Germany. Berlin, Heidelberg: Springer Berlin Heidelberg, 31-32, 2008. DOI: 10.1007/978-3-540-85156-1\_16. ISBN 978-3-540-85154-7. Available from: [http://link.springer.com/10.1007/978-3-540-85156-1\\_16](http://link.springer.com/10.1007/978-3-540-85156-1_16)
- [31] KRIVANEK, O. L., DELLBY, N., KEYSE, R. J., et al. *Chapter 3 Advances in Aberration-Corrected Scanning Transmission Electron Microscopy and Electron Energy-Loss Spectroscopy. Advances in IMAGING AND ELECTRON PHYSICS - Aberration-Corrected Electron Microscopy*. Elsevier, 121-160, 2008. Advances in Imaging and Electron Physics. DOI: 10.1016/S1076-5670(08)01003-3. ISBN 9780123742209. Available from: <https://linkinghub.elsevier.com/retrieve/pii/S1076567008010033>
- [32] KRIVANEK, O.L., CORBIN, G.J., DELLBY, N., et al. *An electron microscope for the aberration-corrected era*. Ultramicroscopy. 108(3), 179-195, 2008. DOI: 10.1016/j.ultramic.2007.07.010. ISSN 03043991. Available from: <https://linkinghub.elsevier.com/retrieve/pii/S0304399107002331>
- [33] ROSE, H. *Prospects for aberration-free electron microscopy*. Ultramicroscopy. 103(1), 1-6, 2005. DOI: 10.1016/j.ultramic.2004.11.017. ISSN 03043991. Available from: <https://linkinghub.elsevier.com/retrieve/pii/S0304399104002074>
- [34] MÜLLER, H., UHLEMANN S., HARTEL, P., ZACH, J. and HAIDER, M. *Overview of Commercially Available CEOS Hexapole-type Aberration Correctors*. Microscopy and Microanalysis. 20(S3), 934-935, 2014. DOI: 10.1017/S1431927614006394. ISSN 1431-9276. Available from: [https://www.cambridge.org/core/product/identifier/S1431927614006394/type/journal\\_article](https://www.cambridge.org/core/product/identifier/S1431927614006394/type/journal_article)
- [35] MÜLLER, H., UHLEMANN S., HARTEL P. and HAIDER M. *Aberration-corrected optics: from an idea to a device*. Physics Procedia. 1(1), 167-178, 2008. DOI: 10.1016/j.phpro.2008.07.093. ISSN 18753892. Available from: <https://linkinghub.elsevier.com/retrieve/pii/S187538920800103X>
- [36] Corrected Electron Optical Systems GmbH [online]. CEOS: 2020 [cit. 10.5.2020]. Available from: <http://www.ceos-gmbh.de/en/>
- [37] MÜLLER, H., MASSMANN, I., UHLEMANN, S., et al. *Aplanatic imaging systems for the transmission electron microscope*. Nuclear Instruments and Methods in Physics Research Section A: Accelerators, Spectrometers, Detectors and Associated Equipment. 645(1), 20-27, 2011. DOI: 10.1016/j.nima.2010.12.091. ISSN 01689002. Available from: <https://linkinghub.elsevier.com/retrieve/pii/S0168900210028718>

- [38] NAKAMURA, K., INAD, H., TANAKA, H., et al. *Hitachi's spherical aberration corrected STEM: HD2700*. Hitachi Rev. 56(3), 34–38, 2007.
- [39] Nion Company [online]: 2020 [cit. 10.2.2020]. Available from: <http://www.nion.com/index.html>
- [40] DELLBY, N., KRIVANEK, O.L. and MURFITT, M.F. *Optimized Quadrupole-Octupole C3/C5 Aberration Corrector for STEM*. Physics Procedia. 1(1), 179–183, 2008. DOI: 10.1016/j.phpro.2008.07.094. ISSN 18753892. Available from: <https://linkinghub.elsevier.com/retrieve/pii/S1875389208001041>
- [41] KRIVANEK, O. L., CHISHOLM, M. F., NICOLOSI, V., et al. *Atom-by-atom structural and chemical analysis by annular dark-field electron microscopy*. Nature. 464(7288), 571–574, 2010. DOI: 10.1038/nature08879. ISSN 0028-0836. Available from: <http://www.nature.com/articles/nature08879>
- [42] SAWADA, H., TANISHIRO, Y., OHASHI, N., et al. *STEM imaging of 47-pm-separated atomic columns by a spherical aberration-corrected electron microscope with a 300-kV cold field emission gun*. Journal of Electron Microscopy [online]. 58(6), 357–361, 2009. DOI: 10.1093/jmicro/dfp030. ISSN 0022-0744. Available from: <https://academic.oup.com/jmicro/article-lookup/doi/10.1093/jmicro/dfp030>
- [43] SAWADA, H., HOSOKAWA, F., SASAKI, T., et al. *Aberration Correctors Developed Under the Triple C Project*. Advances in Imaging and Electron Physics, Elsevier. 297–336, 2011. DOI: 10.1016/B978-0-12-385983-9.00006-5. ISBN 9780123859839. Available from: <https://linkinghub.elsevier.com/retrieve/pii/B9780123859839000065>
- [44] STAM, M. A., TIEMEIJER, P., FREITAG, B., et al. *The Design and First Results of a Dedicated Corrector (S)TEM*. Microscopy and Microanalysis. 11(S02), 2005. DOI: 10.1017/S1431927605505750. ISSN 1431-9276. Available from: [http://www.journals.cambridge.org/abstract\\_S1431927605505750](http://www.journals.cambridge.org/abstract_S1431927605505750)
- [45] HAIDER, M., HARTEL, P., MÜLLER, H., et al. *Information Transfer in a TEM Corrected for Spherical and Chromatic Aberration*. Microscopy and Microanalysis. 16(4), 393–408, 2010. DOI: 10.1017/S1431927610013498. ISSN 1431-9276. Available from: [https://www.cambridge.org/core/product/identifier/S1431927610013498/type/journal\\_article](https://www.cambridge.org/core/product/identifier/S1431927610013498/type/journal_article)
- [46] UHLEMANN, S., MÜLLER, H., HARTEL, P., et al. *Thermal Magnetic Field Noise Limits Resolution in Transmission Electron Microscopy*. Physical Review Letters. 111(4), 2013. DOI: 10.1103/PhysRevLett.111.046101. ISSN 0031-9007. Available from: <https://link.aps.org/doi/10.1103/PhysRevLett.111.046101>
- [47] URBAN, K. W., MAYER J., JINSCHKE J. R., et al. *Achromatic Elemental Mapping Beyond the Nanoscale in the Transmission Electron Microscope*. Physical Review Letters. 110(18), 2013. DOI: 10.1103/PhysRevLett.110.185507. ISSN 0031-9007. Available from: <https://link.aps.org/doi/10.1103/PhysRevLett.110.185507>

- [48] URBAN, K. W., MAYER, J., JINSCHKE, J. R., et al. *Achromatic Elemental Mapping Beyond the Nanoscale in the Transmission Electron Microscope*. Physical Review Letters. 2013, 110(18). DOI: 10.1103/PhysRevLett.110.185507. ISSN 0031-9007. Available from: <https://link.aps.org/doi/10.1103/PhysRevLett.110.185507>
- [49] KAISER, U., BISKUPEK, J., MEYER, J.C., et al. *Transmission electron microscopy at 20kV for imaging and spectroscopy*. Ultramicroscopy. 111(8), 1239-1246, 2011. DOI: 10.1016/j.ultramic.2011.03.012. ISSN 03043991. Available from: <https://linkinghub.elsevier.com/retrieve/pii/S0304399111001197>
- [50] The Sub-Angstrom Low-Voltage Electron Microscopy Project [online] SALVE: 2020 [cit. 3.5.2020]. Available from: <https://www.salve-project.de/>
- [51] UHLEMANN, S. and HAIDER, M. *Residual wave aberrations in the first spherical aberration corrected transmission electron microscope*. Ultramicroscopy. 72(3-4), 109-119, 1998. DOI: 10.1016/S0304-3991(97)00102-2. ISSN 03043991. Available from: <https://linkinghub.elsevier.com/retrieve/pii/S0304399197001022>
- [52] KAISER, U., BISKUPEK J., MEYER J.C., et al. *Transmission electron microscopy at 20kV for imaging and spectroscopy*. Ultramicroscopy. 111(8), 1239-1246, 2011. DOI: 10.1016/j.ultramic.2011.03.012. ISSN 03043991. Available from: <https://linkinghub.elsevier.com/retrieve/pii/S0304399111001197>
- [53] HAIDER, M., HARTEL P., MÜLLER H., et al. *Information Transfer in a TEM Corrected for Spherical and Chromatic Aberration*. Microscopy and Microanalysis. 16(4), 393-408, 2010. DOI: 10.1017/S1431927610013498. ISSN 1431-9276. Available from: [https://www.cambridge.org/core/product/identifier/S1431927610013498/type/journal\\_article](https://www.cambridge.org/core/product/identifier/S1431927610013498/type/journal_article)
- [54] ROSE, H. *Electron optical correction system for lenses of electron microscope - has series of electric or magnetic and electromagnetic quadrupole elements located in optical path in astigmatic intermediate images*. Patent, DE4204512 A1, 1992.
- [55] Delong Instruments a.s. [online]. LVEM5 [cit. 14.2.2020]. Available from: <http://www.delong.cz/products/lvem5/>
- [56] Delong Instruments a.s. [online]. LVEM25 [cit. 14.2.2020]. Available from: <http://www.delong.cz/products/lvem25/>
- [57] ROSE, H. *Optics of high-performance electron microscopes*. Science and Technology of Advanced Materials. 9(1), 2008. DOI: 10.1088/0031-8949/9/1/014107. ISSN 1878-5514. Available from <https://iopscience.iop.org/article/10.1088/0031-8949/9/1/014107>
- [58] KRIVANEK, O. L., N. DELLBY , A. J. SPENCE , et al. *Aberration correction in the STEM*, J. M. Rodenburg (Ed.), In: Institute of Physics Conference Series: Proceedings 1997 EMAG Meeting, 153, 35-40.
- [59] CREWE, A. V., D. Kopf *Limitations of sextupole correctors*. Optik 56, 391-39. 1980b.

- [60] CREWE, A. V., D. Kopf *A Sextupole System for the Correction of Spherical Aberration*. Optik 55, 1–10. 1980.
- [61] ROSE, H. *Correction of aperture aberrations in magnetic systems with threefold symmetry*. Nuclear Instruments and Methods in Physics Research. 187(1), 187-199, 1981. DOI: 10.1016/0029-554X(81)90488-2. ISSN 01675087. Available from: <https://linkinghub.elsevier.com/retrieve/pii/0029554X81904882>
- [62] ROSE, H. *Outline of a spherically corrected semiaplanatic medium-voltage transmission electron microscope*. Optik 85, 19-24, 1990.
- [63] HAIDER, M., MÜLLER, H., UHLEMANN S., *Advances in Imaging and Electron Physics*. Volume 153, Hawkes ed., Springer, Heidelberg, 2008. ISBN 978-0123742209
- [64] ROSE, H. *Outline of an ultracorrector compensating for all primary chromatic and geometrical aberrations of charged-particle lenses*. Nuclear Instruments and Methods in Physics Research Section A: Accelerators, Spectrometers, Detectors and Associated Equipment. 519(1-2), 12-27, 2004. DOI: 10.1016/j.nima.2003.11.115. ISSN 01689002. Available from: <https://linkinghub.elsevier.com/retrieve/pii/S0168900203029899>
- [65] REMPFER, G. F., DESLOGE D. M., Walter P., et al. *Simultaneous Correction of Spherical and Chromatic Aberrations with an Electron Mirror: An Electron Optical Achromat*. Microscopy and Microanalysis. 3(1), 14-27, 1997. DOI: 10.1017/S143192769797001X. ISSN 1431-9276. Available from: [https://www.cambridge.org/core/product/identifier/S143192769797001X/type/journal\\_article](https://www.cambridge.org/core/product/identifier/S143192769797001X/type/journal_article)
- [66] REMPFER, G. F. *A theoretical study of the hyperbolic electron mirror as a correcting element for spherical and chromatic aberration in electron optics*. Journal of Applied Physics. 67(10), 6027-6040, 1990. DOI: 10.1063/1.345212. ISSN 0021-8979. Available from: <http://aip.scitation.org/doi/10.1063/1.345212>
- [67] TROMP, R. M., HANNON J.B., ELLIS A.W., et al. *A new aberration-corrected, energy-filtered LEEM/PEEM instrument. I. Principles and design*. Ultramicroscopy. 110(7), 852-861, 2010. DOI: 10.1016/j.ultramic.2010.03.005. ISSN 03043991. Available from: <https://linkinghub.elsevier.com/retrieve/pii/S0304399110000835>
- [68] GABOR, D. *A Space-Charge Lens for the Focusing of Ion Beams*. Nature. 160(4055), 89-90, 1947. DOI: 10.1038/160089b0. ISSN 0028-0836. Available from: <http://www.nature.com/articles/160089b0>
- [69] ASH, E.A., Gabor, D. *Experimental investigations on electron interaction*. Proc. Roy. Soc. (London) A228, 477-490, 1955.
- [70] ASH, E. A. *Use of Space Charge in Electron Optics*. Journal of Applied Physics. 26(3), 327-330, 1955. DOI: 10.1063/1.1721987. ISSN 0021-8979. Available from: <http://aip.scitation.org/doi/10.1063/1.1721987>
- [71] HAUFE, V. G. Optik (Stuttgart) 15, 520, 1958.
- [72] Le Poole, J. B. *Space charge correction of spherical aberration*. In Proceedings of the 5th European Congress Electron Microscopy, pp. 130-131 (Institute of Physics, London). Conference: Manchester, UK, September 5-12, 1972.

- [73] BERNARD, Y. M. *Aberration de sphéricité des lentilles à grilles*. C.R. Acad. Sci. Paris 234, 606-608, 1952.
- [74] BERNARD, Y. M. *Focalisation des particules de grande énergie par des lentilles à grille. I. Défauts des lentilles*. J. Phys. J. Phys. Radium 14, 381-394, 1953. DOI: 10.1051/jphysrad:01953001406038100
- [75] BERNARD, Y. M. *Focalisation des particules de grande énergie par des lentilles à grille. II. Défauts des lentilles*. J. Phys. Radium 14, 451-458, 1953. DOI: 10.1051/jphysrad:01953001407-9045100
- [76] SEMAN, O.I. Zh. Tekh. Fiz. 22, 1581-1591, 1952.
- [77] VERSTER, J. L. *On the use of gauzes in Electron Optics*. Philips Res. Rep. 18(6), 465-605, 1963.
- [78] RUS, P.J. *Correctie van Sferische Aberratie met behulp van een Gaaslens*. Afs-tudeerverslag, Delft. 1965.
- [79] ICHIHASHI M. and MARUSE S. *Correction of Spherical Aberration by Means of a Thin Conducting Foil*. JOURNAL OF ELECTRON MICROSCOPY, Vol. 20, No. 3, 167, 1971.
- [80] ICHIHASHI M. and MARUSE S. *Optical Properties of the Foil Lens for the Correc-tion of the Spherical Aberration*. Journal of Electron Microscopy, Volume 22, Issue 4, pp.321–328, 1973. DOI: 10.1093/oxfordjournals.jmicro.a049889. ISSN 1477-9986. Available from: <https://academic.oup.com/jmicro/article-lookup/doi/10.1093/oxfordjournals.jmicro.a049889>
- [81] ICHIHASHI, M. a MARUSE S. *Correction of the Spherical Aberration of a Mag-netic Lens with a Foil Lens*. Journal of Electron Microscopy, Volume 25, Issue 4. 229-236, 1976. DOI: 10.1093/oxfordjournals.jmicro.a050022. ISSN 1477-9986. Avail-able from: <https://academic.oup.com/jmicro/article/25/4/229/875856/Correction-of-the-Spherical-Aberration-of-a>
- [82] OLDFIELD, L C. *A rotationally symmetric electron beam chopper for picosec-ond pulses*. Journal of Physics E: Scientific Instruments. 9(6), 455-463, 1976. DOI: 10.1088/0022-3735/9/6/011. ISSN 0022-3735. Available from: <https://iop-science.iop.org/article/10.1088/0022-3735/9/6/011>
- [83] KHURSHEED, A., W. K. ANG. *On-Axis Electrode Aberration Correctors for Scanning Electron/Ion Microscopes*. Microscopy and Microanalysis. 21(S4), 106-111, 2015. DOI: 10.1017/S1431927615013227. ISSN 1431-9276. Available from: [https://www.cambridge.org/core/product/identifier/S1431927615013227/type/journal\\_article](https://www.cambridge.org/core/product/identifier/S1431927615013227/type/journal_article)
- [84] KAWASAKI, T., ISHIDA T., TAKAI Y., et al. *Development of electrostatic spheri-cal aberration corrector using annular and circular electrodes*. Surface and Interface Analysis. 48(11), 1160-1165, 2016. DOI: 10.1002/sia.6131. ISSN 01422421. Available from: <http://doi.wiley.com/10.1002/sia.6131>

- [85] HAWKES, P. W. *The geometrical aberrations of general electron optical systems I The conditions imposed by symmetry*. Philosophical Transactions of the Royal Society of London. Series A, Mathematical and Physical Sciences. 257(1086), 479-522, 1965. DOI: 10.1098/rsta.1965.0013. ISSN 0080-4614. Available from: <https://royalsocietypublishing.org/doi/10.1098/rsta.1965.0013>
- [86] HAWKES, P. W. *The geometrical aberrations of general electron optical systems II. The primary (third order) aberrations of orthogonal systems, and the secondary (fifth order) aberrations of round systems*. Philosophical Transactions of the Royal Society of London. Series A, Mathematical and Physical Sciences. 257(1086), 523-552, 1965. DOI: 10.1098/rsta.1965.0014. ISSN 0080-4614. Available from: <https://royalsocietypublishing.org/doi/10.1098/rsta.1965.0014>
- [87] HAWKES P.W. and KRIVANEK O.L. *Aberration Correctors, Monochromators, Spectrometers*. In: Hawkes P.W., Spence J.C.H. (eds) Springer Handbook of Microscopy. Springer, 2019. ISBN 978-3-030-00068-4
- [88] *Aberration-Corrected Analytical Transmission Electron Microscopy, First Edition*. Brydson R. ed. John Wiley & Sons, Ltd., 2011. ISBN 9780470518519
- [89] REIMER, L., KOHL, H. *Transmission electron microscopy: physics of image formation*. 5th ed. New York: Springer, Springer series in optical sciences, 2008. ISBN 978-0-387-40093-8.
- [90] FREITAG, B., KUJAWA S., MUL P.M., et al. *Breaking the spherical and chromatic aberration barrier in transmission electron microscopy*. Ultramicroscopy. 102(3), 209-214, 2005. DOI: 10.1016/j.ultramic.2004.09.013. ISSN 03043991. Available from: <https://linkinghub.elsevier.com/retrieve/pii/S0304399104001834>
- [91] KIM, H. S., YU M. L., THOMSON M. G. R., KRATSCHEMER E., et al. *Energy distributions of Zr/O/W Schottky electron emission*. Journal of Applied Physics. 81(1), 461-465, 1997. DOI: 10.1063/1.364081. ISSN 0021-8979. Available from: <http://aip.scitation.org/doi/10.1063/1.364081>
- [92] FRANSEN, M.J., VAN ROOY Th. L., TIEMEIJER P.C., et al. *On the Electron-Optical Properties of the ZrO/W Schottky Electron Emitter*. Elsevier, Advances in Imaging and Electron Physics. 91-166, 1999. DOI: 10.1016/S1076-5670(08)70217-9. ISBN 9780120147533. Available from: <https://linkinghub.elsevier.com/retrieve/pii/S1076567008702179>
- [93] MORIN, R., FINK H. W. *Highly monochromatic electron point-source beams*. Applied Physics Letters. 65(18), 2362-2364, 1994. DOI: 10.1063/1.112746. ISSN 0003-6951. Available from: <http://aip.scitation.org/doi/10.1063/1.112746>
- [94] EGERTON, R. F. *Electron Energy-Loss Spectroscopy in the Electron Microscope*. Springer Science & Business Media. 2011. ISBN 978-1-4419-9583-4
- [95] ECKERTOŮVÁ, L., FRANK, L., ed. *Metody analýzy povrchů: elektronová mikroskopie a difrakce*. Praha: Academia. 1996. ISBN 80-200-0329-0.

- [96] RUSKA, E. *The Development of the Electron Microscope and of Electron Microscopy*. Nobel lecture, December 8. 1986.
- [97] BAČOVSKÝ, J. *Aberration correction for low voltage optimized transmission electron microscopy*. *MethodsX*. 5, 1033-1047, 2018. DOI: 10.1016/j.mex.2018.08.009. ISSN 22150161. Available from: <https://linkinghub.elsevier.com/retrieve/pii/S2215016118301377>
- [98] VAN DEN BOS, A. *Aberration and the Strehl ratio*. *Journal of the Optical Society of America A*. 17(2), 2000. DOI: 10.1364/JOSAA.17.000356. ISSN 1084-7529. Available from: <https://www.osapublishing.org/abstract.cfm?URI=josaa-17-2-356>
- [99] MAHAJAN, V. N. *Strehl ratio for primary aberrations: some analytical results for circular and annular pupils*. *Journal of the Optical Society of America A*. 10(9), 1993. DOI: 10.1364/JOSAA.10.002092. ISSN 1084-7529. Available from: <https://www.osapublishing.org/abstract.cfm?URI=josaa-10-9-2092>
- [100] INTARAPRASONK, V., XIN H. L., MULLER D. A. *Analytic derivation of optimal imaging conditions for incoherent imaging in aberration-corrected electron microscopes*. *Ultramicroscopy*. 108(11), 1454-1466, 2008. DOI: 10.1016/j.ultra-mic.2008.05.013. ISSN 03043991. Available from: <https://linkinghub.elsevier.com/retrieve/pii/S0304399108001812>
- [101] CHANG, L.Y., KIRKLAND A.I. and TITCHMARSH J.M. *On the importance of fifth-order spherical aberration for a fully corrected electron microscope*. *Ultramicroscopy*. 106(4-5), 301-306, 2006. DOI: 10.1016/j.ultra-mic.2005.09.004. ISSN 03043991. Available from: <https://linkinghub.elsevier.com/retrieve/pii/S0304399105002160>
- [102] MANKOS, M., SHADMAN K. and KOLAŘÍK V. *Novel electron monochromator for high resolution imaging and spectroscopy*. *Journal of Vacuum Science & Technology B, Nanotechnology and Microelectronics: Materials, Processing, Measurement, and Phenomena*. 34(6), 2016. DOI: 10.1116/1.4962383. ISSN 2166-2746. available from: <http://aip.scitation.org/doi/10.1116/1.4962383>
- [103] LENCOVÁ B., HAWKES P. W. *Chromatic aberrations of electrostatic lens doublet*. *Inst. Phys. Conf. Ser. No 179: Section 4, Electron Microscopy and Analysis Group Conf. EMAG2003*. Oxford. 2003.
- [104] ORLOFF, J. *On addition of spherical and chromatic aberration of a pair of electron lenses*. *Optik* 63, No. 4, 369-372, 1983.
- [105] ROSE, H., WAN, W. *Aberration Correction in Electron Microscopy*. *Proceedings of the 2005 Particle Accelerator Conference*. IEEE. 44-48, 2005. DOI: 10.1109/PAC.2005.1590354. ISBN 0-7803-8859-3. Available from: <http://ieeexplore.ieee.org/document/1590354/>
- [106] HAWKES, P. W. *Magnetic electron lenses*. Springer-Verlag, New York. 1982. ISBN: 9783642815188

- [107] BARANOVA, L.A., READ F.H. and CUBRIC D. *Computer simulations of hexapole aberration correctors*. Physics Procedia. 1(1), 185-191, 2008. DOI: 10.1016/j.phpro.2008.07.095. ISSN 18753892. Available from: <https://linkinghub.elsevier.com/retrieve/pii/S1875389208001053>
- [108] LINCK, M., HARTEL P., UHLEMANN S., et al. *Chromatic Aberration Correction for Atomic Resolution TEM Imaging from 20 to 80 kV*. Physical Review Letters. 117(7), 2016. DOI: 10.1103/PhysRevLett.117.076101. ISSN 0031-9007. Available from: <https://link.aps.org/doi/10.1103/PhysRevLett.117.076101>
- [109] CHANG, WEI-Yu, CHEN F-R. *Development of compact Cs corrector for desktop electron microscope*. Ultramicroscopy. 179, 94-99, 2017. DOI: 10.1016/j.ultramicro.2017.04.009. ISSN 03043991. Available from: <https://linkinghub.elsevier.com/retrieve/pii/S0304399116302959>
- [110] ZLÁMAL, J., LENCOVÁ B. *Development of the program EOD for design in electron and ion microscopy*. Nuclear Instruments and Methods in Physics Research Section A: Accelerators, Spectrometers, Detectors and Associated Equipment. 645(1), 278-282, 2011. DOI: 10.1016/j.nima.2010.12.198. ISSN 01689002. Available from: <https://linkinghub.elsevier.com/retrieve/pii/S0168900210030007>
- [111] ROSE, H. *Prospects for realizing a sub-Å sub-eV resolution EFTEM*. Ultramicroscopy. 78(1-4), 13-25, 1999. DOI: 10.1016/S0304-3991(99)00025-X. ISSN 03043991. Available from: <https://linkinghub.elsevier.com/retrieve/pii/S030439919900025X>
- [112] ZACH, J., HAIDER, M. *Aberration correction in a low voltage SEM by a multipole corrector*. Nuclear Instruments and Methods in Physics Research Section A: Accelerators, Spectrometers, Detectors and Associated Equipment. 363(1-2), 316-325, 1995. DOI: 10.1016/0168-9002(95)00056-9. ISSN 01689002. Available from: <https://linkinghub.elsevier.com/retrieve/pii/0168900295000569>
- [113] BAČOVSKÝ, J., KOLAŘÍK, V. *Hexapole corrector for LVEM*. Ultramicroscopy. 212, 2020. DOI: 10.1016/j.ultramicro.2020.112974. ISSN 03043991. Available from: <https://linkinghub.elsevier.com/retrieve/pii/S030439911930004X>

## 12. List of abbreviations

CFE	Cold field emission
EDM	Electric discharge machining
FFT	Fast Fourier transform
HAADF	High-angle annular dark-field imaging
LVEM	Low voltage electron microscopy
TEM	Transmission electron microscopy
LEEM	Low energy electron microscopy
PEEM	Photo electron emission microscopy
P-V	Peak to valley
RMS	Root-Mean-Square
SEM	Scanning electron microscopy
STEM	Scanning transmission electron microscopy
YAG	Yttrium aluminium garnet